PERFORMANCE ANALYSIS OF FREE SPACE OPTICAL COMMUNICATION UNDER THE EFFECT OF SCINTILLATION IN MWANZA AND ARUSHA REGIONS OF TANZANIA

EDSON JOSEPH

MASTER OF SCIENCE IN TELECOMMUNICATIONS ENGINEERING

THE UNIVERSITY OF DODOMA

OCTOBER, 2019

PERFORMANCE ANALYSIS OF FREE SPACE OPTICAL COMMUNICATION UNDER THE EFFECT OF SCINTILLATION IN MWANZA AND ARUSHA REGIONS OF TANZANIA

BY
EDSON JOSEPH

A DISSERTATION SUBMITTED IN PARTIAL FULFILMENT OF THE REQUIREMENTS FOR THE DEGREE OF MASTER OF SCIENCE IN TELECOMMUNICATIONS ENGINEERING

THE UNIVERSITY OF DODOMA
OCTOBER, 2019

DECLARATION

AND

COPYRIGHT

I, **Edson Joseph**, declare that this dissertation is my own original work and that it has not been presented and will not be presented to any other university for a similar or any other degree award.

Signature:……………………..……………

CERTIFICATION

The undersigned certify that they have read and hereby recommend for acceptance by the University of Dodoma, a dissertation entitled "***Performance analysis of Free Space Optical communication under the effect of scintillation in Mwanza and Arusha regions of Tanzania,***" in partial fulfillment of the requirements for the degree of Master of Science in Telecommunications Engineering of the University of Dodoma.

Dr. Florence Rashidi

Signature: FRashidi Date: 31/10/2019

(SUPERVISOR)

Dr. Mustafa H. Mohsin

Signature: Date: 31/10/2019

(SECOND SUPERVISOR)

ACKNOWLEDGEMENTS

First and foremost, praises are entirely devoted to Almighty God for blessing me with health and intellectual power and assisted me all the way to finish this work.

I would like to express my deep and sincere gratitude to my research supervisor, ***Dr. Florence Rashidi***, for her inspirational guidance, valuable suggestions, keen interest, constant help, and encouragement. This work and publications could not been achieved without her discussions and research feedback. I would also like to thank her for her friendship, empathy, and great sense of humor. I am also very grateful to ***Dr. Mustafa H. Mohsin***, my second supervisor for his scientific advice and knowledge and many intuitive discussions and suggestions. I wish to express my gratitude to UDOM- CIVE for awarding me studentship to complete my MSc.

I give my special appreciation to Mr Marko R. Mwalongo who was my classmate and staff from the Department of Telecommunications and Communications Networks for his constructive contribution during my whole study period, I also extend my special thanks to my other fellow classmates Eng. Peter Philip, Mr. Humphrey Mwakalibule and Eng. Khadija O. Mohammed for their team working and super support.

I am sincerely expressing my gratitude to Prof. Abel Makubi, Current Director General of Bugando Medical Centre for granting me the study leave permission.

And last, but not least, I am thankful to my family for their encouragement, patience, love and prayers especially my father Mr. Joseph R Ndyalimo, my step mother Kemilembe Kailembo and my respected brothers and sisters.

DEDICATION

To the memory of my loving mother Feliciana Kaigi.

ABSTRACT

Free Space Optics communications (FSO) has drawn a bunch of attention for a range of applications in telecommunications field. The unregulated bandwidth which is up to 200THz, security, higher speed, unlimited data rate, low deployment cost, and shortest installation time frame are the few reasons to employ FSO system. However, weather attenuation has a massive impact on the FSO transmission channel.

In this study, the effect of scintillation on the performance and FSO link availability evaluation is analyzed in terms of eye diagrams, Bit Error Rate (BER) and Q-factor, the examination of signal to noise ratio (SNR) was also considered.

Two prediction models Submarine Laser Communication (SLC) II and Hufnagel Valley (HV) day were compared to attain the finest prediction model performance for selected data regarding particular meteorological conditions of Mwanza and Arusha regions. HV day model had the best performance for predicting scintillation intensity for the scintillation data taken from January 2015 to December 2018 which totals up to a 48 months period.

The simulation shows, the FSO transmission for below 6km distance produce the better quality signal than transmission for 8km and above distance where at 8km distance, the BER value is 10^{-7} which produce the bad quality signals at receiver for both two regions. However, the FSO link availability decreases with increase in transmission path, FSO link is feasible in both Arusha and Mwanza regions for about 6km range and therefore is recommended for adoption for both regions.

TABLE OF CONTENTS

LIST OF TABLES

LIST OF FIGURES

LIST OF APPENDICES

LIST OF ABBREVIATIONS

APD	Avalanche Photo Diode
BER	Bit Error Rate
CIVE	College of Informatics and Virtual Education
Cm	Centimeter
CSI	Channel State Information
dB	Decibels
FOV	Field of View
FSO	Free Space Optics
GHz	Gigahertz
HAP	High Altitude Platform
HV	Hufnagel Valley
ICT	Information Communication Technology
IT	Information Technology
LPD	Low Probability of Detection
LPI	Low Probability of Interception
M	Meter
MHz	Megahertz
Nm	Nano Meter
NRZ	Non Return to Zero
OOK	On Off Keying
Q factor	Quality Factor
RF	Radio Frequency
RX	Receiver
SLC	Submarine Laser Communication
SNR	Signal to Noise Ratio
TMA	Tanzanian Meteorological Agency
TX	Transmitter
UAV	Unmanned Aerial Vehicles
UDOM	The University of Dodoma

CHAPTER ONE
INTRODUCTION

1.1 General Introduction

The introduction of Information and Communications Technologies (ICT) has created a huge need for use of these technologies in many areas of human endeavor. The health sector has seen ICT being used in diagnosing and controlling of diseases (Mirarchi, Guzzi, Vizza, Tradigo, & Cannataro, 2015). There have been improvements in the education sector in the delivery of learning materials as a result of ICT advances (Stoilescu, 2017). ELearning has made it possible to conduct lessons to large and far flung audiences. This way many people who would have had difficulties to get an education have been reached. The business sector has also not been left out. Companies such as Alibaba, Amazon and Bolt to name a few have been using ICT to reach out to their customers (Sanayei & Faraghian, 2015).

These many uses of ICT have created a scarcity of bandwidth in the last mile. The traditional last mile delivery system which is radio frequency (RF) has seen a huge strain on its system (Nilupulee, Gunathilake, & Shakir, 2017). This strain on RF has enabled the introduction of optical fiber to mitigate this problem. Fiber optic transmit data through glass or plastic in form of light (Yang et al., 2017). This has enabled large amounts of data to be transmitted at extremely high speed. However the digging which is associated with delivery of fiber optic implementation in the last mile not only raises the cost but also creates disruption to the public through digging of roads (Rashid & Semakuwa, 2014). The other option left to deliver information in the last mile is Free Space Optics (FSO).

Free Space Optics (FSO) being an optical technology in which the information signal in the form of light beams propagates in atmospheric channel between the transmitter (TX) and the receiver (RX) (Nazari, Gholami, Vali,Sedghi, & Ghassemblooy, 2016).

However, since the channel of FSO is an atmosphere which encounters enormous challenge and the performance of FSO communication system is subject to rapid changes in atmosphere. For that reason, it is desirable to investigate the diverse atmospheric conditions such as fog, smoke, and scintillation and also analyze the system performance under these atmospheric conditions (Miglani, 2017).

Scintillation occurs when temperature varies with completely different air pockets due to the heat up rising from the surface of the earth. Thereby generating regions of varying refractive index along the transmission path, where by transmission errors may be induced due to the beam spread from the transceiver as they propagate through these heated air pockets (Malik & Singh, 2015). The variations of temperature can result into instability in amplitude of the signal which results "image dancing" at the FSO receiving terminal (Touati, Abdaoui, Touati, Uysal, & Bouallegue, 2017).

According to Ijaz et al. (2012) another challenge that hinders FSO communication visibility is the presence of smoke in channel. Smoke is produced by the burning of numerous substances like carbon, glycerol, and household discharge.

Fog is also a factor that significantly attenuates visible FSO radiation. Optical ray of light is absorbed, scattered, and reflected by the obstruction resulted by fog.

For FSO communications, Mie scattering dominates other atmospheric losses (Majumdar, 2015), Mie Scattering is an atmospheric loss that occurs when laser radiation rapidly scattered from particulates (aerosols or clouds) of sizes similar to the wavelengths of radiation with no variation of frequency (Larry B. Stotts, 2017)

Mie Scattering is the result of fog in channel (Esmail & Fathallah, 2016). According to a survey done by Demers et al. (2011), snow and rain can result into attenuation up to around 100 dB/km and 40 dB/km respectively, fog is the leading problem by far. In exceedingly heavy fog, attenuation is as high as 480 dB/km.

In examining FSO performance, it is vital to take several system parameters into consideration. In general, these parameters can be divided into two different categories: internal parameters and external parameters. Internal parameters are associated with the design of a FSO system which incorporate optical power, wavelength, transmission bandwidth, divergence angle, optical loss on the transmit side and receiver sensitivity, BER, receiver lens diameter, and receiver field of view (FOV) on the receive side. Furthermore the external parameters are associated with the weather patterns on which the system are being deployed including visibility and atmospheric attenuation, scintillation, transmission distance, pointing loss, loss due to window (Gunathilake & Shakir, 2017).

FSO uses lasers, or lightweight pulses, to send packetized information within the rate (THz) spectrum vary, air being the transport medium. This suggests that urban businesses needing quick information and web access have a considerably lower cost possibility. An FSO system for native loop access contains many optical device terminals, every one residing at a network node to form one, point-to-point link; associate degree optical mesh architecture; or a network topology that is typically point-to-multipoint.

FSO delivers more advantages over other traditional wireless technologies (e.g Microwave systems). It can avoid some challenges facing optical fiber communications such as high cost of digging roads, impractical physical link between transmitters and receivers (Rashid & Semakuwa, 2014). FSO systems provide very high data rates without the requirement of spectrum license, The attained data rate is almost equivalent to the optical fiber cable’s data rate and due to narrow laser beam facilitates unlimited number of FSO links that can be deployed. Due to the narrow laser beam high data security with low probability of interception and low probability of detection (LPI/LPD) properties can be achieved (Raja, 2013).

It is easier to deploy the FSO link, the total time taken to become operational from its begin of installation to its alignment is comparatively short. The main demand is to ensure clear Line Of Sight (LOS) with none variety of obstruction between the transmitter and receiver. This can be in contrast to the utilization of fiber optic cables which needs right of method and trenching adding further value to the installation. FSO system can be used to extend any network system including Wireless Local Area Network (WLAN), and Fiber optic or satellite using invisible beams of light which results into a very fast broadband speed (Carrozzo, Mori, & Marzano, 2014).

According to Singhal et al (2015) another major advantage of FSO communication is insensitivity to electromagnetic interference (EMI), due to immunity to EMI FSO link provides opportunity for unlimited frequency reuse as of this property. A narrow

beam ensures good spatial selectivity so there is no interference with other links surrounding the transmission atmosphere (Henniger & Wilfert, 2010).
Despite of great potential of FSO communication, its transmission capacity depends on atmospheric changes such as absorption, scattering and turbulence found in atmospheric channel. According to Kaushal & Kaddoum (2015) atmospheric turbulence affects bit error rate (BER) of FSO performance which is the proportion of bits that have errors relative to the overall variety of bits received in a very transmission and that results into communication link infeasibility. Due to intensity fluctuations in beam phase of light may result into scintillation effect.

Scintillation is the effect of solar energy heating small pockets of air to some extent in different temperatures, thereby generating regions of varying refractive index along the transmission path, where by transmission errors may be induced due to the beam spread from the transceiver as they propagate through these heated air pockets (Shumani, Abdullah, & Suriza, 2016), thus creating FSO data transmission difficult due to errors. Sun radiation increase atmospheric temperature near the earth surface and consequently, the atmosphere density will be decreased. This causes random fluctuation of the atmosphere temperature and accordingly the atmosphere refractive index will change randomly with time and space. Random variation of refractive index leads to deflection of optical beam and power fluctuation at the Rx, which is described in term of scintillation. $C_n^{\ 2}$ is a key parameter for describing the fluctuation of refraction index. The refractive index or index of refraction of a material is a dimensionless number that describes how fast light propagates through the material (Nor et al., 2017). The index of refraction value in the atmosphere depends on temperature, pressure, and humidity of air and on the wavelength used for the transmission (Roberto Ramirez-Iniguez, Sevia M. Idrus, 2008).

1.2 Statement of the Problem

There has been a marked increase in mobile phone users in Tanzania. From 2010 to 2018 there has been an increase of 44.9% of users. This has created a huge demand for bandwidth on the traditional RF and Optical Fiber systems (TCRA, 2018)
That demonstrates the highly use of smart phones and other accessories such as laptops and tablets. Eventually there are number of applications being installed on

these mobile and fixed devices which require significant use of bandwidth to function properly.

Telecommunication companies in Tanzania are now investing much capital in laying optical fiber cables as milestone communication solution so as to meet the bandwidth demand, since Radio Frequency (RF) communication systems can no longer suffice the high demand of bandwidth needed by subscribers.

Moreover, there are challenges on laying these optical fiber cables especially in cities where the infrastructure like roads and buildings have been developed and renovations still continue.

Thus digging and laying cables are very complex if not impossible in a few suburbs. In such areas, telecom companies are strained to depend on microwave links (Miglani, 2017). Again, due to continuity development of network infrastructure design in Tanzania, underground fiber cables are cut during road and other infrastructure constructions. An alternative to fiber cables in unreachable sites could be the employing of FSO system. FSO communication can be used to offer backup links in the experience of fiber cable destruction or as a backbone network.

According to Zabidi et al. (2010) it was observed that FSO channel is more affected by scintillation attenuation up to 12dBm. Also according to Touati et al. (2017) the scintillation is the main vital factor that hinder the performance of wireless optical communications in subtropical region. In order to evaluate the feasibility of FSO link in Arusha and Mwanza regions, this study analyses the atmospheric condition in terms of scintillation attenuation from meteorological data of the particular regions.

To the best of my knowledge, evaluation of FSO performance in Arusha and Mwanza regions has not been investigated to determine its practicability under scintillation effect. No work has been done in the region to find out whether the Arusha and Mwanza weather patterns in terms of scintillation will tolerate FSO communication link. After the evaluation, the study proposes if FSO communication can be used in the mentioned cities under scintillation effect.

1.3 Research Objectives

1.3.1 Main Objective

The main of objective of this study is to investigate the feasibility of Free space optic communication under the scintillation effect in Arusha and Mwanza regions.

1.3.2 Specific Objectives

i. To simulate the FSO transmission link under two mathematical models Hufnagel Vallay (HV) Day and Submarine Laser Communication (SLC II) Day using the calculated scintillation attenuation in Arusha and Mwanza regions.
ii. To compare the FSO transmission link performance of the two mathematical models, HV day and SLC II day.
iii. To propose the feasibility of free space optical communication in Mwanza and Arusha regions based on the comparison results in ii above.

1.4 Research Questions

To attain the specified objectives, this study work will answer the following questions.

1. What is the individual and total average signal attenuation in Arusha and Mwanza regions under scintillation?
2. Which mathematical model between HV Day and SLC II day performs better based on best BER?
3. Can FSO communication be implemented in Arusha and Mwanza regions?

1.5 Significance of the Research

The findings of this research is beneficial to the society considering that data and voice communication require high bandwidth transmission media like FSO link. The ever increasing bandwidth demand of current and emerging telecommunication systems in Arusha and Mwanza cities is the major driving force behind this study (Halotel et al., 2018). The study highlights the best link margin in terms of transmission power and wavelength so as to improve the transmission quality and best Bit error rate (BER). Through investigating scintillation effect on FSO link performance the better link parameter settings such as wavelength, beam divergence, and transmitting power is obtained. The results of this study helps to describe the effect of scintillation in Arusha and Mwanza regions, Hence practical FSO link efficiency under scintillation effect is achieved.

CHAPTER TWO

LITERATURE REVIEW

2.1 Introduction

Free Space Optics (FSO) communication is the transmission of information/data under long distances using modulated optical signals through free space (or an unguided media) (Esmail, Member, Fathallah, & Member, 2016). The unguided media could be space, water, atmosphere or a combination of any of these media. Since this study is about terrestrial transmissions, the medium of interest is the atmosphere. FSO communication has grown to be more and more interesting as an addition or alternative to radio frequency communication (Pesek, Bohata, Zvanovec, Perez, & Valencia, 2016). FSO communication is deployed in links connecting satellites, ground stations, deep-space probes, aircraft, unmanned aerial vehicles (UAVs), high altitude platforms (HAPs), and other traveling communication technologies are of practical interest. Furthermore, all links can be used in both military and civilian circumstances (Henniger & Wilfert, 2010). Fig 2.1 shows a association of FSO with a range of wireless technologies and fiber.

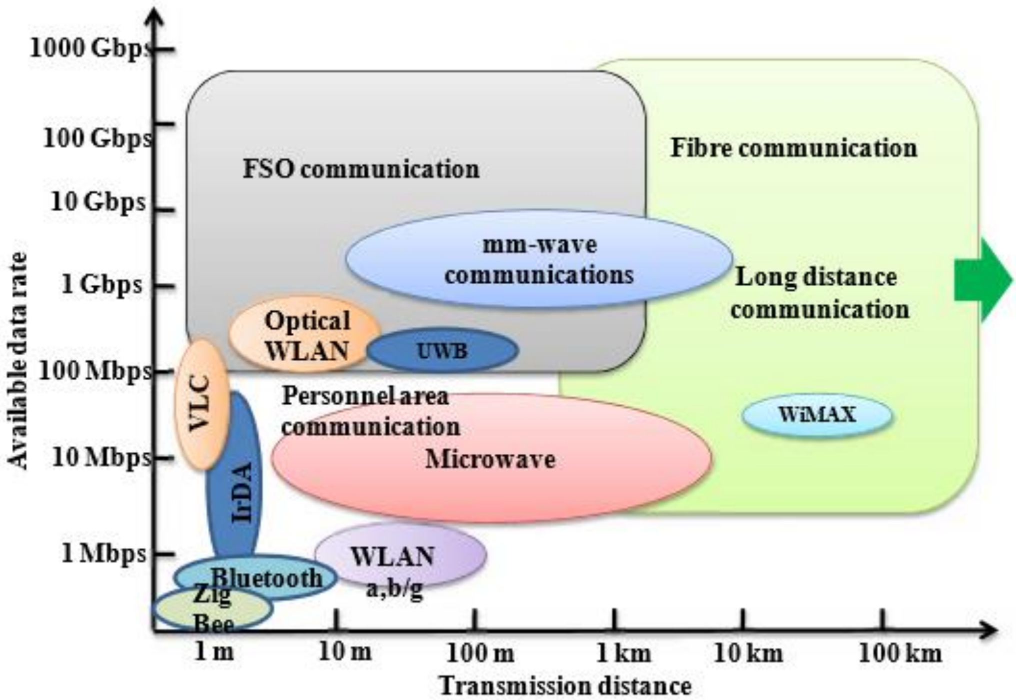

Figure 2. 1 Comparison of a range of optical and RF wireless technologies

Source: (Z.Ghaseemlooy, W. Poopola, 2012)

2.1.1 FSO Block Diagram

The major subsystems in an FSO communication system are illustrated in Fig. 1. A source producing data input is to be transmitted to a remote destination. This source

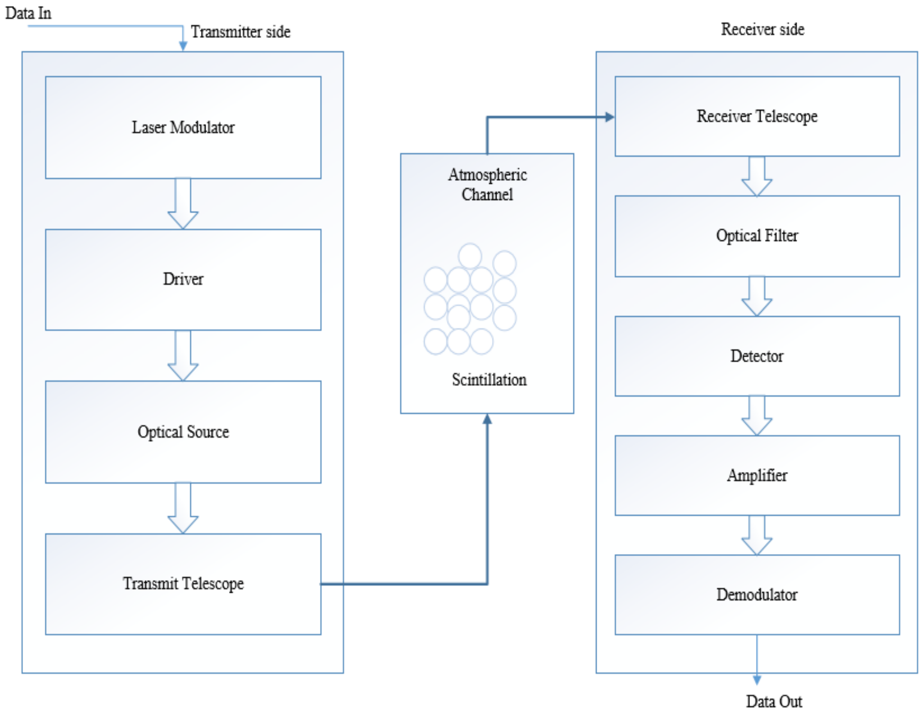

Figure 2. 2 FSO communication Block diagram

has its output modulated onto an optical carrier; laser or LED, which is then transmitted as an optic al field through the atmospheric channel. The important aspects of the optical transmitter system are size, power, and beam quality, which determine laser intensity and minimum divergence obtainable from the system. At the receiver, the field is optically collected and detected, generally in the presence of noise interference, signal distortion, and background radiation.

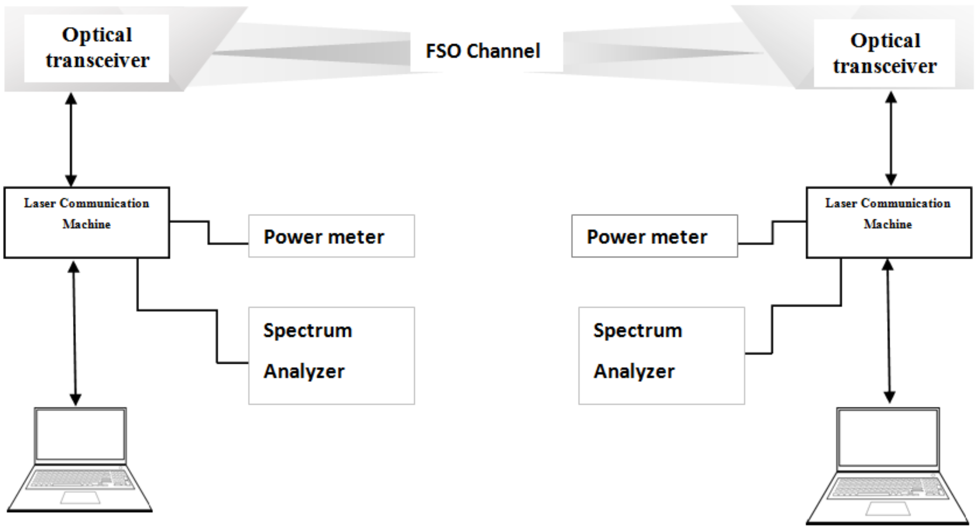

Figure 2. 3 FSO communication Block diagram with connections

2.2 Atmospheric Turbulence

When solar radiation heats surface of the earth, the air surrounded becomes hotter. The warm air molecules unfold apart; consequently, it becomes less dense and lighter than the air on top of it. The unstable heat air rises and also the cooler denser air quickly descends to interchange it. This development generates separate air cells with totally different temperatures unsteady vertically thus leads to fluctuations in the index of refraction. This interrupts atmospheric pressure equilibrium and produce horizontal movements of the air cells. The resultant of the mentioned effects, forms eddy air currents within the atmosphere termed as atmospheric turbulence (Ghassemlooy et al., 2010). Optical turbulence is termed as the fluctuations in the index of refraction, and is denoted by the refractive index structure C_n^2, which is a quantity of the amount of refraction present in the air. Irregularly solar power heats the atmosphere and different cells in the atmosphere reveals different temperatures and results to turbulences. Table 2.1 shows different ranges of C_n^2 (Vitásek et al., 2011)(Madhuri & Mahaboob, 2017).

Table 2. 1 Atmospheric Turbulences

C_n^2 ($m^{-2/3}$)	Atmospheric Turbulences
10^{-16}	Weak
10^{-14}	Middle
10^{-13}	Strong

Where C_n^2 is the refractive index structure in $m^{-2/3}$.

2.3 Turbulence and Scintillation

Thermal turbulence available in atmospheric channel creates random distributed cells and wave fronts fluctuate resulting into focusing and defocusing of the beam at the receiver, these fluctuations are called scintillations (Fiser, Brazda, & Rejfek, 2014). It is turbulence-related phenomena that results BER degradation in FSO systems (Willebrand & Ghuman, 2002). Turbulence has three major effects. First is the deflection of the beam caused by changes of index of refraction in a random way, called beam wander. Second is fluctuations in intensity of the beam wave front that results into scintillation. Last is the additional divergence of the beam. Under these three turbulence effects, FSO communication is mainly affected by scintillation (Sidarta, 2016). Figure 2.2 illustrates atmospheric turbulence.

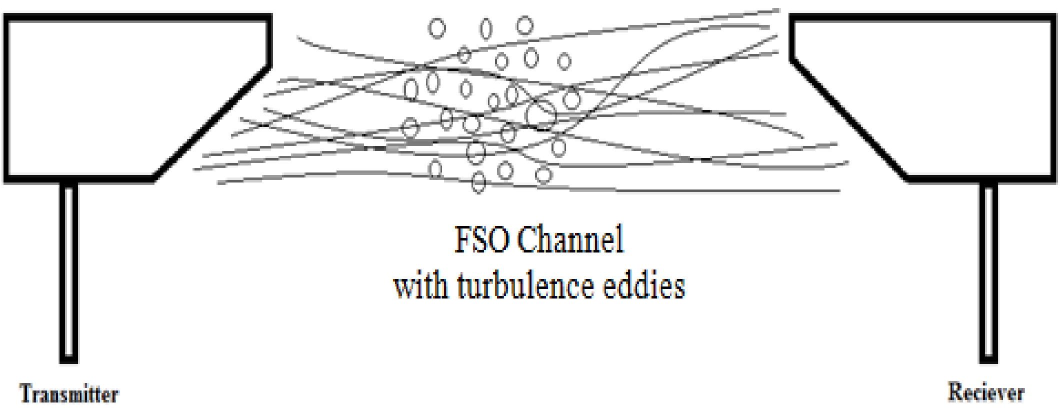

Figure 2. 4 Atmospheric Turbulence

2.4 Index of Refraction Structure Constant (C_n^2) and Modeling.

The index of refraction structure parameter C_n^2 is defined as a critical parameter for describing optical turbulence and used to compute the intensity of optical turbulence. Refractive index structure parameter (C_n^2) is mainly considerable parameter that determines the attenuation due to scintillation (Majumdar, 2015). This parameter can be modeled basing on theoretical and/or empirical, moreover, by using numerical under given input parameters or analytical form this parameter can be presented (Son & Mao, 2016). In this study numerical approach was used to present the index of refraction structure parameter C_n^2 under theoretical model.

According to Ricklin et al. (2006) and Prokes (2009), the refractive index structure parameter lies on different variables of meteorological on the altitude, geographical location, temperature gradient, wind strength, humidity and day-time. Characteristics of temperature circulation varies with different location and reflected under assumed values of C_n^2.

Theoretical/mathematical models used to model the index of refraction structure parameter C_n^2 are Hufnagel Valley(HV) Day, Hufnagel Valley (HV) Night, Greenwood (GW), Submarine laser communication I (SLC I) Day, Submarine laser communication II (SLC I) Day, Submarine laser communication III (SLC III) Day and PAMELA models (Majumdar, 2015). In this thesis, Hufnagel Valley Day and Submarine laser communication (SLC II) Day were used in this study since they are commonly used (Larry C. Andrews, Ronald L. Phillips, 2001) (Propagation et al., 2014). Furthermore, the two models were selected because according to the table 2.2, showing models and specific limitation patterning this study, only the two models HV day and SLC II day complied with the study requirements.

Equation 2.1 and 2.2 represents the Submarine laser communication (SLC II) Day and Hufnagel Valley (HV) Day models respectively (Uysal & Yu, 2006)(Carrozzo et al., 2014).

Table 2. 2: Shows different models used to describe the refractive index structure parameter C_n^2 and their limitations.

Model	Altitude(h)	Input Parameter(s)	Limitation according to this study
Hufnagel Valley Day	Nil	Wind velocity, Altitude	None (Ricklin et al., 2006).
Hufnagel Valley Night	Nil	Altitude	nighttime model (Ricklin et al., 2006).
Greenwood Night	Nil	Elevation angle, altitude	nighttime model (Greenwood, 1977).
SLC I-model	20m<h<230m	Altitude	Low Altitude requirement (Ricklin et al., 2006)
SLC II-model Day	850m<h7000m	Altitude	None (Ricklin et al., 2006).
SLC III-model	7000m<h<20000	Altitude	High Altitude requirement (Ricklin et al., 2006).
PAMELA	Nil	Altitude, Latitude, longitude, day time, percent cloud cover, terrain type, date, temperature, pressure and wind velocity.	large set of input parameter (Oh et al., 2004) (Han, Ricklin, Oh, Doss-hammel, & Eaton, 2004).

$$C_n^2(h) = 6.352 \times 10^{-7} h^{-2.966} \quad (2.1)$$

$$C_n^2(h) = 0.00594\left({}^{v}/_{27}\right)^2 (10^{-5}h)^{10}\, e^{\left({}^{h}/_{1000}\right)} + 2.7 \times 10^{-6} e^{\left({}^{-h}/_{1500}\right)} + Ae^{{}^{-h}/_{1000}} \quad (2.2)$$

Whereby,

A is the refractive-index structure constant parameter at ground level 1.7×10^{-14} $(m^{-2/3})$

v is the velocity of wind (m/s)

h is the altitude (m)

While taking into consideration the performance of C_n^2 is affected by temperature fluctuations along different layers within the Earth's atmosphere, hence, the refractive-index structure parameter turn into a function of the altitude above the ground and expressed in equation 2.3 (J Armstrong, 2009).

$$C_n^2(SF, T, WS, RH, TCSA) = 5.9 \times 10^{-15} W_{th} + 1.6 \times 10^{-15} T - 3.7 \times 10^{-15} RH - 3.7 \times 10^{-15} WS + 2.8 \times 10^{-14} SF - 1.8 \times 10^{-14} TCSA - 3.9 \times 10^{-13} \quad (2.3)$$

Whereby,

W_{th} is a temporal hour weight (0.1)

RH is the relative humidity (%)

SF is the solar flux (kW/m^2)

WS is the wind speed (m/s)

$TCSA$ is the aerosol particles' total cross sectional area and it expressed in equation 2.4

$$TCSA = 7.3 \times 10^{-3} + 9.96 \times 10^{-4} RH - 2.75 \times 10^{-5} RH^2 - 1.37 \times 10^{-5} SF^4 \quad (2.4)$$

As a result the refractive index structure parameter, C_n^2 can be calculated by adding equation 2.1 and 2.3 for SLC II day model, and equation 2.2 and 2.3 for HV day model.

$$C_n^2 = C_n^2(h) + C_n^2(hT, WS, RH, TCSA, SF) \quad (2.5)$$

The relationship between C_n^2 and optical intensity fluctuation relative variance is represented in equation 2.1 (Larry C. Andrews and Ronald Phillips, 2005)

$$\propto_{Scint} = \sqrt{\left(0.5 \frac{2\pi}{\lambda}^{7/6} * C_n^2 * L^{11/6}\right)} \quad (2.6)$$

Whereby,

$\propto_{Scint}$ is the attenuation coefficient due to scintillation (dB)

λ is the wavelength (nm)

L is the optical link distance (m)

2.5 Performance Measurements

2.5.1 Measured Eye Diagrams

Eye diagram is a measurement method for assessing the transmission quality of FSO system in a statistical way (Guo, Lin, Lin, Huang, & Member, 2009). The eye diagram is an important Bit-Error-Rate **(**BER) measurement for simulated FSO systems, and allows essential parameters of the electrical signal quality to be swiftly visualized and analyzed. Eye diagram has three major parts which shows useful information as shown in Fig 2.3. First, jitter is the time divergence from the best timing of a data-bit event and is possibly one of the main significant characteristics of a high speed signal for digital data, second inter-symbol interference (ISI) is a structure of signal distortion in which one symbol interferes by subsequent symbols caused by high-speed transmission and multipath fading, and the third one is the width of the eye opening that represents the time interval through which the received signal can be sampled with no error from ISI (Larry B. Stotts, 2017). Through the eye diagram analyzer, Q-factor and BER can be visualized as shown in Fig 2.4 and 2.5 respectively. Q-factor as a measure of the eye opening, is associated to the electrical signal-to-noise power ratio and it is broadly used to calculate the BER, The BER is a evaluation of the total amount of bits incorrectly received to the total amount sent (Milosevic, Petkovic, Member, & Djordjevic, 2017). It is normally measured by transmitting a pseudorandom binary chain across a link and counting the number of inaccurate bits received at the other terminal and is the ultimate signal quality determinant in optical communication links (Diagram et al., 2012). The typical BER requirement is $< 10^{-9}$ (less than one error in one billion bits) for most practical optical receivers applications (Navidpour, Uysal, & Kavehrad, 2007). BER performance is the supportive in presenting broad investigation amid different FSO configurations, which was the key focus of this study.

2.5.2 Signal –to-Noise Ratio (SNR)

Signal –to-noise ratio (SNR) is defined as the ratio of the preferred signal power to noise power. SNR points out the communication link reliability of among the transmitter and receiver. Always SNR is increased to a large degree with simultaneous decrease in BER (Pandey, Awasthi, & Srivastava, 2013). SNR was used in this study to estimate the quality of free space optical communication systems.

According to MS Alam et. (2008), SNR can be calculated from the refractive index structure C_n^2 obtained in equation 2.5 as follows.

$$SNR(dB) = 10log\left(\frac{1}{0.31C_n^2\left(\frac{2\pi}{\lambda}\right)^{7/6}L^{11/6}}\right) \qquad (2.7)$$

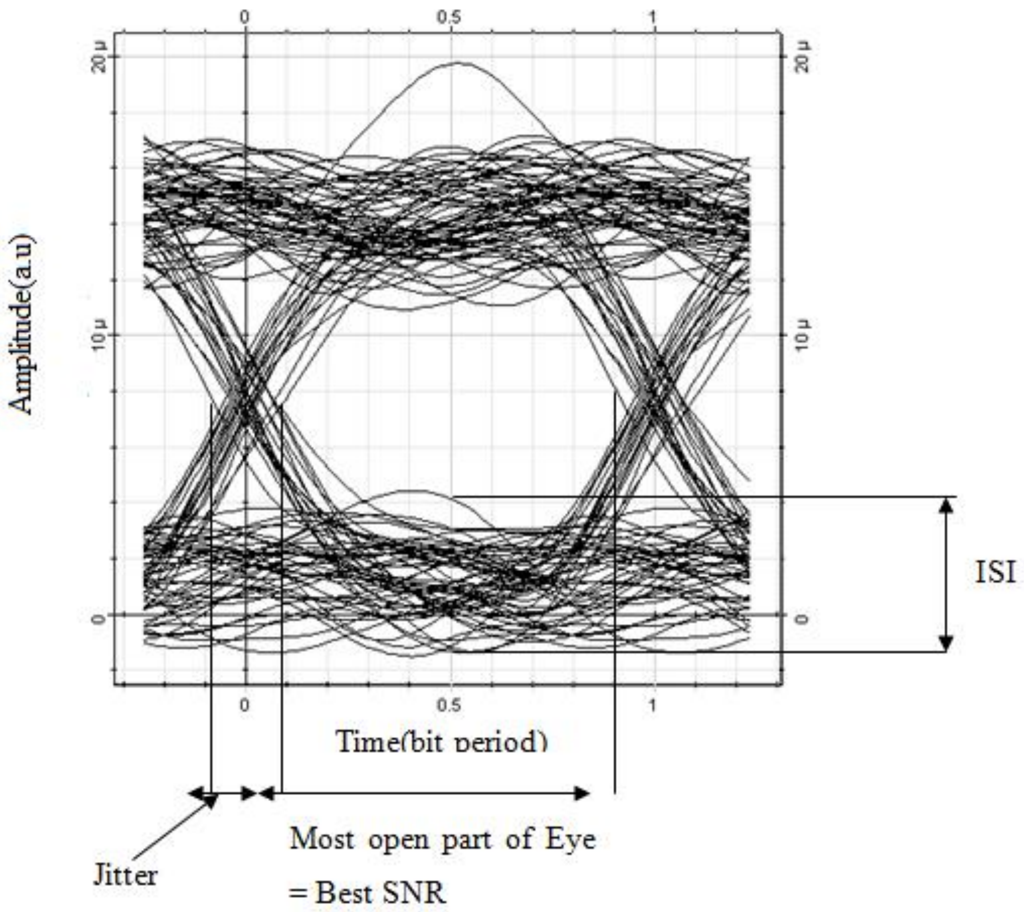

Figure 2. 5 Eye diagram and its interpretation

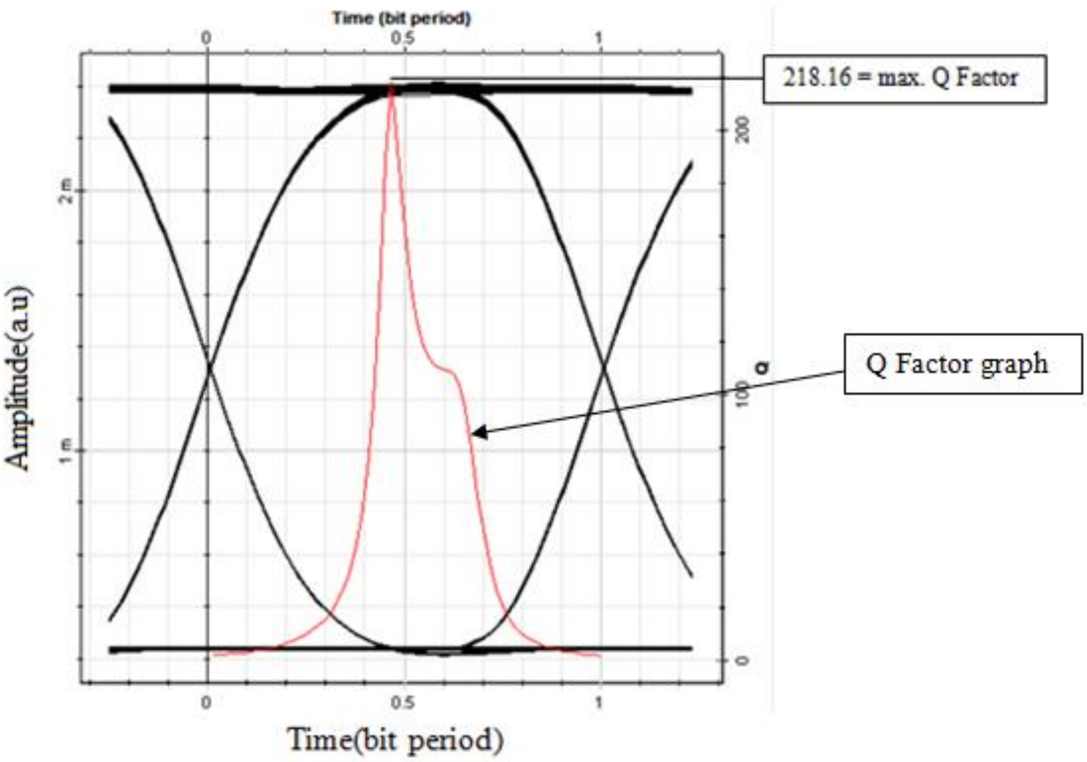

Figure 2. 6 Eye diagram illustrating max Q Factor

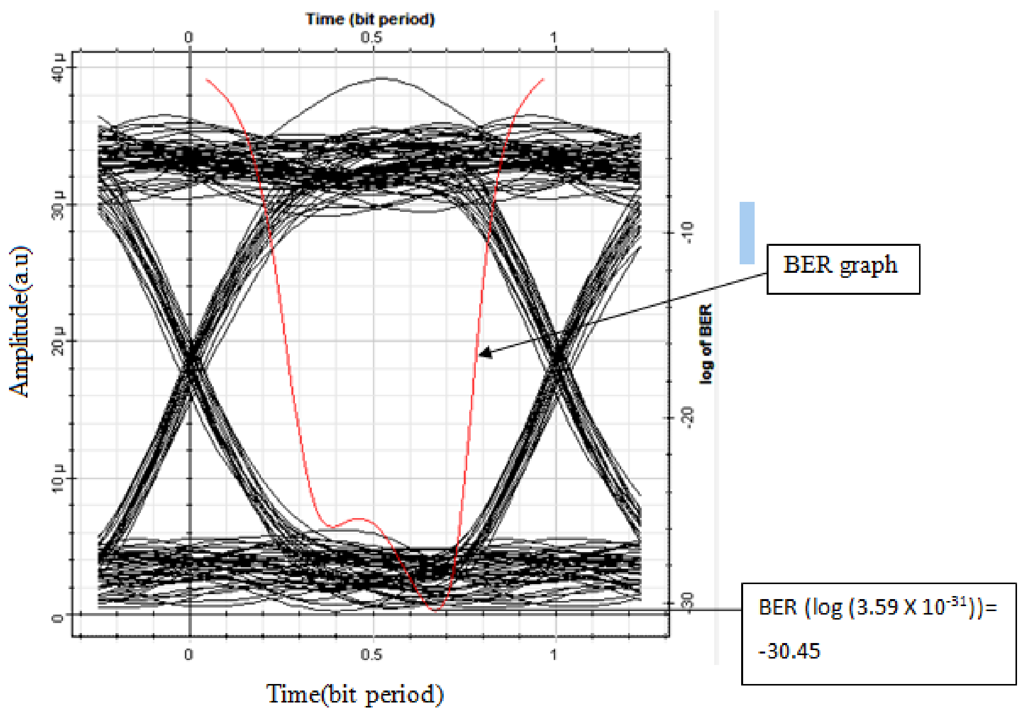

Figure 2. 7 Eye diagram illustrating Min BER

2.6 Modulation Schemes

We mostly use modulation scheme in communication so as to be able to utilize a small available spectrum with a squeezed large amount of data. That point is termed as spectral efficiency and measures how fast data propagates in an allocate bandwidth (MRS, 2016). However, it is also important to consider power efficient in the modulation scheme selection, but according to Elganimi (2013) power efficient is not only factor for modulation technique selection. There are number of modulation techniques available, In this study On-off keying Non Return to Zero (OOK-NRZ) were used for modulating data. Because it is the most frequently utilized modulation techniques in FSO communication systems relying on the specific necessities of the certain optical system such as system simplicity, bandwidth and power efficiency (MRS, 2016)(Sahota, 2017)(Dong & Aminian, 2014). Comparing with other modulation formats NRZ signal has the better compact spectrum, hence it is bandwidth efficient (Tejkal, Filka, Šporik, & Reichert, 2010). Furthermore, according to the research done by Mohammed et al. (2012) a significant performance was achieved on maintaining the received signal power and BER thresholds over NRZ modulation scheme with 1550nm as operating wavelength using APD photo detector. The NRZ and RZ data signal formats are illustrated in Fig. 2.5

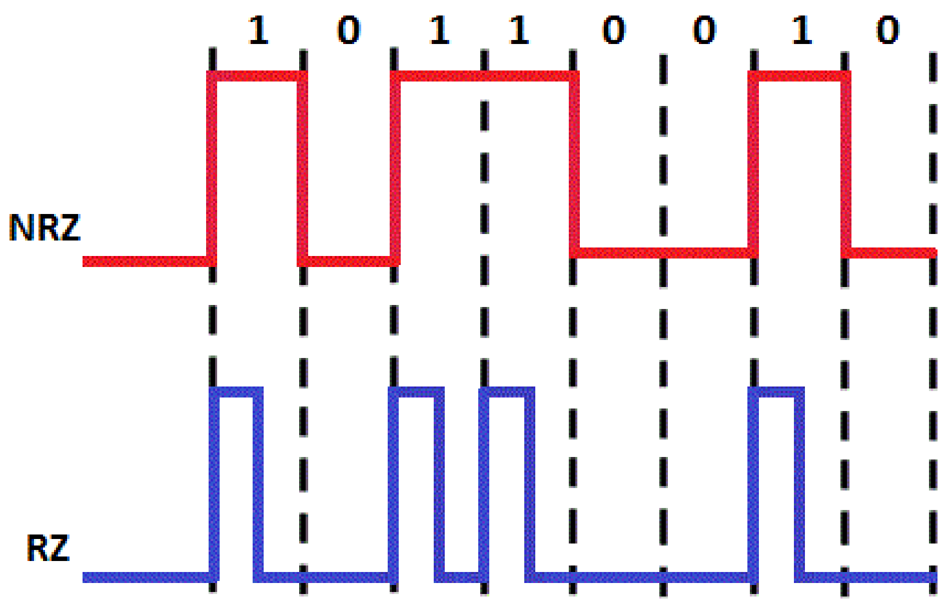

Figure 2. 8 NRZ and RZ data signal formats

Source (Norazimah, Aljunid, Al-khafaji, Fadhil, & Anuar, 2013)

2.7 Related Studies

The study done in University of the West of Scotland (UWS) Paisley campus during the summer 2017, for the purpose of evaluating FSO accessibility empirically and statistically depending on different weather conditions qualified in the West of Scotland. The empirical link tests was conducted for five days in five different sites at the campus area, and for statistical analysis the researcher straight focused on statistical historical weather data in Paisley (UK) (2016) to approximate weather attenuation margins in the town yearly. According to the study the researcher revealed that a very high FSO feasibility can be estimated in Paisley (UK) throughout the year, thus, this validates the area is appropriate for stable FSO transmission for range may be limited up to 100m regardless of weather volatility (Nilupulee et al., 2017). Thus arising the need to investigate on other places depending on weather conditions.

Analysis done by Rashid and Semakuwa (2014) on FSO Communication in two regions of Tanzania under rain effect, after designing the model of FSO system using opt-system version 7 to set up an FSO link by a range of 5 to 15 km and 3 to 5 km in Dar-es-Salaam and Dodoma respectively, the study revealed that the deployment of FSO communication is better compared to optical fiber since it can circumvent a number of challenges such as huge cost of trenching roads, impractical physical connection between transmitters and receivers and data insecurity. The results showed that 37dBm/km and 80dBm/km as an optical attenuated loss need be taken into thought in deployment designing FSO link in Dodoma and Dar Es Salaam respectively. While 30dBm of transmission power is required to maintain bit error rate (BER) of 1 and receiving power of -100dBm. The researchers left other atmospheric attenuation factors such as scintillation as it wasn't in their scope of the research.

The study done in Arusha – Tanzania on analyzing the FSO performance under rain effect. The analysis was done basing on statistical weather rainfall rate data for April and November from 2002 to 2012 as obtained from Tanzania Meteorological Agency (TMA), through simulation software opti - system version 7 the researchers observed that in order to attain low BER and maintain minimal power loss then transmission power is required to be 30dBm and above for 15km transmission distance (Rashid &

Semakuwa, 2014). The study also left other atmospheric attenuation factors such as scintillation as it wasn't in their scope of the research. Since the above studies were done to study the rain effect on FSO link in the targeted cities, therefore this study proposes the study of FSO link under scintillation effect in Dodoma.

Navidpour (2007) studied the BER routine of FSO communications with spatial diversity by using lognormal atmospheric turbulence fading channels, with assumption that both independent and correlated channels among transmitter/receiver apertures over FSO link. A BER of 10^{-7} is achieved. However a BER of only 10^{-5} is achieved if the receiver knows only the Channel State Information (CSI). The downside of this paper is that the received signal loss is severe if the correlation among multiple transmitters/receivers raises. The design therefore requires enough separation involving transmitters/receivers apertures and exacting co-alignment. Both circumstances are tricky to achieve practically.

Ijaz et al (2009) characterized the strength of turbulence as it affects the FSO link by creating the simulation chamber with 140 x 30 x 30 cm dimension. The main target was to evaluate the BER as it is affected during scintillation environment. Turbulence is simulated by blowing hot and cold air to the chamber. The cold air is set at about 20°C and hot air cover up a temperature range of 20°C to 80 °C. By means of air vents sequence, extra heat control is attained thus guarantee a steady temperature gradient between the transmitter and receiver. Through the experiment carried it was observed that if scintillation is not taken into consideration during FSO link design it would cause serious link performance impairment. From the experiment it was revealed that high BER caused by scintillation, the simulated turbulence lowered the link BER performance as of being error-free to about 10^{-4}. Furthermore there was a need to perform a study in open space instead of evaluating the BER in controlled environment.

Furthermore, an experimental study was done at Isfahan University of Technology(Iran), for the FSO network link of 220m distance connecting transmitter (TX) and receiver (RX), the results showed the refractive index affecting the transmitted beam of light was much affected by the time of the day and temperature are of important parameter, therefore FSO link performance depends on the time of the day (Nazari, Gholami, Vali, Sedghi, & Ghassemblooy, 2016).

According to the study conducted by Sidarta (2016) in Singapore about scintillation effect for rain and non-rain period from the variation of air refractive index, FSO link were affected at higher rate during midday and peak-to-peak scintillation resulted to be lower in midday compared to morning and evening. 6 dB transmission power of peak-to-peak scintillation could be observed during rain period and -34dBm transmission power during non-rain period. Thus, indicating the scintillation effect varies according to environment therefore creating the demand for us to investigate on this scintillation effect on how it will affect FSO communication in our surroundings.

A survey done by Khalighi et al. (2014) has detailed a variety of issues in FSO link in accordance to communication theory prospective. Different nature of losses encountered in terrestrial FSO link was presented, facts on FSO transceiver, channel coding, modulation and ways to alleviate fading effects of atmospheric turbulence. However, most of their study is concentrated around terrestrial FSO communication. From the survey it was observed that scintillation index C_n^2 is elevation dependent and is larger at lower altitudes due to the additional significant heat transfer between the surface and air and does not depend on distance lather varies mostly during daytime and at a given location. Thus, creating the need for the researches to be done on different locations to investigate the scintillation variations and effects on FSO link.

Also Bloom et al. (2003) pointed out that the performance of a FSO link is primarily reliant upon the meteorological and the physical distinctiveness of its installation site located. The article discusses main factors affecting FSO performance include atmospheric attenuation, window attenuation, scintillation, alignment or point motion, solar interference, and line-of-sight barriers. Furthermore, Bloom et al. (2003) described that scintillation can alter by more than an order of degree through the course of a day, being the worst, or most scintillated, during midday when the heat is the highest. The article suggested that more than enough link margin need to be taken into consideration to compensate for scintillation.

Study done by Mandeep and Dao (2012) comparing the cumulative distribution of six tropospheric scintillation models namely Karasawa, ITU-R, Van de Kamp, OTUNG and Ortgies (Ortgies-N and Ortgies- T) with the measured scintillation data for the purpose of determining which model suits better for prediction. These models are based on data collection from countries like Germany, United Kingdom, Japan, Finland, US. The best model for scintillation fades is the Ortgies N. and Karasawa being the best model for scintillation enhancement prediction. However, The authors also recommended that, these models could not be practiced for tropical countries with different climate patterns like Singapore, Malaysia, Thailand, Indonesia and etc. compared to the four seasons' countries.

CHAPTER THREE

METHODS AND MATERIALS

3.1 Introduction

This study present the methods and materials used to achieve the objectives the first one being to simulate the FSO transmission link under two mathematical models Hufnagel Vallay (HV) Day and Submarine Laser Communication (SLC II) Day using the calculated scintillation attenuation in Arusha and Mwanza regions. Second, to compare the two mathematical models HV day and SLC II day and the last is to propose the feasibility of free space optical communication in Mwanza and Arusha regions. Furthermore, it presents technique used for analysis that were used for the purpose of complying with the research questions. Also, the hardware and software tools, simulation environment used.

3.2 Research Design

Research design is a plan or blueprint that guides the process of data collection and analysis. The study used quantitative data for analysis basing on case study of Arusha and Mwanza regions. The research investigated the feasibility of Free Space Optic communication under the scintillation effect in Arusha and Mwanza regions.

3.3 Data Collection

Quantitative data was used in this study, the data involved humidity, temperature, wind speed and altitude. The data was secondary data from Tanzania Meteorological Agency (TMA) for 48 months as from 2015 to 2018 as shown in APPENDIX JJJ. Because the target was to capture the general C_n^2 trend across two regions (Arusha and Mwanza), it was necessary to collect an extensive quantity of data that spans this array.

3.4 Area of Study

The study mainly focused on two regions Arusha and Mwanza as the study area. This is due to the fact that the two regions have developed infrastructure (i.e. buildings and roads) which makes tunneling and laying cables very complex if not impracticable in some suburbs. According to TCRA (2010), Arusha and Mwanza regions are the next regions after Dar-es-Salaam for internet subscribers. Mwanza is the second largest city in Tanzania with population of 706,543 people, and population of 416,442 people makes Arusha be the third largest city in Tanzania (Sousa, 2017). In his thesis titled "Analysing the Effect of Visibility and Scintillation on Free Space Optical Communication: A CaseStudy of Dar es Salaam and Dodoma Regions" Teck Kinte Chiyaba, did the feasibility of FSO in Dar es Salaam region, the reason which made the author of this thesis to not consider Dar es Salaam and Dodoma as the study area.

3.5 Data Analysis

The following section expresses how each of the specific objectives of this study was analyzed;

Specific Objective 1: To simulate the FSO transmission link under two mathematical models Hufnagel Vallay (HV) Day and Submarine Laser Communication (SLC II) Day using the calculated scintillation attenuation in Arusha and Mwanza regions.

Equation 2.6 was used to achieve this objective by calculating the attenuation in decibel (dB) then the calculated data were fed into the simulation software.

Specific Objective 2: To compare the two mathematical models HV day and SLC II day. Quality factor (Q factor), Bit error rate (BER) and Signal to Noise Ratio (SNR) were used to perform comparison analysis under two models.

Specific Objective 3: To propose the feasibility of free space optical (FSO) communication in Mwanza and Arusha regions. Bit error rate (BER) and Q-factor values were used to draw conclusion on feasibility analysis of FSO communication in two regions (Mwanza and Arusha).

3.6 Simulation Setups and Components

The simulation setup depicted in figure 3.1 was performed in OptiSystem version 16 with the following components included in the simulation setup. The setup was run to about 384 times under different ranges, months, models and regions to obtain BER and Q factors. Depending on the modeling equations analysis and the listed set of the operating parameters are shown in Table 3.1.

3.6.1 Components

- **Optical Transmitter** - Converts data from digital bit sequence to optical stream.

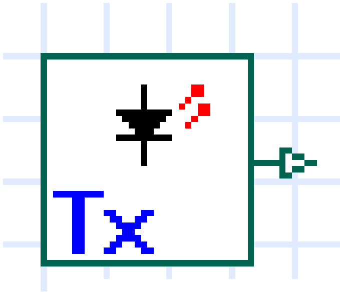

Figure 3. 1 Optical Transmitter

Source (OptiSystem)

- **FSO channel** – represents the atmospheric channel where attenuation is taking effect.

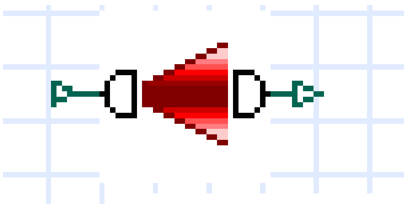

Figure 3. 2 FSO channel

- **Optical Receiver -** detects the transmitted optical power and extract from it the signal (either digital or analog) transmitted.

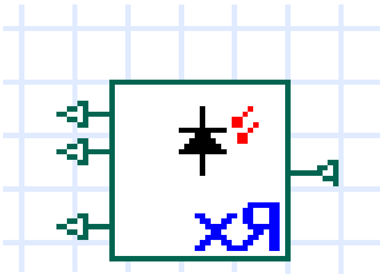

Figure 3. 3 Optical Receiver

Source (OptiSystem)

- **Eye Diagram Analyzer –** presents the eye diagram along with the calculated BER and Q factor of the simulated link.

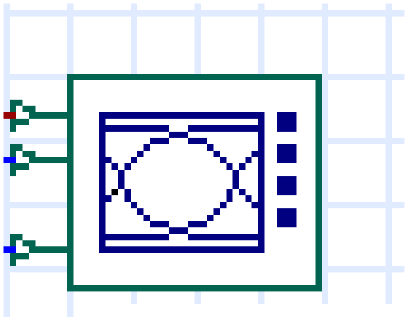

Figure 3. 4 Eye Diagram Analyzer

Source (OptiSystem)

- **Optical Power Meter** - This measures either power transmitted or power received in FSO system.

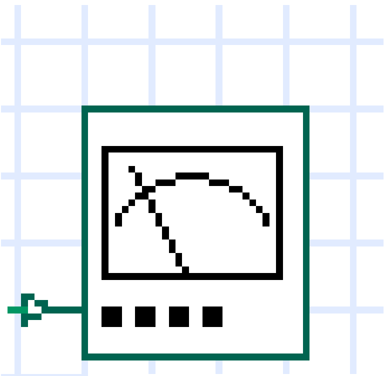

Figure 3. 5 Optical Power Meter

Source (OptiSystem)

3.6.2 Parameters

Table 3. 1 Values and units of the parameters

Parameters	Value	Unit
Operating optical signal wavelength, λ	1550	nm
Link range, L	$2 \leq L \leq 8$	km
Receiver aperture diameter.	20	cm
Transmitter aperture diameter.	5	cm
Beam divergence	2	mrad
Optical power, pt	20	dBm
Receiver Type	APD	
Cut off frequency	7.5	GHz
Modulation Scheme	NRZ	
Transmission Bit Rate	1.25	GBits/s

3.6.2.1 Parameters Selection Justification

i. Operating optical signal wavelength of 1550nm, the appropriate wavelength selection has major influence on the attenuation coefficient, which leads to extended transmission in free space. According the study done by Ali (2014) , it was shown that the performance of 1550nm is more suitable for FSO communication system. Moreover, 1550nm is more desirable due to its eye safety and third window compatibility (Rashidi & Semakuwa, 2014).

ii. Optical power of 20dBm, by considering the FSO equipment available in a market, most of their default optical transmitting power is set to 20dBm.

iii. Receiver Type/Photo detector, the main function of the photo detector is to convert the transmitted optical signal into electronic signal. The selected APD type is because of its applicability in most of the high speed long-haul systems, however APD proves to have lower SNR compared to PIN (Dong & Aminian, 2014). Moreover, APD offers better Q factor compared to PIN receiver (Shafi & Gokul, 2016).

i. Modulation Scheme – NRZ, Its low power consumption and system simplicity makes it more preferable, it offers the finest attainable link power budget margin through least power dissipation (Wei, Ingham, Cunningham, Penty, & White, 2012). Additionally, according to the study done by

Mohammed et al. (2012) a significant performance was achieved on retaining the received signal power and BER thresholds under NRZ with 1550nm using APD receiver.

ii. Transmission Bit Rate,1.25 Gbps was opted because most of the FSO systems in a market are running at 1.25 Gbps connecting two mounted points (Muhammad Ijaz, 2013).

iii. Beam divergence of 2mrad, for increasing level of protection from unauthorized link access, as the narrow beam increases more secure is the link.

3.6.3 Simulation Setup Interface

Figure 3.6 represents the simulation setup where by only two parameters (attenuation coefficient, range) were altered while others remained constant.

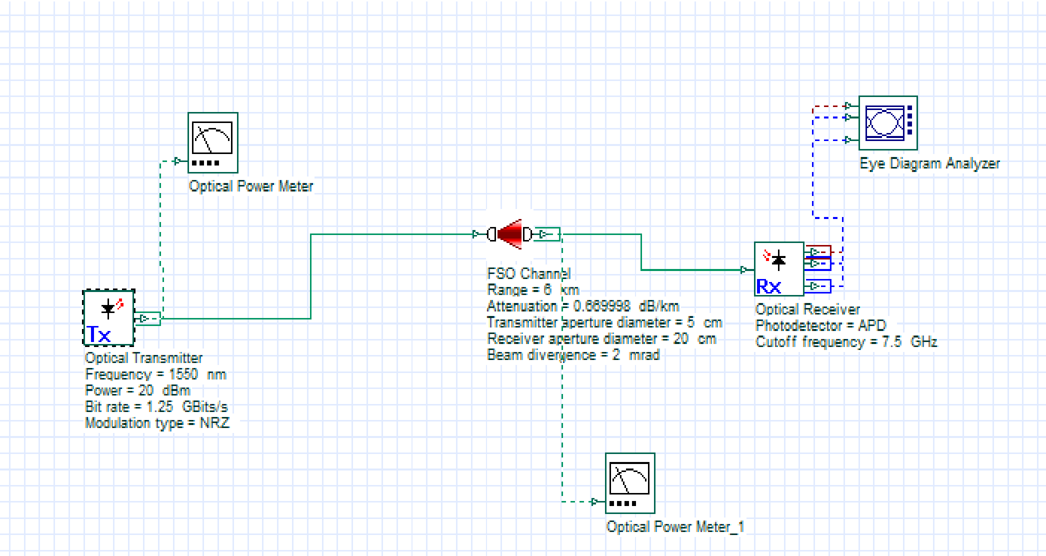

Figure 3. 6 The detailed structure of the FSO system via OptiSystem interface

CHAPTER FOUR
PRESENTATION OF FINDINGS

4.1 Introduction

This chapter presents the findings of the study patterning to the research questions. In this chapter, scintillation has been modeled using Submarine Laser communication (SLC II) Day and Hufnagel Valley (HV) Day and analyzed using OptiSystem version 16 software under one modulation scheme Non return to zero (NRZ).

4.2 Scintillation Attenuation

Using monthly average data in APPENDIX A and APPENDIX B, objective no. 1 which involves scintillation attenuation calculation in Arusha and Mwanza regions using mathematical model. Through application of equation 2.6 with different ranges from 2km to 8km under two models (Submarine Laser Communication(SLC II) Day and Hufnagel Valley (HV) Day, scintillation attenuation in dB was obtained and presented in table 4.1, 4.2, 4.3, 4.4.

Table 4. 1 Arusha Monthly Average Attenuation (dB) 2015 – 2018 under Submarine Laser Communication (SLC II) Day Model

	Attenuation(dB)			
Month	**2km**	**4km**	**6km**	**8km**
January	1.4705	2.7759	4.0255	5.2402
February	1.4530	2.7430	3.9778	5.1780
March	1.4441	2.7261	3.9533	5.1462
April	1.3978	2.6387	3.8265	4.9811
May	1.3422	2.5338	3.6744	4.7832
June	1.3270	2.5051	3.6328	4.7289
July	1.3158	2.4839	3.6020	4.6889
August	1.3215	2.4947	3.6178	4.7094
September	1.3317	2.5139	3.6456	4.7456
October	1.3600	2.5673	3.7231	4.8465
November	1.4046	2.6515	3.8451	5.0053
December	1.4513	2.7396	3.9729	5.1717

Table 4. 2 Arusha Monthly Average Attenuation (dB) 2015 - 2018 under Hufnagel Valley Day Model

	Attenuation(dB)			
Month	**2km**	**4km**	**6km**	**8km**
January	1.4685	2.7721	4.0200	5.2330
February	1.4510	2.7391	3.9722	5.1708
March	1.4421	2.7222	3.9477	5.1389
April	1.3957	2.6346	3.8207	4.9735
May	1.3400	2.5296	3.6684	4.7753
June	1.3248	2.5008	3.6266	4.7210
July	1.3135	2.4796	3.5958	4.6808
August	1.3193	2.4905	3.6116	4.7014
September	1.3295	2.5097	3.6394	4.7376
October	1.3578	2.5632	3.7171	4.8387
November	1.4025	2.6475	3.8393	4.9978
December	1.4492	2.7357	3.9673	5.1644

Table 4. 3 Mwanza Monthly Average Attenuation (dB) 2015 - 2018 under Submarine Laser Communication (SLC II) Day Model

Month	Attenuation(dB)			
	2km	4km	6km	8km
January	1.4688	2.7727	4.0209	5.2342
February	1.4668	2.7690	4.0154	5.2271
March	1.4619	2.7597	4.0020	5.2096
April	1.4804	2.7947	4.0527	5.2756
May	1.4618	2.7596	4.0018	5.2094
June	1.4559	2.7484	3.9856	5.1882
July	1.4356	2.7100	3.9299	5.1158
August	1.4337	2.7065	3.9249	5.1092
September	1.4486	2.7346	3.9655	5.1621
October	1.4568	2.7501	3.9881	5.1915
November	1.4615	2.7590	4.0010	5.2083
December	1.4591	2.7543	3.9943	5.1995

Table 4. 4 Mwanza Monthly Average Attenuation (dB) 2015 - 2018 under Hufnagel Valley Day Model

Month	Attenuation(dB)			
	2km	4km	6km	8km
January	1.4647	2.7650	4.0097	5.2197
February	1.4627	2.7612	4.0042	5.2125
March	1.4578	2.7519	3.9907	5.1949
April	1.4764	2.7870	4.0416	5.2612
May	1.4577	2.7518	3.9906	5.1947
June	1.4518	2.7406	3.9743	5.1735
July	1.4314	2.7021	3.9185	5.1009
August	1.4295	2.6986	3.9134	5.0942
September	1.4444	2.7267	3.9542	5.1474
October	1.4527	2.7423	3.9768	5.1768
November	1.4574	2.7512	3.9897	5.1936
December	1.4549	2.7466	3.9830	5.1848

4.2.1 Scintillation Attenuation in dB/Km

To achieve objective number one, Scintillation attenuation in dB values obtained in Table 4.1, 4.2, 4.3, 4.4 were used to calculate attenuation in dB/km presented in Table 4.5, 4.6, 4.7, 4.8, so as to input the dB/km values into the simulation software under FSO channel component which requires values to be in dB/km and perform the simulation for two regions under different models.

Table 4. 5 Arusha Monthly Average Attenuation (dB/Km) 2015 – 2018 under Submarine Laser Communication (SLC II) Day Model

	Attenuation(dB/Km)			
Month	**2km**	**4km**	**6km**	**8km**
January	0.73524283	0.69397682	0.67091993	0.65502690
February	0.72651935	0.68574295	0.66295963	0.64725516
March	0.72205779	0.68153180	0.65888839	0.64328036
April	0.69889057	0.65966485	0.63774796	0.62264071
May	0.67111841	0.63345143	0.61240545	0.59789853
June	0.66350805	0.62626821	0.60546089	0.59111847
July	0.65788716	0.62096279	0.60033174	0.58611083
August	0.66077234	0.62368604	0.60296451	0.58868123
September	0.66584449	0.62847351	0.60759292	0.59320000
October	0.68000009	0.64183462	0.62051012	0.60581121
November	0.70228781	0.66287143	0.64084799	0.62566731
December	0.72562973	0.68490326	0.66214784	0.64646260

Table 4. 6 Arusha Monthly Average Attenuation (dB/Km) 2015 - 2018 under Hufnagel Valley Day Model

	Attenuation(dB/Km)			
Month	**2km**	**4km**	**6km**	**8km**
January	0.73423232	0.69302302	0.66999782	0.65412663
February	0.72549668	0.68477768	0.66202642	0.64634406
March	0.72102860	0.68056038	0.65794924	0.64236346
April	0.69782735	0.65866131	0.63677775	0.62169349
May	0.67001107	0.63240624	0.61139499	0.59691201
June	0.66238790	0.62521093	0.60443874	0.59012053
July	0.65675751	0.61989654	0.59930092	0.58510442
August	0.65964754	0.62262437	0.60193811	0.58767914
September	0.66472818	0.62741986	0.60657428	0.59220549
October	0.67890710	0.64080297	0.61951274	0.60483746
November	0.70122982	0.66187281	0.63988255	0.62472474
December	0.72460580	0.68393680	0.66121348	0.64555038

Table 4. 7 Mwanza Monthly Average Attenuation (dB/Km) 2015 - 2018 under Submarine Laser Communication (SLC II) Day Model

	Attenuation(dB/Km)			
Month	**2km**	**4km**	**6km**	**8km**
January	0.73440412	0.69318518	0.67015460	0.65427969
February	0.73340095	0.69223832	0.66923919	0.65338596
March	0.73094524	0.68992044	0.66699832	0.65119818
April	0.74021268	0.69866773	0.67545499	0.65945453
May	0.73091339	0.68989037	0.66696925	0.65116980
June	0.72794738	0.68709083	0.66426272	0.64852739
July	0.71778632	0.67750007	0.65499061	0.63947491
August	0.71685805	0.67662390	0.65414355	0.63864792
September	0.72428881	0.68363760	0.66092422	0.64526797
October	0.72840503	0.68752279	0.66468033	0.64893510
November	0.73076555	0.68975083	0.66683435	0.65103809
December	0.72953241	0.68858690	0.66570909	0.64993949

Table 4. 8 Mwanza Monthly Average Attenuation (dB/Km) 2015 - 2018 under Hufnagel Valley Day Model

	Attenuation(dB/Km)			
Month	**2km**	**4km**	**6km**	**8km**
January	0.732357645	0.691253569	0.668287157	0.652456488
February	0.731351694	0.690304078	0.667369212	0.651560287
March	0.728887414	0.687978107	0.66512052	0.649364863
April	0.738182502	0.696751501	0.673602425	0.657645845
May	0.728856882	0.687949289	0.665092659	0.649337662
June	0.725882556	0.685141898	0.662378542	0.646687838
July	0.71569217	0.675523455	0.653079665	0.637609236
August	0.714760457	0.674644035	0.652229463	0.636779175
September	0.722213487	0.681678758	0.659030463	0.64341907
October	0.726341666	0.68557524	0.662797487	0.647096859
November	0.728709112	0.687809812	0.664957816	0.649206014
December	0.727472464	0.686642572	0.663829357	0.648104286

4.3 Calculated BER and Q factor from Simulation

Objective no. 2 : To simulate the FSO transmission link under two mathematical models HV Day and SLC II Day, was attained by simulating the FSO link under different ranges 2km, 4km, 6km and 8km. Through alternating range and the corresponding attenuations obtained from Table 4.5, 4.6, 4.7 and 4.8 under constant parameters from Table 3.1, the Q factor and BER were recorded from the eye diagram analyzer. Table 4.5 and 4.6 presents the Q factor for two models (SLC II, HV) for Arusha and Mwanza regions respectively, Table 4.7 and 4.8 presents the BER for two models (SLC II, HV) for Arusha and Mwanza regions respectively.

Table 4. 9 Calculated Q factor for SLC II day and HV day models in Arusha Region

Q factor- ARUSHA								
	Submarine Laser Communication(SLC II) Day Model				Hufnagel Valley (HV) Day Model			
Month	**2km**	**4km**	**6km**	**8km**	**2km**	**4km**	**6km**	**8km**
January	92.37	27.41	10.85	5.04	92.40	27.72	10.86	5.05
February	92.60	27.87	11.01	5.11	92.63	27.89	10.97	5.12
March	92.53	27.96	10.01	5.14	92.75	27.89	10.02	5.15
April	93.35	28.42	11.27	5.32	93.38	28.44	11.31	5.33
May	94.11	28.97	11.65	5.54	94.14	29.00	11.67	5.55
June	94.32	29.13	11.75	5.61	94.35	29.15	11.77	5.62
July	94.47	29.24	11.83	5.65	94.51	29.26	11.84	5.66
August	94.40	28.18	11.79	5.63	94.43	29.21	11.80	5.64
September	94.26	29.08	11.72	5.59	94.29	29.10	11.74	5.60
October	93.87	28.80	11.54	5.47	93.90	28.82	11.55	5.48
November	93.26	28.35	11.26	5.30	93.29	28.37	11.27	5.30
December	92.63	27.89	10.97	5.12	92.66	27.91	10.98	5.12

Table 4. 10 Calculated Q factor for SLC II day and HV day models in Mwanza Region

Q factor – MWANZA								
	Submarine Laser Communication(SLC II) Day Model				Hufnagel Valley (HV) Day Model			
Month	**2km**	**4km**	**6km**	**8km**	**2km**	**4km**	**6km**	**8km**
January	92.39	27.72	10.86	5.05	92.45	28.72	10.88	5.07
February	92.42	27.74	10.87	5.06	92.47	27.78	10.90	5.07
March	92.48	27.79	10.90	5.08	92.54	27.83	10.93	5.09
April	92.23	27.61	10.79	5.01	92.29	27.65	10.81	5.02
May	92.49	27.79	10.90	5.08	92.54	27.83	10.93	5.09
June	92.57	27.85	10.94	5.10	92.62	27.87	10.96	5.11
July	92.84	28.05	11.06	5.18	92.90	28.09	11.09	5.19
August	92.87	28.06	11.07	5.18	92.92	28.11	11.10	5.20
September	92.66	27.92	10.98	5.13	92.72	27.96	11.01	5.14
October	92.55	27.84	10.93	5.10	92.61	27.88	10.96	5.11
November	92.49	27.79	10.90	5.08	92.55	27.83	10.93	5.09
December	92.52	27.82	10.92	5.09	92.58	28.86	10.94	5.10

Table 4. 11 Calculated BER for SLC II day and HV day models in Arusha Region

BER- ARUSHA								
	Submarine Laser Communication(SLC II) Day Model				Hufnagel Valley (HV) Day Model			
Month	**2km**	**4km**	**6km**	**8km**	**2km**	**4km**	**6km**	**8km**
Jan	0	3.08E-169	1.01E-27	2.27E-07	0	1.78E-169	8.81E-28	2.19E-07
Feb	0	2.71E-171	1.71E-28	1.61E-07	0	1.55E-171	2.72E-28	1.55E-07
Mar	0	2.37E-172	1.71E-28	1.35E-07	0	1.35E-172	1.48E-28	1.29E-07
Apr	0	5.98E-178	6.65E-30	5.15E-08	0	3.28E-178	5.71E-30	4.92E-08
May	0	7.07E-185	1.10E-31	1.49E-08	0	3.70E-185	9.28E-32	1.41E-08
June	0	8.11E-187	3.42E-32	1.04E-08	0	4.19E-187	2.88E-32	9.82E-09
July	0	2.89E-188	1.43E-32	7.90E-09	0	1.47E-188	1.20E-32	7.48E-09
Aug	0	1.61E-187	2.24E-32	9.09E-09	0	8.27E-188	1.88E-32	8.61E-09
Sept	0	3.21E-186	4.91E-32	1.16E-09	0	1.67E-186	4.13E-32	1.10E-08
Oct	0	1.23E-182	4.19E-31	2.25E-08	0	6.55E-183	3.56E-31	2.14E-08
Nov	0	4.05E-177	1.08E-29	5.95E-08	0	2.24E-177	9.29E-30	5.68E-08
Dec	0	1.67E-171	2.77E-28	1.56E-07	0	9.55E-172	2.41E-28	1.49E-07

Table 4. 12 Calculated BER for SLC II day and HV day models in Mwanza Region

BER – MWANZA								
	Submarine Laser Communication(SLC II) Day Model				Hufnagel Valley (HV) Day Model			
Month	**2km**	**4km**	**6km**	**8km**	**2km**	**4km**	**6km**	**8km**
Jan	0	1.96E-169	9.01E-28	2.20E-07	0	1.19E-181	6.86E-28	2.03E-07
Feb	0	1.14E-169	7.88E-28	2.12E-07	0	3.75E-170	5.99E-28	1.95E-07
Mar	0	3.01E-170	5.68E-28	1.92E-07	0	9.85E-171	4.31E-28	1.77E-07
Apr	0	4.45E-168	1.94E-27	2.76E-07	0	1.50E-168	1.48E-27	2.55E-07
May	0	2.96E-170	5.65E-28	1.92E-07	0	9.69E-171	4.29E-28	1.77E-07
June	0	5.91E-171	3.79E-28	1.71E-07	0	2.83E-171	2.87E-28	1.57E-07
July	0	2.26E-173	9.49E-29	1.13E-07	0	7.12E-174	7.10E-29	1.04E-07
Aug	0	1.36E-173	8.34E-29	1.09E-07	0	4.25E-174	6.24E-29	1.00E-07
Sept	0	8.03E-172	2.31E-28	1.47E-07	0	2.56E-172	1.74E-28	1.36E-07
Oct	0	7.58E-171	4.03E-28	1.73E-07	0	2.46E-171	3.05E-28	1.60E-07
Nov	0	2.70E-170	5.54E-28	1.93E-07	0	8.94E-171	4.20E-28	1.76E-07
Dec	0	1.40E-170	4.70E-28	1.82E-07	0	4.56E-171	3.56E-28	1.67E-07

4.4 Scintillation Models Comparison

Model comparisons were carried out to determine the best scintillation analyst for a given set of optical parameters. The Q factor, atmospheric attenuation, BER values were used to plot the graph for maximum Q factor versus link range (2,4,6,8) km in Fig 4.1 and maximum Q factor versus atmospheric attenuation in Fig 4.2. Thereafter the plotted graphs showed the best model as explained in next chapter.

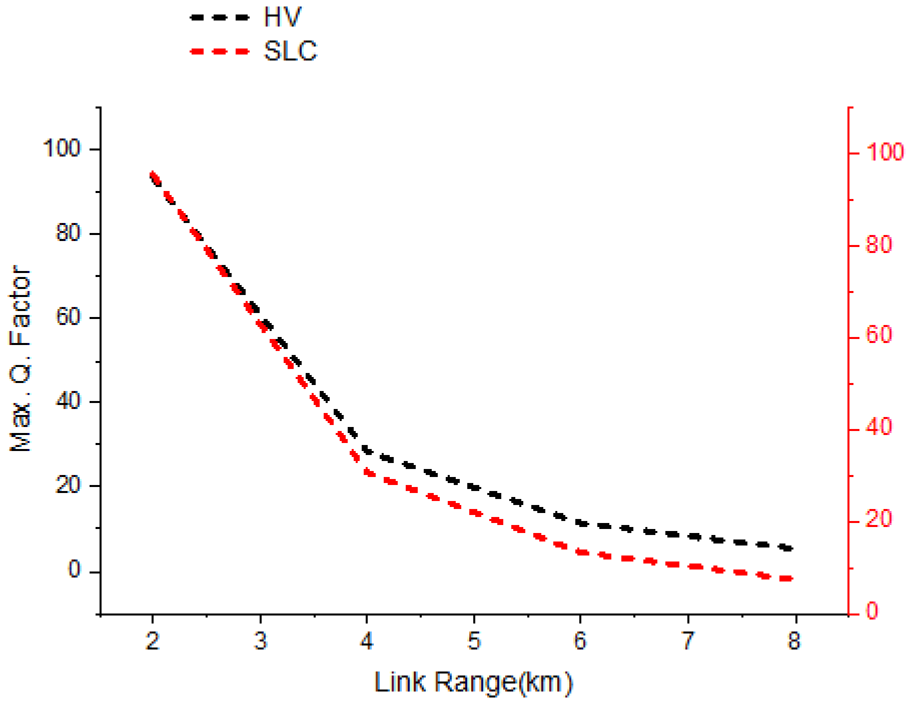

Figure 4. 1 Max. Q factor vs Link Range (2-8) Km

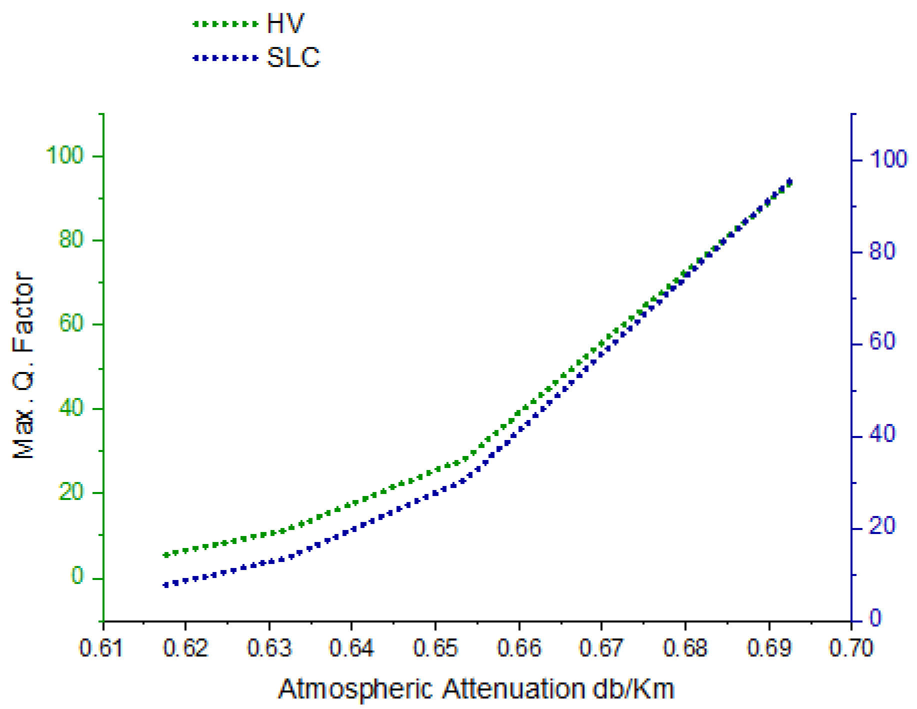

Figure 4. 2 Max. Q factor vs atmospheric attenuation (dB/Km)

Furthermore, by applying equation 2.7, Signal –to-noise ratio (SNR) values were calculated from the scintillation index and presented in Table 4.9. Thereafter, Log BER versus SNR for two models (SLC II, HV) under range of 2km, 4km, 6km and 8km curve has been demonstrated in Fig 4.3. Logarithm was applied to BER so as to respond to skewness towards large SNR values. Also the plotted graph Fig 4.3 were used in chapter 5 to draw modulation scheme comparison.

Table 4. 13: Average SNR for SLC II day and HV day under 2-8km

Range(Km)	**SNR**	
	SLC II DAY	**HV DAY**
2	0.00	0.00
4	1701.14	1698.77
6	278.37	278.12
8	85.52	85.39

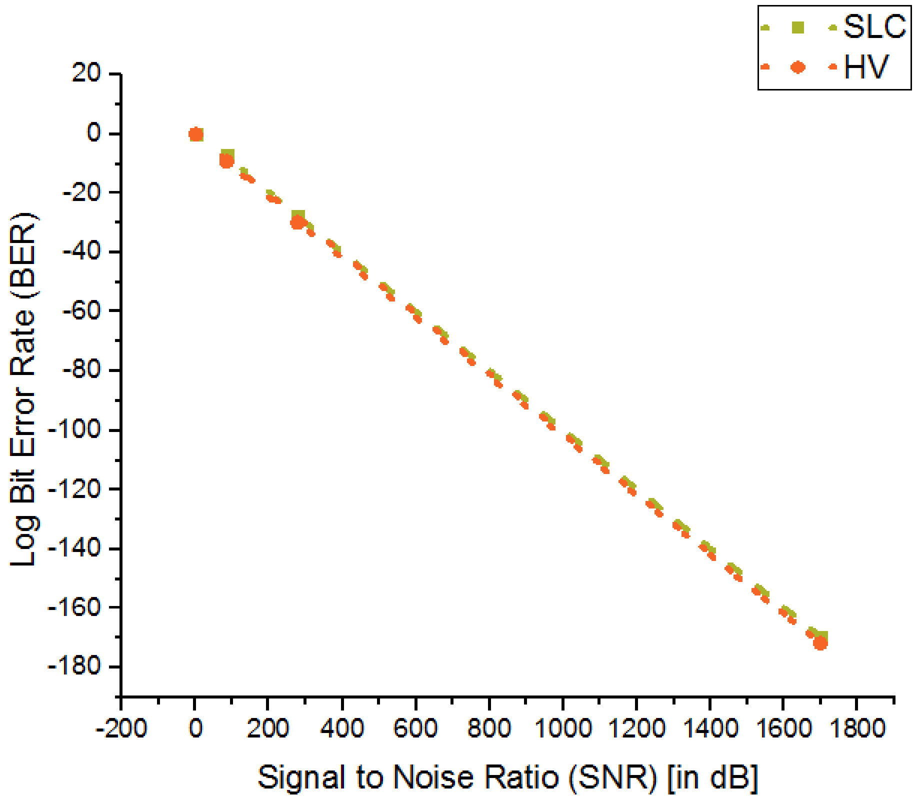

Figure 4. 3 LogBER vs SNR for different models (SLC II , HV) for (2,4,6,8)km

4.5 Monthly FSO Transmission.

The region dependence of scintillation is generally the meteorological dependence (Vasseur, H., 1999)(Mandeep & Dao, 2012). The scintillation data were taken from January 2015 till December 2018 which totals up to a 48 month period from TMA. These meteorological data were averaged over a period in the series of a month so the short-term scintillation variations could not be predicted with daily weather fluctuations. Fig 4.4 and 4.5 presents the worst months for FSO transmission for both regions Arusha and Mwanza from data in APPENDIX K.

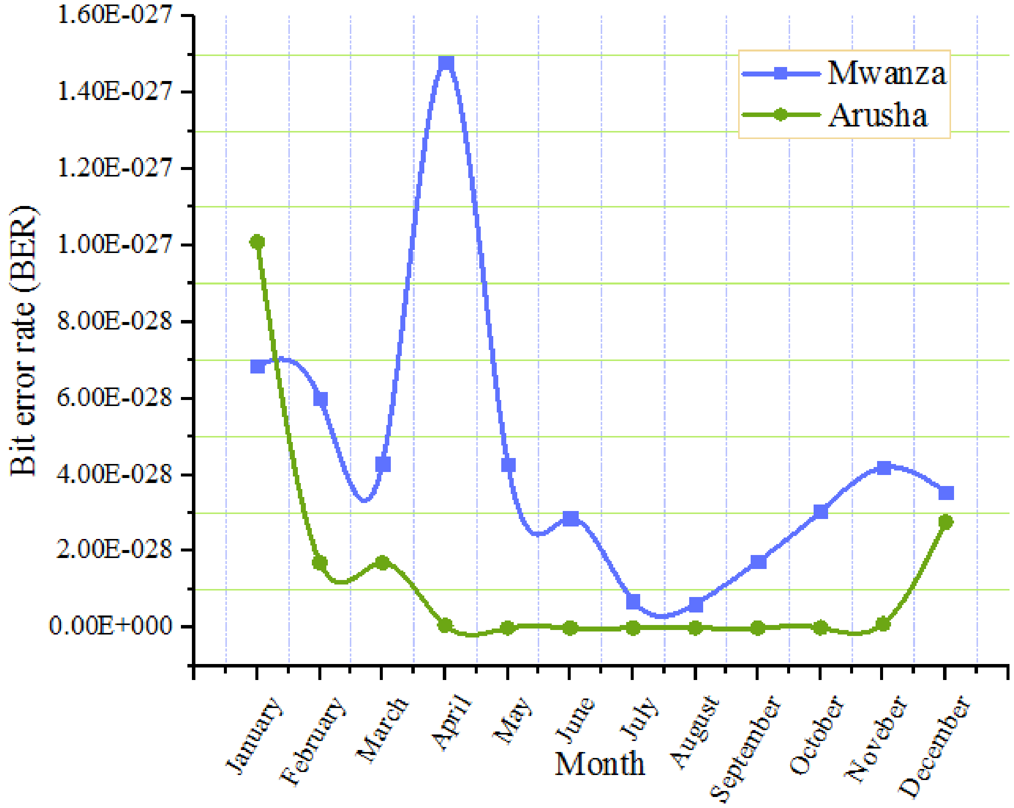

Figure 4. 4 BER vs Months for Arusha and Mwanza regions

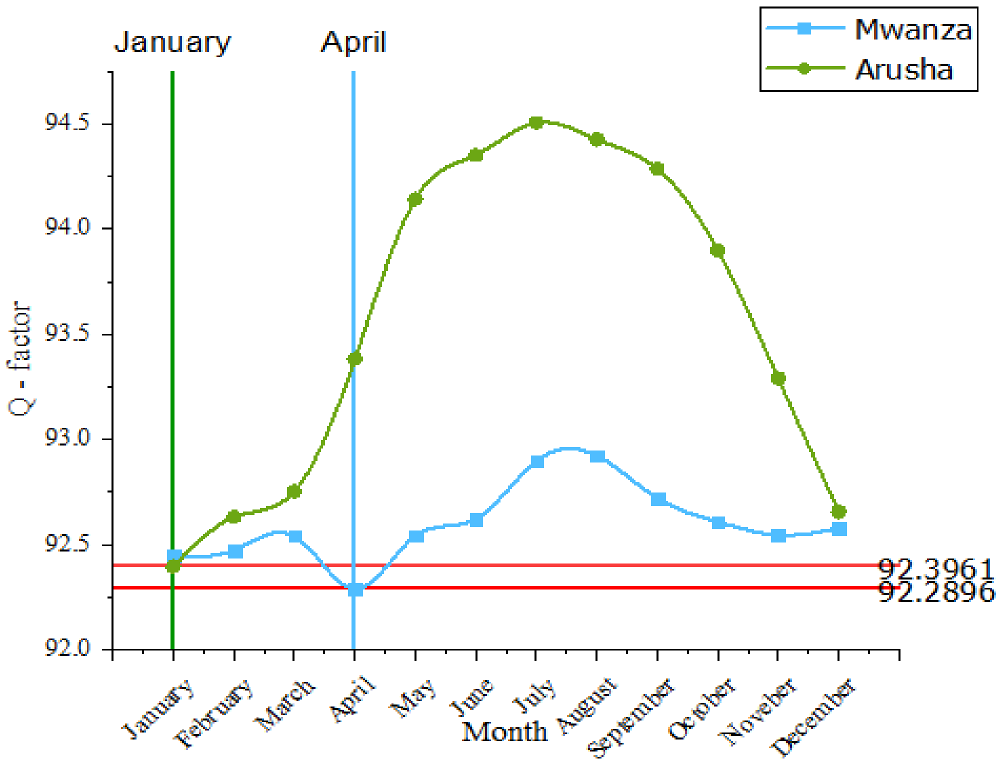

Figure 4. 5 Q factor vs Months for Arusha and Mwanza regions

4.6 FSO Feasibility Analysis

The findings of the analysis can present extra knowledge on the feasibility of FSO deployment under tropical weather condition mostly for a long range link (Zabidi et al., 2010). Considering the BER threshold of 10^{-6} for the reliable link in telecommunication standard (Navidpour et al., 2007), FSO feasibility can be analyzed. Therefore, using the calculated BER from Table 4.7 and 4.8 for SLC II day and HV day models, the graph representing the BER versus range was plotted in Fig 4.6, and the feasibility analysis was discussed in chapter 5.

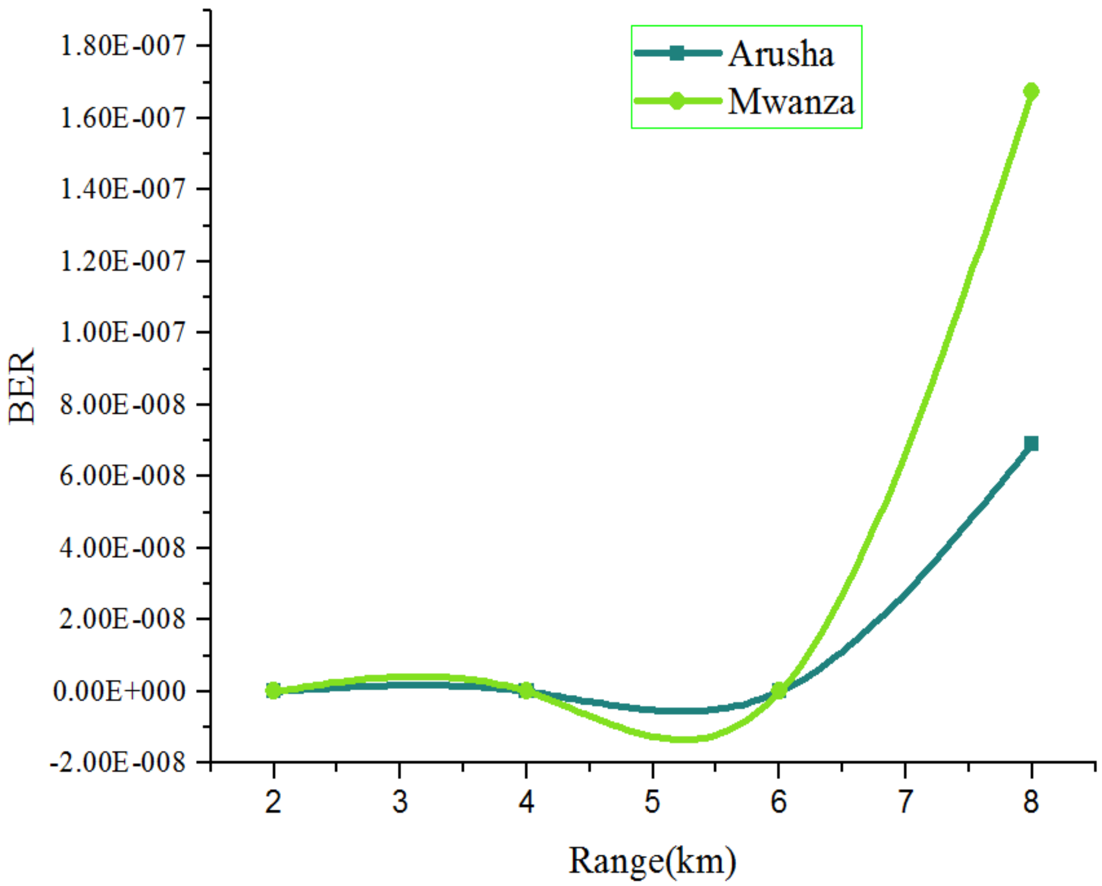

Figure 4. 6 BER vs Range (km) for Arusha and Mwanza regions

4.7 Eye Diagram Analyzer

In telecommunication applications eye diagram is considered a principally useful tool for received signal quality measurement at the receiver, the better eye-opening the less noise to the received signal (Dorrer et al., 2005). The system performances can be evaluated and analyzed by using eye diagram analyzer. Fig 4.7 – 4.22 shows the eye diagram for the both Arusha and Mwanza regions under different models and ranges with the corresponding average BER values.

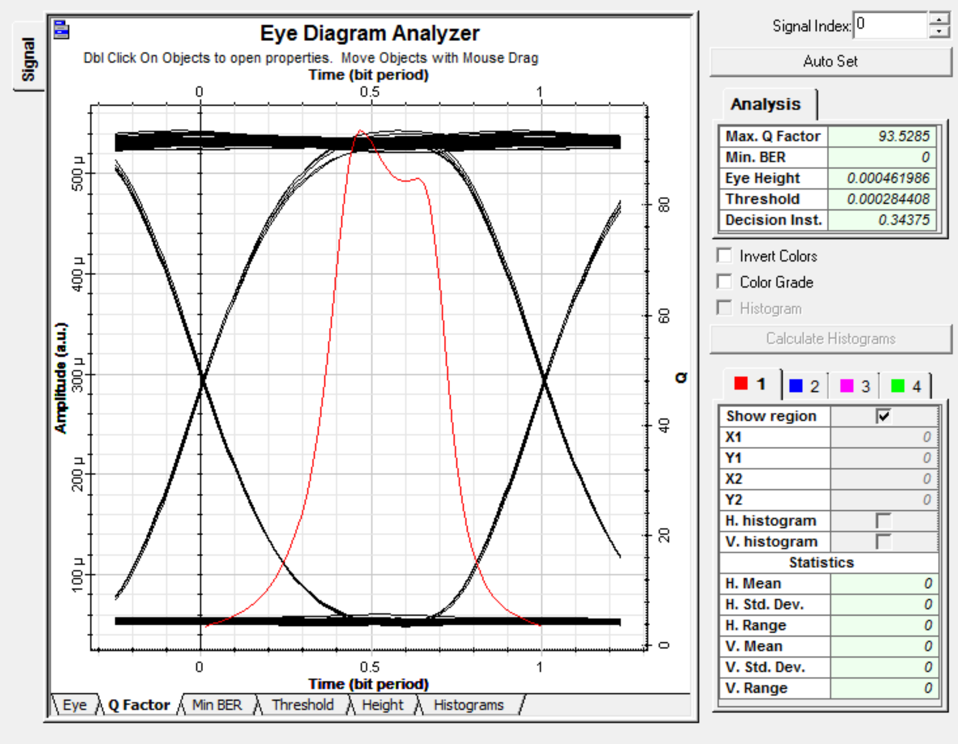

Figure 4. 7 Eye diagram for Arusha Range in 2km, BER = 0 under SLC II day

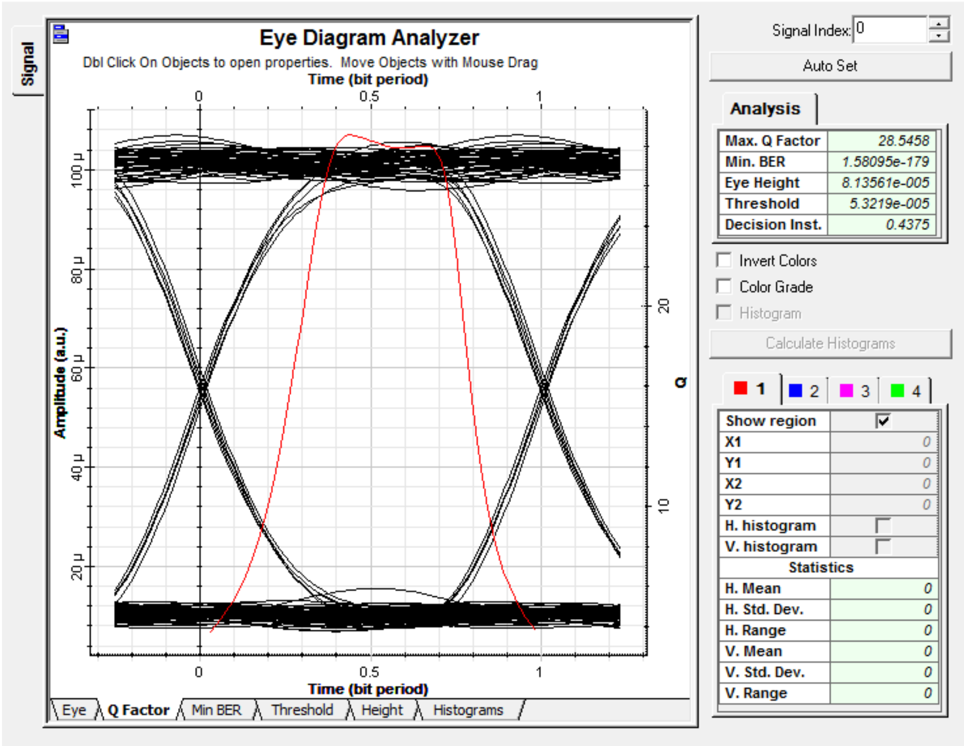

Figure 4. 8 Eye diagram for Arusha Range in 4km, BER = 10^{-179} under SLC II day

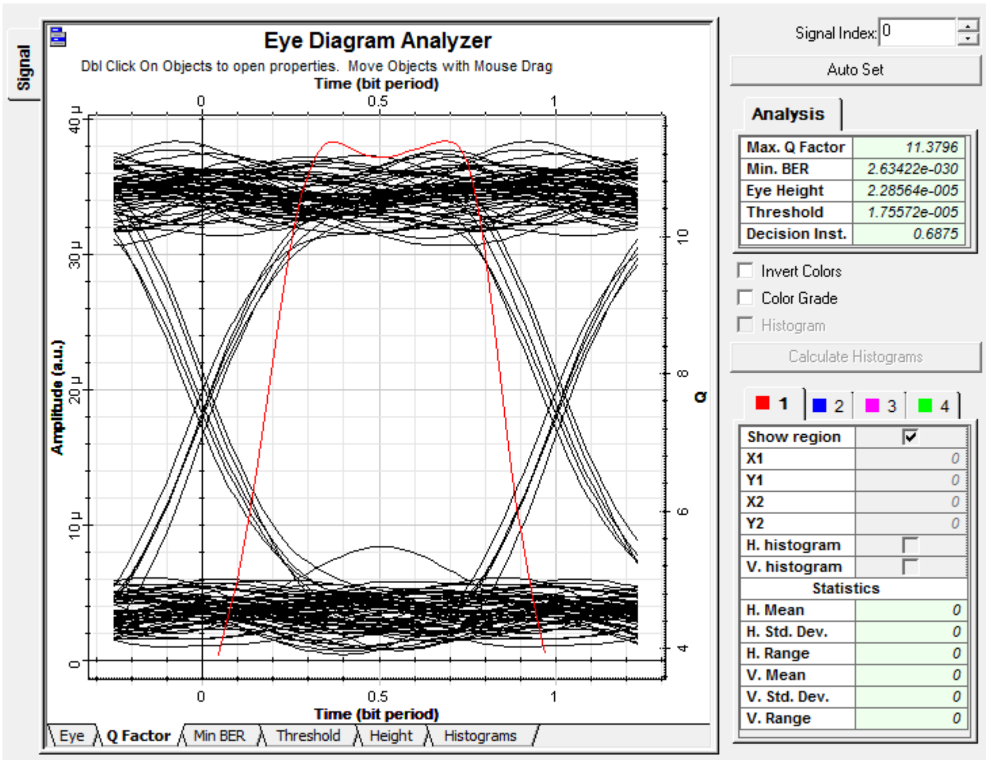

Figure 4. 9 Eye diagram for Arusha Range in 6km, BER = 10^{-30} under SLC II day

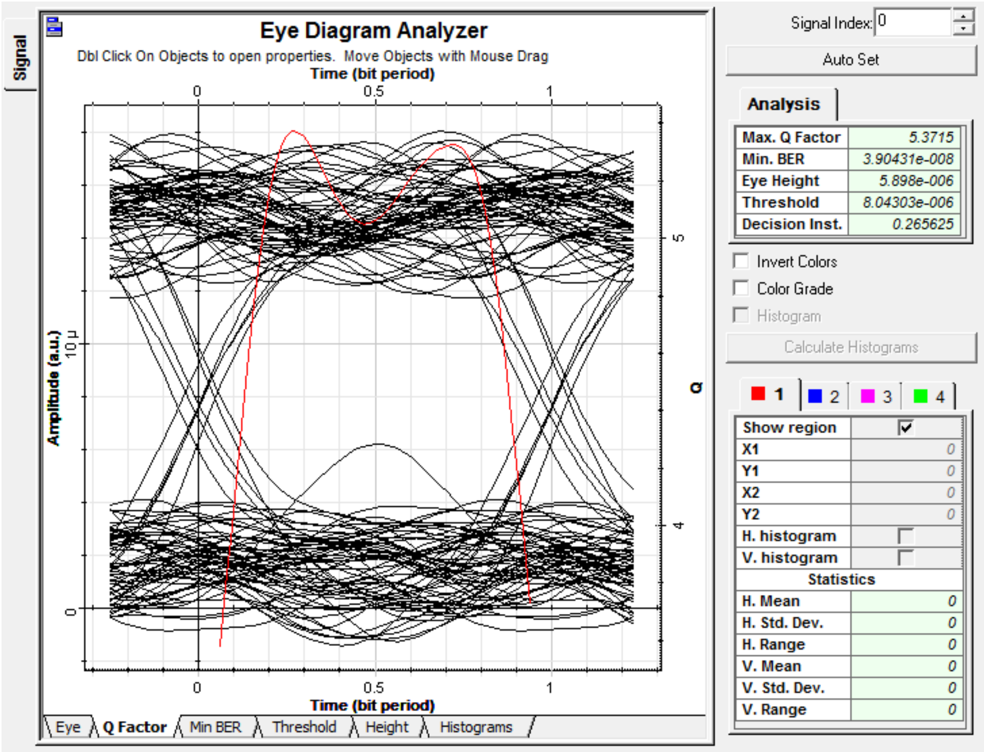

Figure 4. 10 Eye diagram for Arusha Range in 8km, BER = 10^{-8} under SLC II day

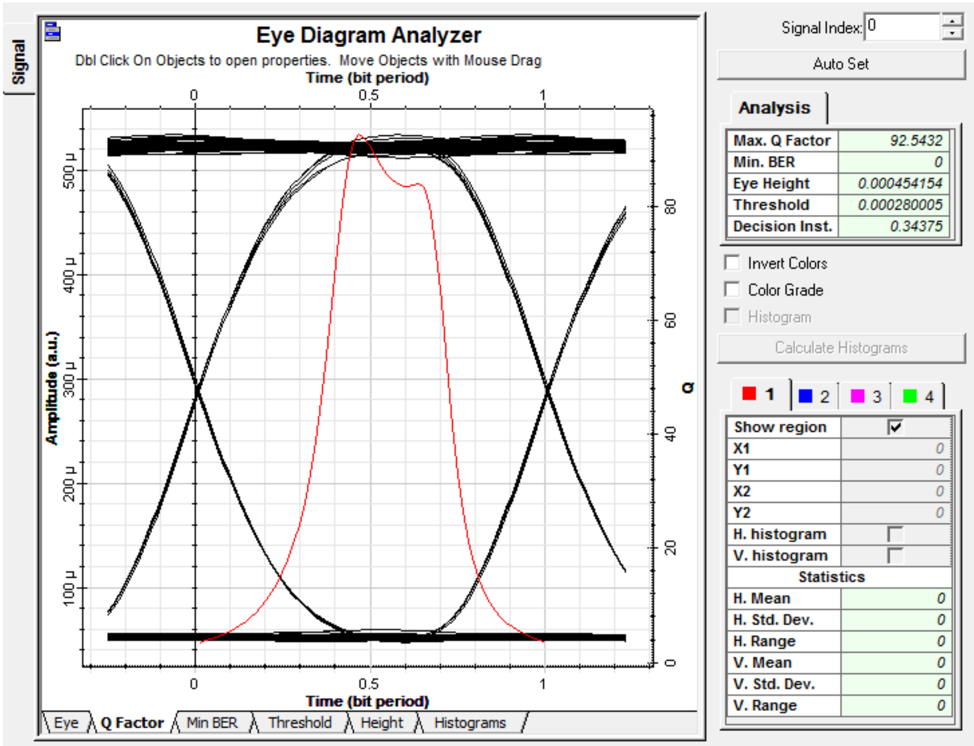

Figure 4. 11 Eye diagram for Mwanza Range in 2km, BER = 0 under SLC II day

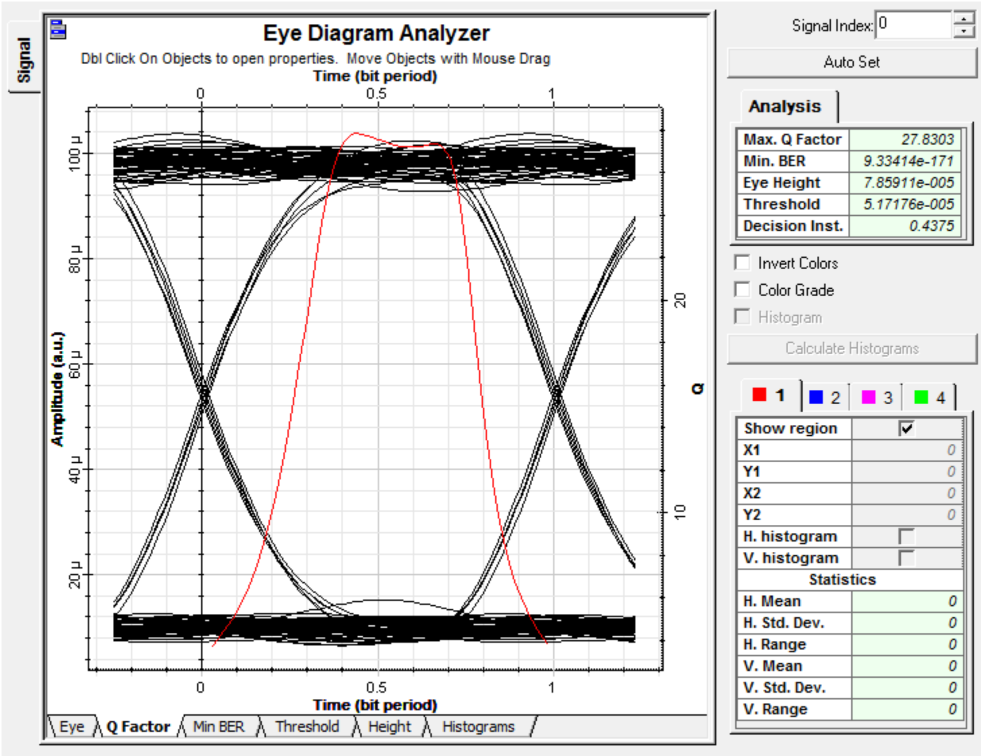

Figure 4. 12 Eye diagram for Mwanza Range in 4km, BER = 10^{-171} under SLC II day

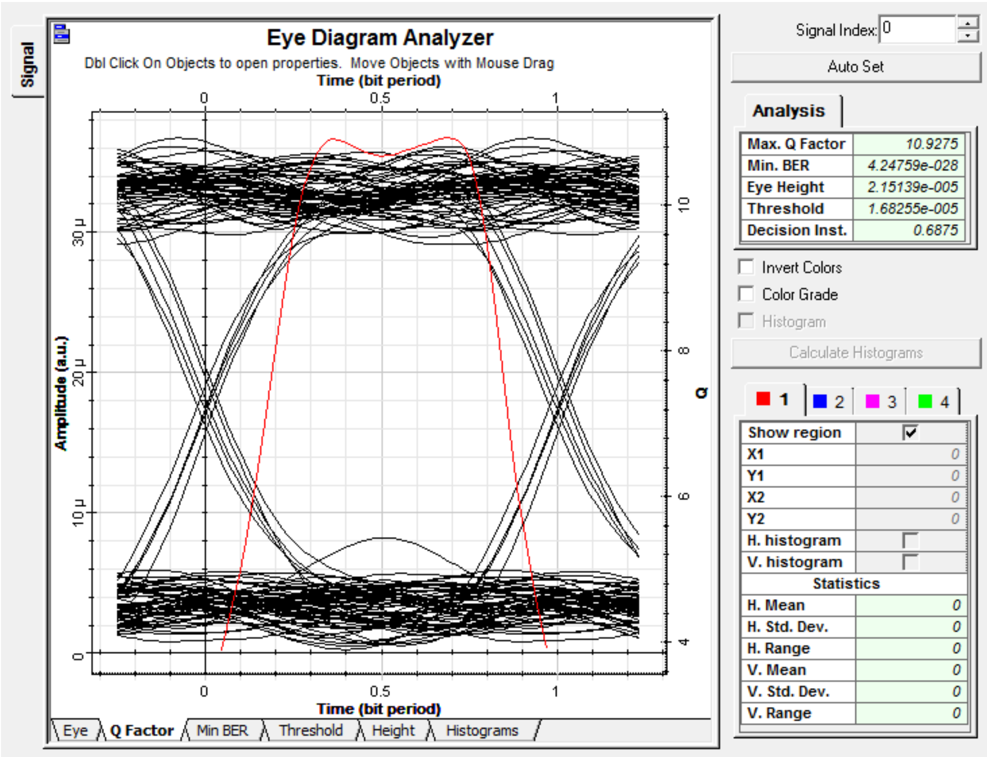

Figure 4. 13 Eye diagram for Mwanza Range in 6km, BER = 10^{-28} under SLC II day

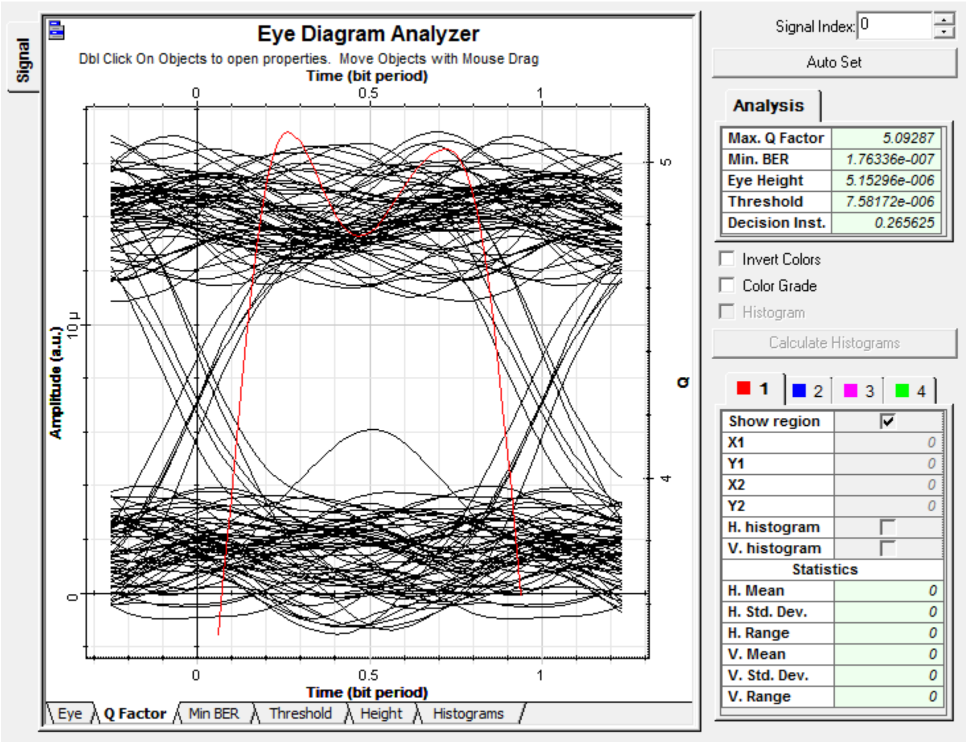

Figure 4. 14 Eye diagram for Mwanza Range in 8km, BER = 10^{-7} under SLC II day

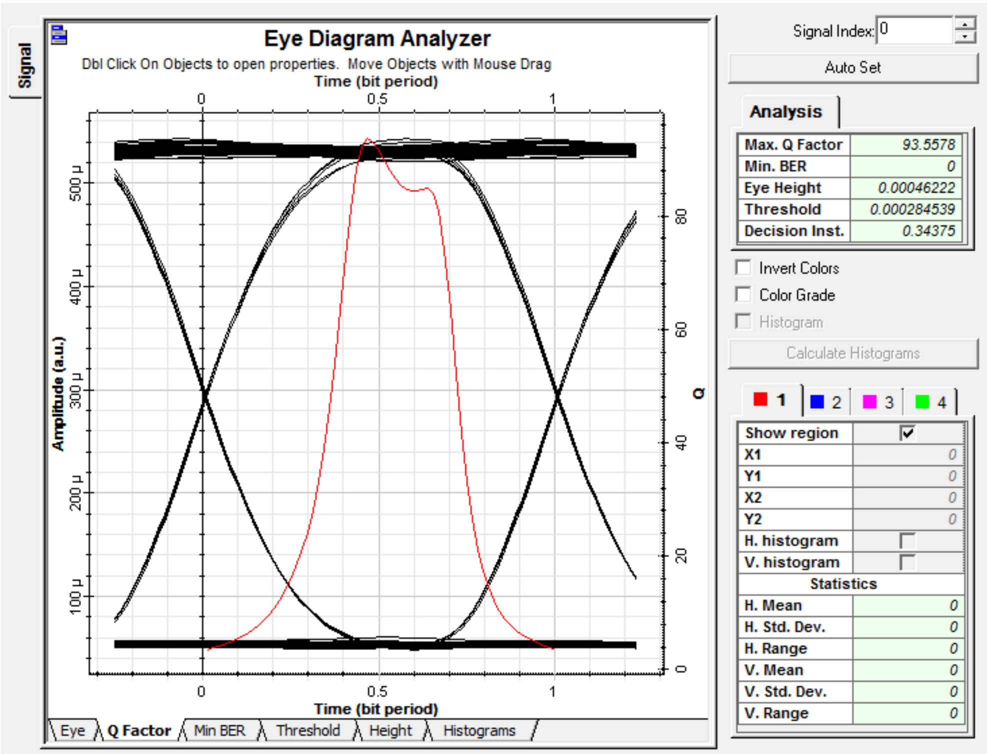

Figure 4. 15 Eye diagram for Arusha Range in 2km, BER = 0 under HV day model

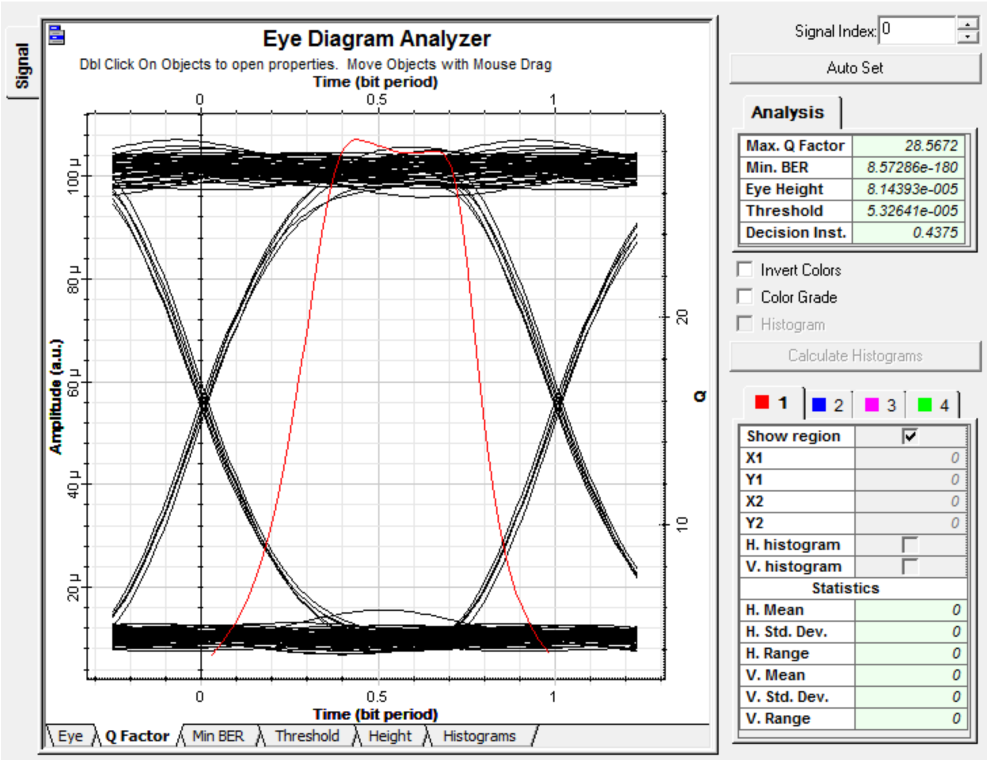

Figure 4. 16 Eye diagram for Arusha Range in 4km, BER = 10^{-180} under HV day

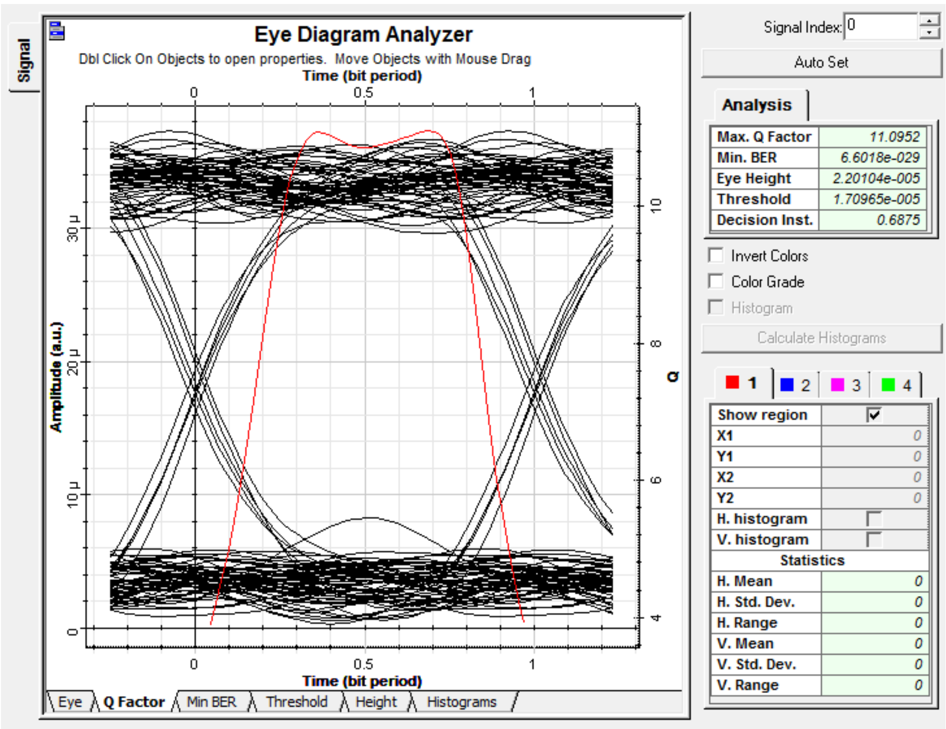

Figure 4. 17 Eye diagram for Arusha Range in 6km, BER = 10^{-29} under HV day

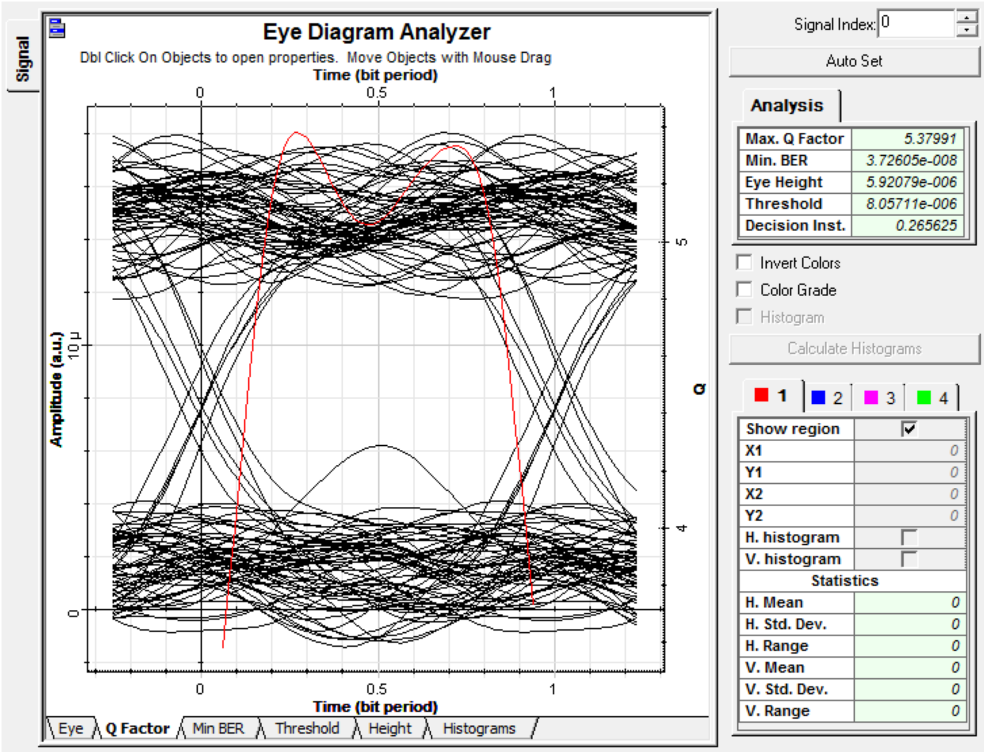

Figure 4. 18 Eye diagram for Arusha Range in 8km, BER =10^{-8} under HV day

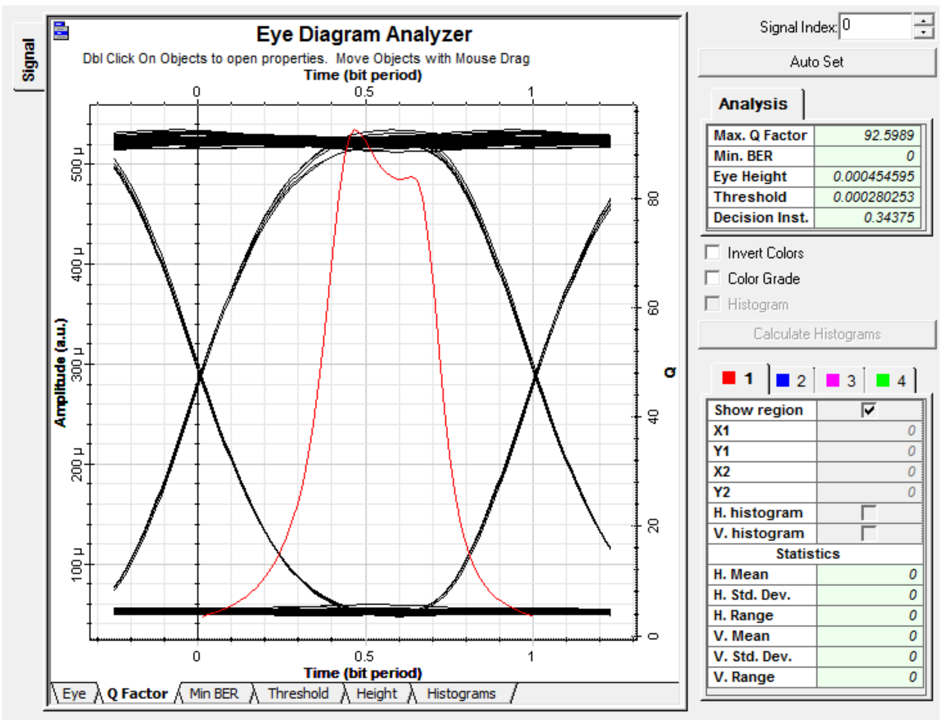

Figure 4. 19 Eye diagram for Mwanza Range in 2km, BER = 0 under HV day

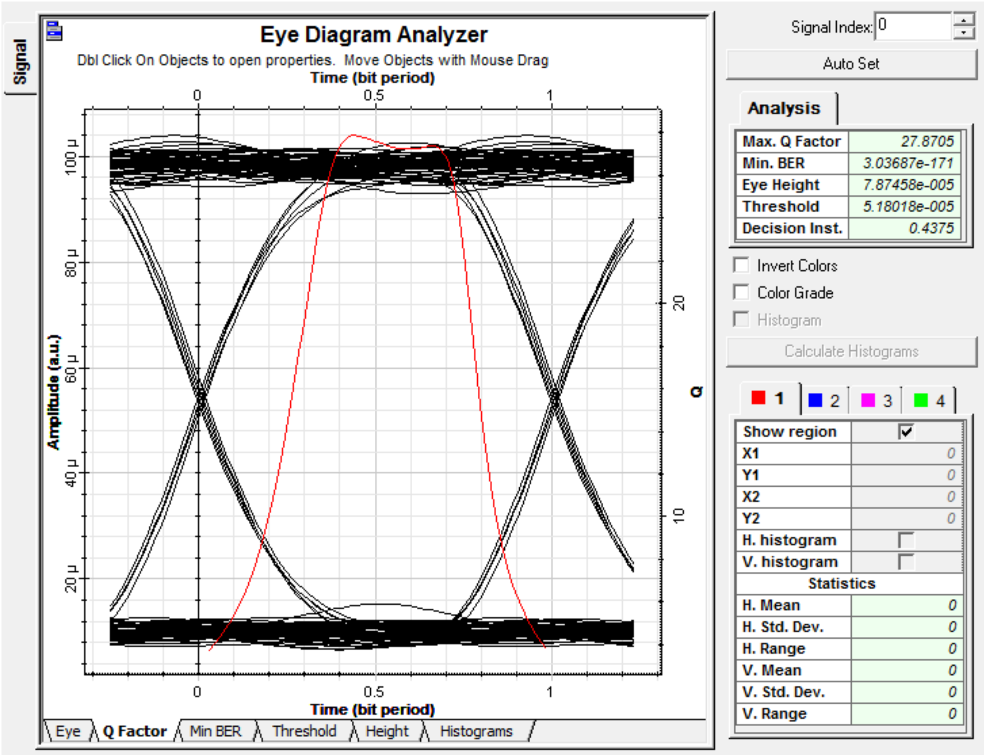

Figure 4. 20 Eye diagram for Mwanza Range in 4km, BER = 10^{-171} under HV day

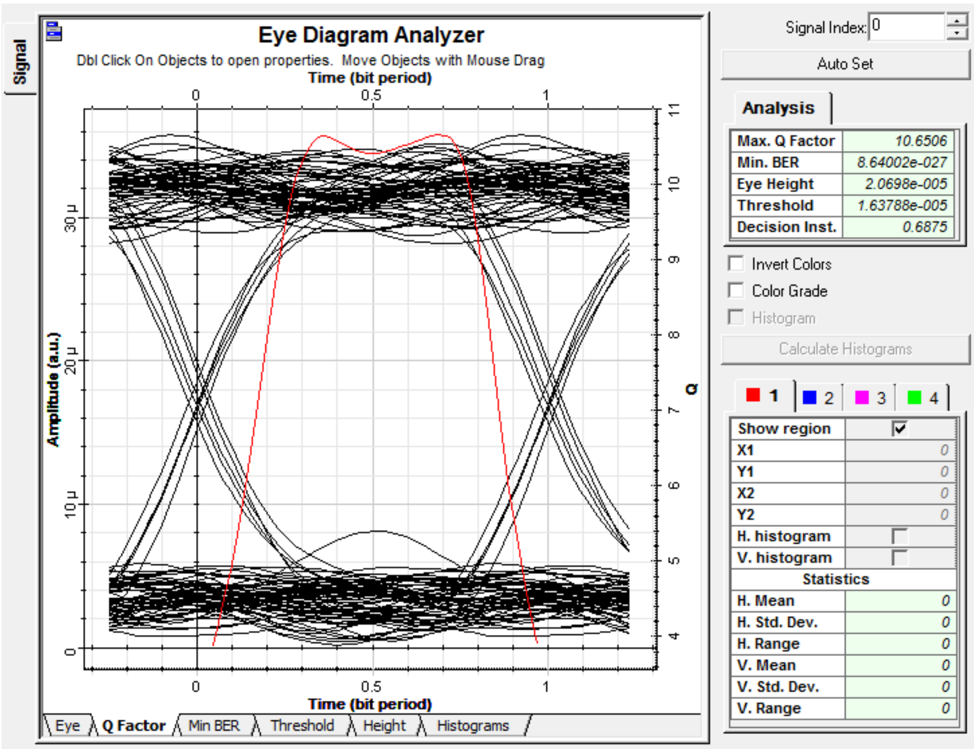

Figure 4. 21 Eye diagram for Mwanza Range in 6km, BER = 10-27 under HV day

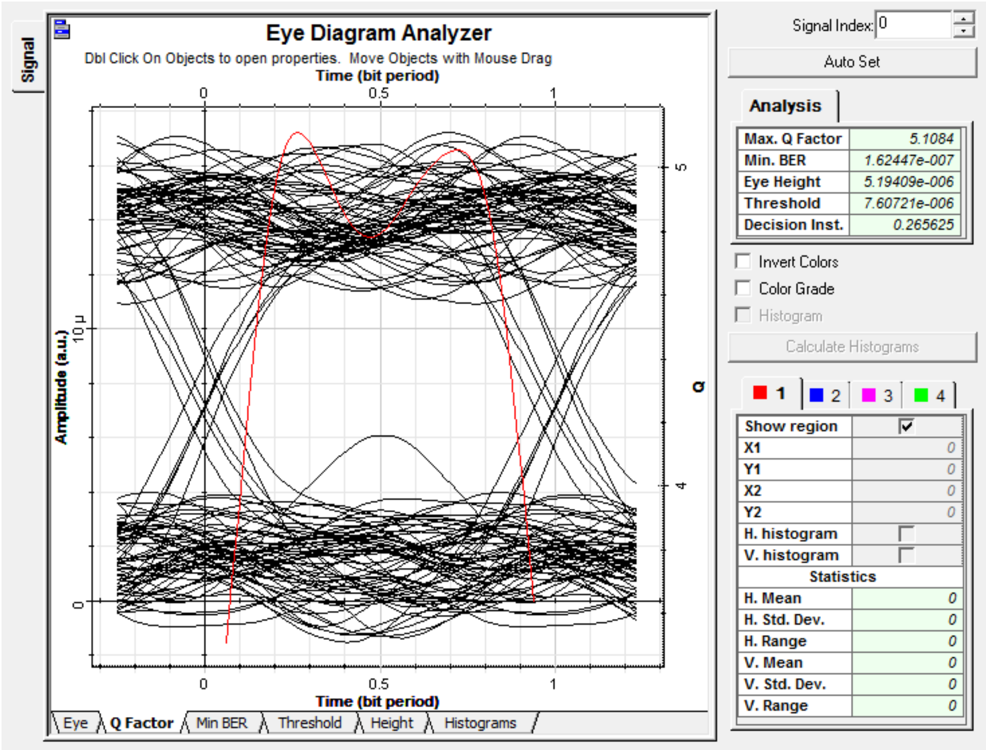

Figure 4. 22 Eye diagram for Mwanza Range in 8km, BER =10^{-7} under HV day

CHAPTER FIVE
DISCUSSION OF FINDINGS

5.1 Atmospheric Scintillation Attenuation

The availability of FSO link in all the two Tanzania cities was further estimated as shown in Table 4.5 – 4.8. In Arusha, the highest attenuation estimated was 0.735dB /km using SLC II day model, 0.734 dB/km on HV day model. The lowest attenuation estimated was 0.588 dB/km using SLC II day model, 0.585 dB/km on HV day model. In Mwanza, the highest attenuation estimated was 0.740dB /km using SLC II day model, 0.738dB/km on HV day model. The lowest attenuation estimated was 0.638 dB/km using SLC II day model, 0.636 dB/km on HV day model.

5.2 Scintillation Models Comparison

The Q-factor versus range curve in Fig. 4.1 shows that, HV has slightly higher Q factor compared to SLC II, which indicates low BER for the transmission. Moreover, results in Fig 4.2 Q- factor versus atmospheric attenuation curve, demonstrates slightly higher Q factor attained when using HV compared to SLC II. However, as atmospheric attenuation increases the divergence between the two declines.

Moreover, Log BER versus SNR for different models (SLC II ,HV) under 2km, 4km, 6km and 8km curve results has been demonstrated in Fig 4.3. This shows that, HV day model requires the least amount of transmission power compared to SLC II day model. Also, the required SNR of SLC II day model is about “0.92dB” more than the required SNR of HV day to obtain a desired BER performance. So, the best model is HV day, is suitable to predict scintillation data in Arusha and Mwanza regions.

5.3 Monthly Scintillation Analysis.

BER versus Months for Arusha and Mwanza regions graph plotted in Fig 4.4 and Q factor versus Months for Arusha and Mwanza regions graph plotted in Fig 4.5, Shows that, For Arusha, January is worst transmission month because of the demonstrated lower Q-factor of 92.3961 for 2km, 27.7242 for 4km, 10.8611 for 6km and 5.05207 for 8km and atmospheric attenuation of up to 0.78 dB per km. The attenuation results for Arusha are summarized in Table 4.5 and 4.8.

BER versus Months for Arusha and Mwanza regions graph plotted in Fig 4.4 and Q factor versus Months for Arusha and Mwanza regions graph plotted in Fig 4.5 Shows that, For Mwanza, April is worst transmission month because of the demonstrated lower Q-factor of 92.2896 for 2km, 27.6475 for 4km, 10.8132 for 6km and 5.02262 for 8km and atmospheric attenuation of up to 0.79 dB per km. The attenuation results for Mwanza are summarized in Table 4.3 and 4.4.

5.4 Arusha and Mwanza regions FSO feasibility.

Fig. 4.6 illustrates the graph of BER versus range for Arusha and Mwanza regions. The plotted graph shows, BER for Arusha and Mwanza is less than 10^{-6} for 2km, 4km and 6km, and higher to about 10^{-7} for 8km. This indicates the reliability of FSO transmission link range is 6km for both Arusha and Mwanza. It clearly shows that the reliability of the link increases as BER decreases.

5.4.1 Received Signal Quality

Fig 4.7 – 4.22 shows the eye diagram generated after simulation for the both Arusha and Mwanza regions under different models and ranges with the corresponding average BER values. It is clear that, eye diagrams of 2km, 4km and 6km for both cities and under two models having a large eye-opening between the top and bottom level. The eye pattern is clear and opens apparently up to 6km, when the propagation distance is increased to 8km, the eye pattern track begins to confound. Therefore, FSO communication can be deployed to the maximum of 6km for both cities.

CHAPTER SIX

CONCLUSION AND RECOMMENDATIONS

6.1 Conclusions and Recommendations

The feasibility of Free Space Optic communication under the scintillation effect in Arusha and Mwanza regions have been investigated in this study. Two models namely Submarine Laser Communication (SLC II) Day and Hufnagel Valley (HV) Day models were compared with the calculated scintillation data on 1500nm wavelength. The best model is Hufnagel Valley (HV) Day for scintillation data prediction.

The FSO system availability decreases with increase in transmission path. Moreover, the increase of the optical transmission power results into better FSO system availability. From this study, it concludes that FSO communication is feasible in both Arusha and Mwanza regions for about 6km range.

By comparing the turbulence ranges represented in Table 2.1, the study has revealed that turbulence level in both cities is middle since the scintillation index was 10^{-14} . Moreover, the study concludes that, the worst-month for FSO transmission is January for Arusha and March for Mwanza since lower Q-factor were revealed compared with other months.

6.2 Recommendation.

This study work has accomplished the objective and aims listed in Chapter One. From this study, Free Space Optical communication can be implemented in both Arusha and Mwanza regions under six (6) km. It can be used for last mile access and milestone communication solutions, Fiber Optic Back-up link, Cellular communication back haul and Temporary Links.

6.3 Future Study

Attenuation conditions are location dependent from the scintillation statistics analysis done in this research, it is essential to have a transparent understanding of what attenuation will be encountered in a given area before physical installation. The study mentioned in 3.4 was done under two modulation schemes Non Return to Zero (NRZ) and Return to Zero (RZ) with single mathematical model (Hufnagel Valley) . Therefore, it is important for future studies to be conducted for other regions and also by taking into consideration on other different atmospheric effects conditions such as fog, smoke and rain together with different modulation schemes and different model.

REFERENCES

Ali, M. A. A. (2014). Comparison of NRZ, RZ-OOK Modulation Formats for FSO Communications under Fog Weather Condition. *International Journal of Computer Applications*, *Volume 108*.

Bloom, S., Korevaar, E., & Schuster, J. (2003). Understanding the performance of free-space optics [Invited], *2*(6), 178–200.

Carrozzo, D., Mori, S., & Marzano, F. S. (2014). Modeling Scintillation Effects on Free Space Optical Links using Radiosounding Profile Data, *2*(3), 40–44.

Demers, F., Yanikomeroglu, H., & St-hilaire, M. (2011). A Survey of Opportunities for Free Space Optics in Next Generation Cellular Networks, 210–216.

Diagram, E., Freude, W., Schmogrow, R., Nebendahl, B., Winter, M., Josten, A., … Leuthold, J. (2012). Quality Metrics for Optical Signals :, *1*, 3–6.

Dong, Y., & Aminian, M. S. (2014). Routing in Terrestrial Free Space Optical Ad-Hoc Networks Yao Dong Routing in Terrestrial Free Space Optical Ad-Hoc Networks Examensarbete utfört i Transportsystem.

Dorrer, C., Doerr, C. R., Kang, I., Ryf, R., Leuthold, J., & Winzer, P. J. (2005). Measurement of Eye Diagrams and Constellation Diagrams of Optical Sources Using Linear Optics and Waveguide Technology, *23*(1), 178–186.

Elganimi, T. Y. (2013). Studying the BER Performance , Power- and Bandwidth-Efficiency for FSO Communication Systems under Various Modulation Schemes, 0–5.

Esmail, M. A., & Fathallah, H. (2016). Improved wavelength independent empirical model for Fog attenuation in FSO communication systems. *2016 7th International Conference on Information and Communication Systems, ICICS 2016*, 196–200.

Esmail, M. A., Member, S., Fathallah, H., & Member, S. (2016). An Experimental Study of FSO Link Performance in Desert Environment, *XX*(X), 1–4.

Fiser, O., Brazda, V., & Rejfek, L. (2014). Two ways to consider atmospheric turbulences in FSO propagation, (2), 3–6.

Ghassemlooy, Z., Ijaz, M., Rajbhandari, S., Adebanjo, O., Ansari, S., & Leitgeb, E. (2010). Experimental Study of Bit Error Rate of Free Space Optics

Communications in Laboratory Controlled Turbulence, *1*, 1072–1076.

Greenwood, D. P. (1977). Bandwidth specification for adaptive optics systems *. *OpticalSociety of America*, *119*(April 1972), 390–393.

Gunathilake, N. A., & Shakir, M. Z. (2017). Empirical Performance Evaluation of FSO Availability under Different Weather Conditions, 156–158.

Guo, W., Lin, J., Lin, C., Huang, T., & Member, S. (2009). Fast Methodology for Determining Eye Diagram Characteristics of Lossy Transmission Lines, *32*(1), 175–183.

Halotel, B., Zantel, V., Halotel, B., Zantel, V., Halotel, B., Zantel, V., … Zantel, V. (2018). October - December 2018 Operators ' Submissions, (December).

Han, Y., Ricklin, J. C., Oh, E., Doss-hammel, S., & Eaton, F. D. (2004). Estimating optical turbulence effects on free-space laser communication : modeling and measurements at ARL ' s A _ LOT facility, *5550*, 247–255.

Henniger, H., & Wilfert, O. (2010). An introduction to free-space optical communications. *Radio Engineering*, *19*(2), 203–212.

Ijaz, M. (2013). Experimental characterisation and modelling of atmospheric fog and turbulence in FSO, 275.

Ijaz, M., Ghassemlooy, Z., Minh, H. Le, Rajbhandari, S., & Perez, J. (2012). Analysis of Fog and Smoke Attenuation in a Free Space Optical Communication Link under Controlled Laboratory Conditions, (3), 3–5.

Ijaz, M., Wu, S., Fan, Z., Popoola, W. O., & Ghassemlooy, Z. (2009). Study of the Atmospheric Turbulence in Free Space Optical Communications.

J Armstrong. (2009). OFDM for optical communications. *IEEE/OSA J Lightw Technol*, *27*, *No. 3*.

Kaushal, H., & Kaddoum, G. (2015). Free Space Optical Communication: Challenges and Mitigation Techniques. *IEEE Conference Journal*, *1*, 1–28.

Khalighi, M. A., Uysal, M., Marseille, C., & Engineering, E. (2014). Survey on Free Space Optical Communication : A Communication Theory Perspective, (c), 1–29.

Larry B. Stotts. (2017). Free Space Optical Systems Engineering: Design and

Analysis. *Free Space Optical Systems Engineering*, 1–2.

Larry C. Andrews, Ronald L. Phillips, C. Y. H. (2001). L. C. Andrews, R. L. Phillips, and C. Y. Hopen, Laser Beam Scintillation with Applications. *SPIE Press*, 357.

Larry C. Andrews and Ronald Phillips. (2005). Laser Beam Propagation through Random Media, Washington USA. *SPIE PRESS*.

Madhuri, A. S., & Mahaboob, S. T. (2017). International Journal of Advance Engineering and Research Evaluating the Performance of Free Space Optical Link in Tropical Climate, 273–278.

Majumdar, A. K. (2015). *Theory of Free-Space Optical (FSO) Communication Signal Propagation Through Atmospheric Channel*.

Malik, A., & Singh, P. (2015). Free Space Optics : Current Applications and Future Challenge. *International Journal of Optics*, *2015*(c), 7 pages.

Mandeep, J. S., & Dao, H. (2012). Comparison of Tropospheric Scintillation Models on Earth-Space Paths in Tropical Region, *4*(11), 1616–1623.

Miglani, R. (2017). Journal of Lasers , Optics & Photonics Free Space Optical Communication : The Last Mile Solution to High Speed Communication Networks, *4*(3), 3–4.

Milosevic, N. D., Petkovic, M. I., Member, S., & Djordjevic, G. T. (2017). Average BER of SIM-DPSK FSO system with multiple receivers over M -distributed atmospheric channel with pointing errors, *0655*(c), 1–6.

Mirarchi, D., Guzzi, P. H., Vizza, P., Tradigo, G., & Cannataro, M. (2015). 2015 IEEE 28th International Symposium on Computer-Based Medical Systems ICT solutions for health education model.

Mohammed, N. A., El-wakeel, A. S., & Aly, M. H. (2012). Performance Evaluation of FSO Link Under NRZ-RZ Line Codes , Different Weather Conditions and Receiver Types in the Presence of Pointing Errors, 28–35.

MRS, W. (2016). Technology Performance Analysis of FSO Modulation Schemes with Diversity Reception. *Engineering and Technology*, *5*(3), 83–90.

MS Alam, SA Shawkat, K Gontaro, M. M. (2008). IrBurst modeling and performance evaluation for large data block exchange over high-speed IrDA links. *IEICE Trans Commun*, *91*, 274–285.

Navidpour, S. M., Uysal, M., & Kavehrad, M. (2007). BER Performance of Free-Space Optical Transmission with Spatial Diversity, *6*(8), 2813–2819.

Nazari, Z., Gholami, A., Vali, Z., Sedghi, M., & Ghassemblooy, Z. (2016). Experimental Investigation of Scintillation Effect on FSO Channel. *IEEE Conference Journal*, 1–8.

Nilupulee, M., Gunathilake, A., & Shakir, M. Z. (2017). Empirical Performance Evaluation of FSO Availability under Different Weather Conditions Empirical Performance Evaluation of FSO Availability under Different Weather Conditions. *IEEE Conference Journal*, (November), 156–158.

Nor, N. A. M., Ghassemlooy, Z., Bohata, J., Saxena, P., Komanec, M., Zvanovec, S., … Khalighi, M. A. (2017). Experimental investigation of all-optical relay-assisted 10Gb/s FSO link over the atmospheric turbulence channel. *Journal of Lightwave Technology*, *35*(1), 45–53.

Norazimah, M. Z., Aljunid, S. A., Al-khafaji, H. M. R., Fadhil, H. A., & Anuar, M. S. (2013). Performance of Different SAC-OCDMA Detection Schemes with NRZ and RZ Data Formats, 66–70.

Oh, E., Ricklin, J., Eaton, F., Gilbreath, C., Doss-hammel, S., & Moore, C. (2004). Estimating Optical Turbulence Using the PAMELA Model, *5550*, 256–266.

Pandey, R., Awasthi, A., & Srivastava, V. (2013). Comparison between Bit Error Rate And Signal To Noise Ratio in OFDM Using LSE, *2013*(Cac2s), 463–466.

Pesek, P., Bohata, J., Zvanovec, S., Perez, J., & Valencia, U. P. De. (2016). FSO for C-RAN Architecture, 1–4.

Prokeš, A. (2009). Modeling of Atmospheric Turbulence Effect on Terrestrial FSO Link, (3), 42–47.

Propagation, A., Ed, V. I., Wasiczko, L. M., Orlando, G. C. G., Michael, S., Parenti, R. R., … Murphy, R. (2014). Comparison of scintillation measurements from a 5 km communication link to standard statistical models The MIT Faculty has made this article openly available . Please share Citation Accessed Citable Link Detailed Terms Comparison of Scintillation Measurem.

Raja, A. S. (2013). Investigations on Free space optics communication system. *EInternationalConferenceonInformationCommunication& Embedded Systems (ICICES '13)*.

Rashid, F. U., & Semakuwa, S. K. (2014). Performance Analysis of Free Space Optical Communication Under the Effect of Rain in Arusha Region, Tanzania, *3*(9), 1523–1526.

Rashidi, F. U., & Semakuwa, S. K. (2014). Analysis of Rain Effect in Free Space Optical Communication under NRZ Modulation in Two Regions of Tanzania, (10), 13–16.

Ricklin, J. C., Hammel, S. M., Eaton, F. D., & Svetlana, L. (2006). Atmospheric channel effects on free-space laser communication, *158*, 111–158.

Roberto Ramirez-Iniguez, Sevia M. Idrus, Z. S. (2008). Optical Wireless Communications, (March), 376. Retrieved from http://books.google.at/books/about/Optical_Wireless_Communications.html?id=pHPuEGZcv-YC&redir_esc=y

Sahota, J. K. (2017). Analyzing the Effect of Scintillation on Free Space Optics, (June), 493–496.

Sanayei, A., & Faraghian, H. (2015). on e-Commerce The Impact ofE-Business on Structural Factors and Its Role in Middle Management Positions in the Organization on e-Commerce, (April), 1–7.

Shafi, N., & Gokul, P. G. (2016). Performance Analysis of Photodetectors and Effect of Photodetection Noises in Optical, 1631–1637.

Shumani, M. M., Abdullah, M. F. L., & Suriza, A. Z. (2016). The Effect of Haze Attenuation on Free Space Optics Communication (FSO) at Two Wavelengths under Malaysia Weather, (1). https://doi.org/10.1109/ICCCE.2016.102

Sidarta, A. E. (2016). Free Space Optics (FSO) Links in Singapore : Scintillation Effects. *International Journal on Recent and Innovation Trends in Computing and Communication*, 2–6.

Singhal, P., Sharma, A., & Singh, S. P. (2015). To Study the Various Weather Effect on FSO Link. *Proceedings - 2015 2nd IEEE International Conference on Advances in Computing and Communication Engineering, ICACCE 2015*, 339–

344.

Son, I. K., & Mao, S. (2016). Author ’ s Accepted Manuscript A Survey of Free Space Optical Networks Reference : To appear in : Digital Communications and Networks. *Digital Communications and Networks*. Retrieved from http://dx.doi.org/10.1016/j.dcan.2016.11.002

Sousa, G. (2017). Biggest Cities In Tanzania. Retrieved from www.worldatlas.com

Stoilescu, D. (2017). An Analysis of Content and Policies in ICT Education in Australia, 10–11. https://doi.org/10.1109/ICALT.2017.162

TCRA. (2010). The United Republic Of Tanzania Report on Internet and Data Services in Tanzania a Supply-Side Survey, (September).

Tejkal, V., Filka, M., Šporik, J., & Reichert, P. (2010). Possibilities of increasing Power Budget in optical networks, *1*(4), 42–47.

Touati, A., Abdaoui, A., Touati, F., Uysal, M., & Bouallegue, A. (2017). On The Effects of Temperature on The Performances of FSO Transmission Under Qatar ’ s Climate, 1–5.

Uysal, M., & Yu, M. (2006). Error Rate Performance Analysis of Coded Free-Space Optical Links over Gamma-Gamma Atmospheric Turbulence Channels, *5*(6), 1229–1233.

Vasseur, H., 1999. (1999). Prediction of tropospheric scintillation on satellite links from radiosonde data. *IEEE T. Antenn. Propag*.

Vitásek, J., Látal, J., Hejduk, S., Koudelka, P., Skapa, J., Šiška, P., & Vašinek, V. (2011). Atmospheric Turbulences in Free Space Optics Channel, 104–107.

Wei, J. L., Ingham, J. D., Cunningham, D. G., Penty, R. V, & White, I. H. (2012). Comparisons between 28 Gb / s NRZ , PAM , CAP and optical OFDM systems for Datacommunication Applications, *2*, 28–29.

Willebrand, H., & Ghuman, B. S. (2002). Free-Space Optics : Enabling Optical Connectivity in Today ’ s Networks.

Yang, D., Li, D., Tao, J., Fang, Y., Mao, X., & Tong, W. (2017). An Optical Fiber Comprehensive Analysis System for Spectral-Attenuation and Geometry Parameters Measurement.

Z.Ghaseemlooy, W. Poopola, and S. R. (2012). Optical wireless communications, system and channel modelling with matlab. *CRC Press, London, UK*.

Zabidi, S. A., Khateeb, W. Al, Islam, M. R., & Naji, A. W. (2010). The effect of weather on Free Space Optics communication (FSO) under tropical weather conditions and a proposed setup for measurement. *International Conference on Computer and Communication Engineering, ICCCE'10*, (May), 11–13.

APPENDICES

Appendix A: Temperature, Relative Humidity and Wind Speed Average data for the year from 2015 to 2018 for Arusha region.

Month	Temperature(C)	Relative Humidity (%)	Wind Speed (knots)	Altitude(m)
January	22.15	72.75	4.25	1372
February	22.45	69.25	5.5	1372
March	22.9	74	6.25	1372
April	21.525	86.75	7.25	1372
May	19.725	87.25	8.5	1372
June	18.725	82	8.5	1372
July	18.3	78.75	8.75	1372
August	19.1	73.25	9.25	1372
September	20.2	69.75	9.75	1372
October	21.875	70.75	9.75	1372
November	22	76.75	7.5	1372
December	21.9	76	5	1372

Appendix B: Temperature, Relative Humidity and Wind Speed Average data for the year from 2015 to 2018 for Mwanza region.

Month	Temperature(C)	Relative Humidity (%)	Wind Speed (knots)	Altitude(m)
January	23.45	75.25	5.5	1140
February	24.15	72.5	6.25	1140
March	23.6	73.5	6	1140
April	23.675	78.75	5	1140
May	23.525	71.75	6	1140
June	23.3	65.5	6.25	1140
July	22.825	61.5	7	1140
August	22.45	62.5	6.75	1140
September	24.35	66.5	7.5	1140
October	24.1	72	6.75	1140
November	23.6	76.25	6	1140
December	23.45	76.5	6	1140

Appendix C: Mwanza Monthly Attenuation (dB/Km) 2015 under Submarine Laser Communication (SLC II) Day Model

Attenuation(dB/Km)				
Month	**2km**	**4km**	**6km**	**8km**
January	0.787247667	0.74306285	0.718375112	0.701357937
February	0.771840827	0.72852073	0.704316143	0.687632003
March	0.784469727	0.740440825	0.715840201	0.698883074
April	0.790559712	0.746189004	0.721397401	0.704308634
May	0.785437655	0.741354427	0.716723449	0.6997454
June	0.786807511	0.742647398	0.717973463	0.700965803
July	0.769593499	0.726399535	0.702265423	0.685629862
August	0.767094593	0.724040882	0.699985134	0.68340359
September	0.779039215	0.735315103	0.710884778	0.694045038
October	0.782193806	0.738292641	0.713763389	0.696855459
Noveber	0.774189383	0.730737472	0.706459235	0.689724329
December	0.772515937	0.729157949	0.704932191	0.688233458

Appendix D: Mwanza Monthly Attenuation (dB/Km) 2016 under Submarine Laser Communication (SLC II) Day Model

Attenuation(dB/Km)				
Month	**2km**	**4km**	**6km**	**8km**
January	0.779573925	0.735819803	0.711372709	0.694521411
February	0.787141749	0.742962877	0.71827846	0.701263575
March	0.793254444	0.748732493	0.723856384	0.706709367
April	0.77755273	0.733912049	0.709528339	0.69272073
May	0.782962207	0.739017915	0.714464567	0.697540027
June	0.762470944	0.719676738	0.695765986	0.679284387
July	0.762837363	0.720022592	0.696100349	0.679610829
August	0.772695719	0.72932764	0.705096244	0.688393625
September	0.7474804	0.705527549	0.682086894	0.66592933
October	0.76915377	0.725984486	0.701864164	0.685238107
November	0.775187021	0.731679117	0.707369594	0.690613123

December	0.766233445	0.723228066	0.699199324	0.682636394

Appendix E: Mwanza Monthly Attenuation (dB/Km) 2017 under Submarine Laser Communication (SLC II) Day Model

Attenuation(dB/Km)				
Month	**2km**	**4km**	**6km**	**8km**
January	0.762224356	0.71944399	0.695540971	0.679064702
February	0.777048205	0.73343584	0.709067952	0.69227125
March	0.732894625	0.69176041	0.668777159	0.652934882
April	0.781200827	0.737355394	0.712857281	0.695970815
May	0.763242016	0.720404533	0.696469601	0.679971333
June	0.757251735	0.714750461	0.691003382	0.6746346
July	0.760574083	0.71788634	0.694035073	0.677594476
August	0.727319761	0.686498439	0.663690013	0.647968242
September	0.76960402	0.726409466	0.702275024	0.685639235
October	0.769408656	0.726225067	0.702096751	0.685465186
November	0.77125629	0.727969	0.703782744	0.68711124
December	0.775827568	0.732283712	0.707954103	0.691183786

Appendix F: Mwanza Monthly Attenuation (dB/Km) 2018 under Submarine Laser Communication (SLC II) Day Model

Attenuation(dB/Km)				
Month	**2km**	**4km**	**6km**	**8km**
January	0.774577641	0.731103938	0.706813526	0.690070227
February	0.763329735	0.720487329	0.696549646	0.680049482
March	0.778298466	0.734615929	0.710208834	0.693385105
April	0.778995202	0.735273561	0.710844615	0.694005827
May	0.757145993	0.714650653	0.69090689	0.674540394
June	0.769652924	0.726455625	0.702319649	0.685682803
July	0.739992817	0.698460212	0.675254364	0.659258652
August	0.761939228	0.719174865	0.695280788	0.678810682
September	0.764510507	0.721601829	0.697627118	0.681101431
October	0.757372522	0.714864469	0.691113601	0.674742209
November	0.767528948	0.724450858	0.70038149	0.683790556
December	0.768343963	0.72522013	0.701125203	0.684516652

Appendix G: Arusha Monthly Attenuation (dB/Km) 2015 under Submarine Laser Communication (SLC II) Day Model

Attenuation(dB/Km)				
Month	**2km**	**4km**	**6km**	**8km**
January	0.779016168	0.73529335	0.710863748	0.694024506
February	0.772429148	0.729076031	0.704852995	0.688156138
March	0.746478473	0.704581855	0.681172621	0.665036715
April	0.744696741	0.702900124	0.679546764	0.663449372
May	0.705683631	0.666076652	0.643946725	0.628692642
June	0.705459005	0.665864634	0.643741751	0.628492524
July	0.684672025	0.646244337	0.624773325	0.60997343
August	0.682082369	0.643800027	0.622410226	0.607666308
September	0.684447547	0.646032458	0.624568485	0.609773442
October	0.703807655	0.664305966	0.642234869	0.627021337
November	0.740774002	0.699197552	0.675967207	0.659954609
December	0.768152522	0.725039434	0.700950511	0.684346098

Appendix H: Arusha Monthly Attenuation (dB/Km) 2016 under Submarine Laser Communication (SLC II) Day Model

Attenuation(dB/Km)				
Month	**2km**	**4km**	**6km**	**8km**
January	0.782256463	0.738351781	0.713820564	0.69691128
February	0.771455409	0.728156944	0.703964443	0.687288635
March	0.775665318	0.732130568	0.707806047	0.691039237
April	0.731495437	0.690439753	0.667500379	0.651688347
May	0.705831782	0.666216488	0.644081915	0.628824629
June	0.688005171	0.649390408	0.62781487	0.612942925
July	0.701994597	0.662594667	0.640580427	0.625406086
August	0.700542877	0.661224427	0.639255712	0.624112751
September	0.707893801	0.668162775	0.645963538	0.63066168
October	0.713029585	0.67301031	0.650650017	0.635237144
November	0.741585313	0.699963328	0.67670754	0.660677405
December	0.769385332	0.726203052	0.702075468	0.685444406

Appendix I: Arusha Monthly Attenuation (dB/Km) 2017 under Submarine Laser Communication (SLC II) Day Model

Attenuation(dB/Km)				
Month	**2km**	**4km**	**6km**	**8km**
January	0.774491097	0.731022252	0.706734553	0.689993125
February	0.763896846	0.72102261	0.697067143	0.680554721
March	0.767984399	0.724880747	0.700797095	0.684196316
April	0.73449155	0.693267707	0.670234377	0.654357581
May	0.704766077	0.665210596	0.643109443	0.627875194
June	0.698674353	0.659460775	0.637550656	0.622448085
July	0.704262782	0.664735549	0.64265018	0.62742681
August	0.70725641	0.667561158	0.645381909	0.630093829
September	0.709719636	0.669886133	0.647629639	0.632288314
October	0.731685202	0.690618867	0.667673543	0.651857408
November	0.745240695	0.703413549	0.68004313	0.66393398
December	0.771396108	0.728100971	0.70391033	0.687235804

Appendix J: Arusha Monthly Attenuation (dB/Km) 2018 under Submarine Laser Communication (SLC II) Day Model

attenuation(dB/Km)				
Month	**2km**	**4km**	**6km**	**8km**
January	0.775804438	0.732261881	0.707932996	0.691163179
February	0.766766424	0.723731132	0.699685676	0.683111225
March	0.765484595	0.722521246	0.698515987	0.681969244
April	0.746605551	0.704701801	0.681288581	0.665149928
May	0.723126538	0.682540564	0.659863635	0.644232506
June	0.714963622	0.674835797	0.652414854	0.636960174
July	0.692311957	0.653455473	0.631744876	0.616779835
August	0.705607226	0.666004536	0.643877005	0.628624573
September	0.714958933	0.674831371	0.652410575	0.636955997
October	0.728585606	0.687693238	0.664845115	0.649095982
Noveber	0.744108432	0.702344835	0.679009923	0.662925248
December	0.761838452	0.719079745	0.695188828	0.6787209

Appendix K: Average BER for Arusha and Mwanza under 2km, 4km,6km and 8km.

km	Average BER	
	Arusha	**Mwanza**
2	0	0
4	1.5E-170	1.3E-169
6	1.3E-28	4.42E-28
8	6.92E-08	1.67E-07

Appendix L: Running commands for OptiSystem parameters calculations

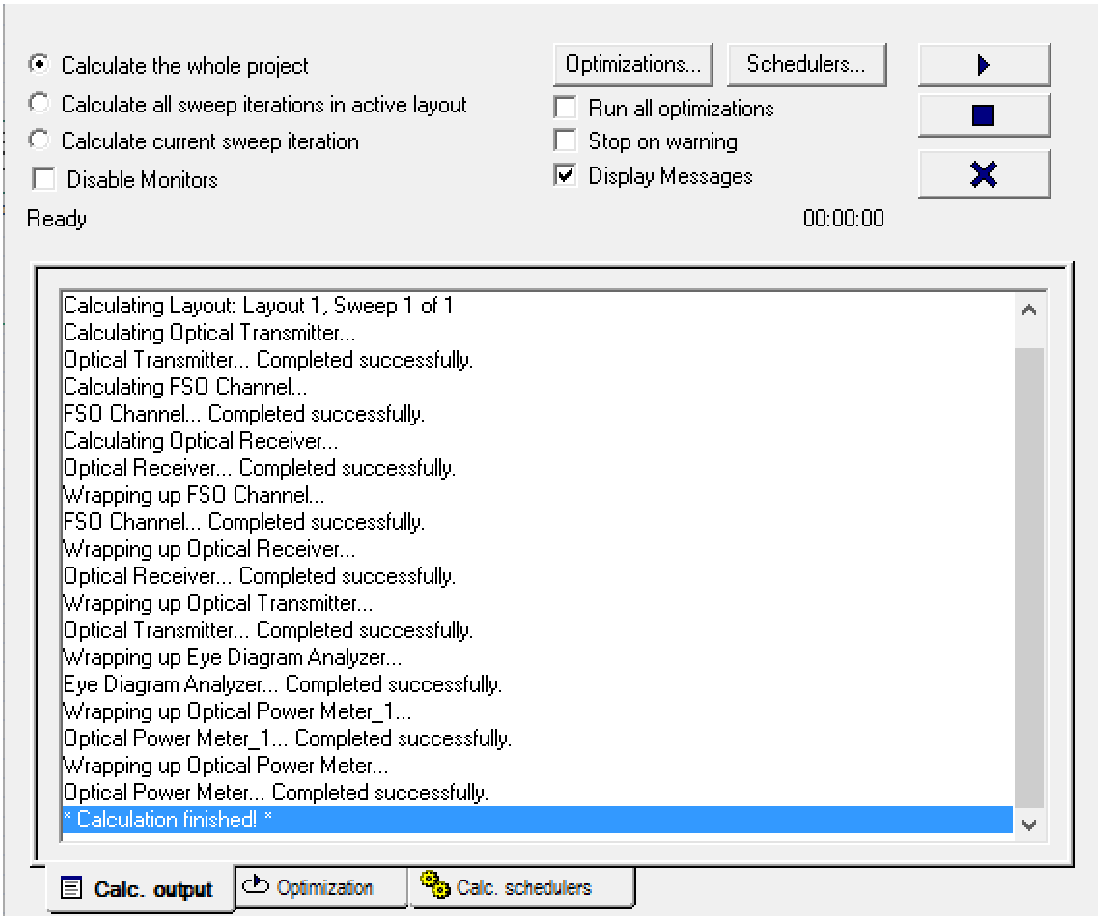

Appendix M: Optical Power results under different ranges.

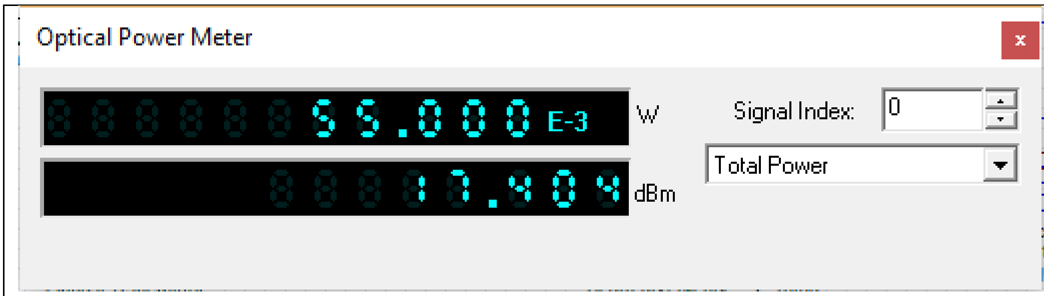

17dBm optical power transmitted

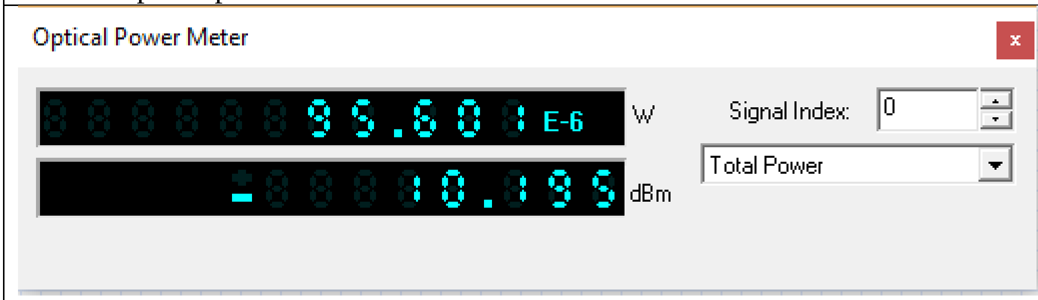

-10.195dBm optical power received under 2km

-17.464dBm optical power received under 4km

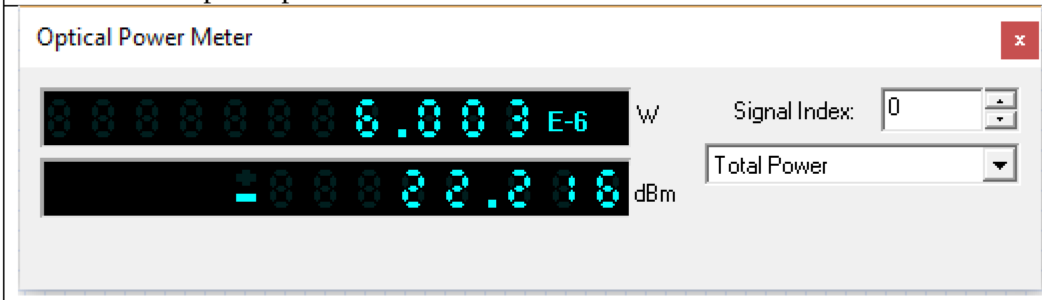

-22.216dBm optical power received under 6km

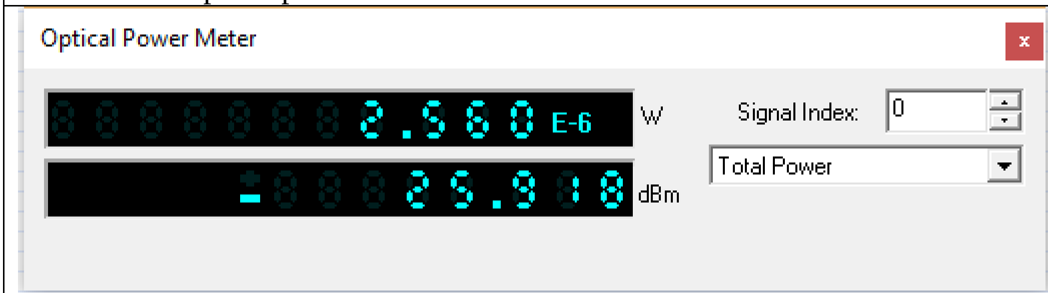

-25.918dBm optical power received under 8km

Appendix N: Arusha Eye Diagram for January under 2km with Q factor of 92.3961 and BER of 0

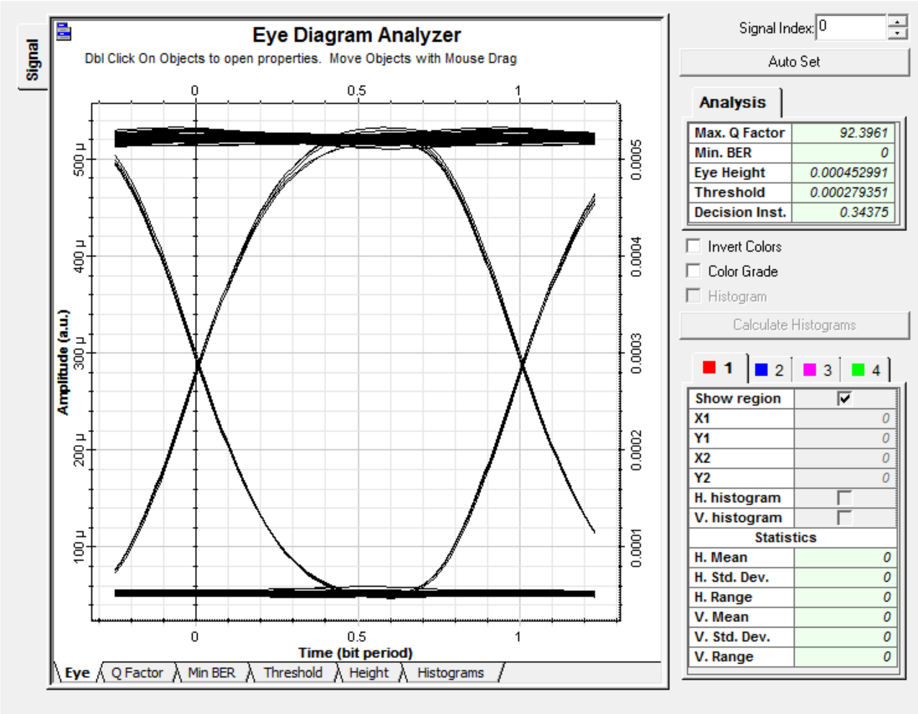

Appendix O: Arusha Eye Diagram for February under 2km with Q factor of 92.6322 and BER of 0

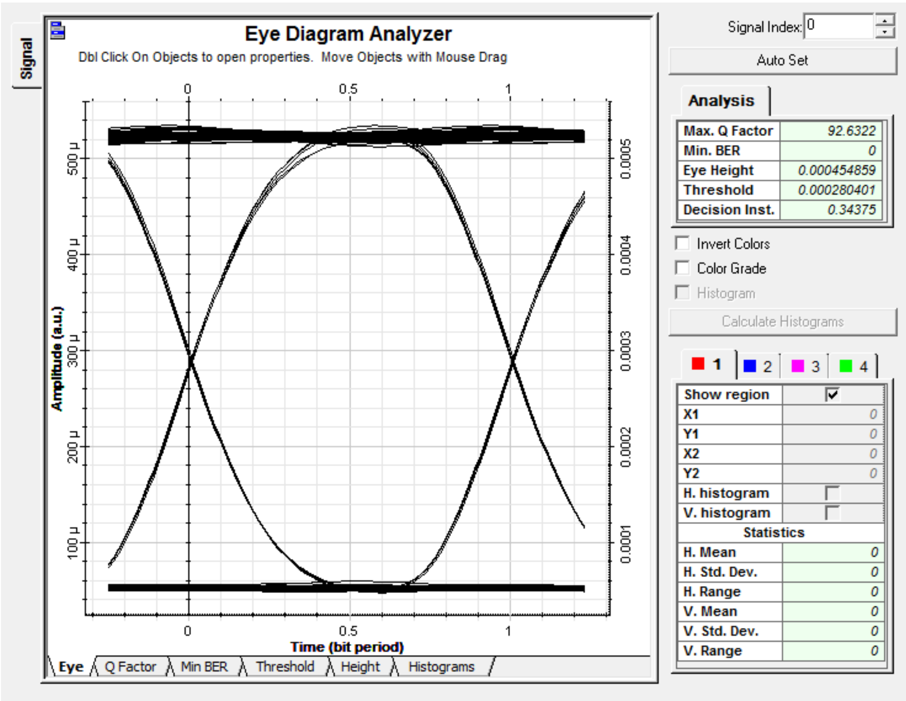

Appendix P: Arusha Eye Diagram for March under 2km with Q factor of 92.7531 and BER of 0

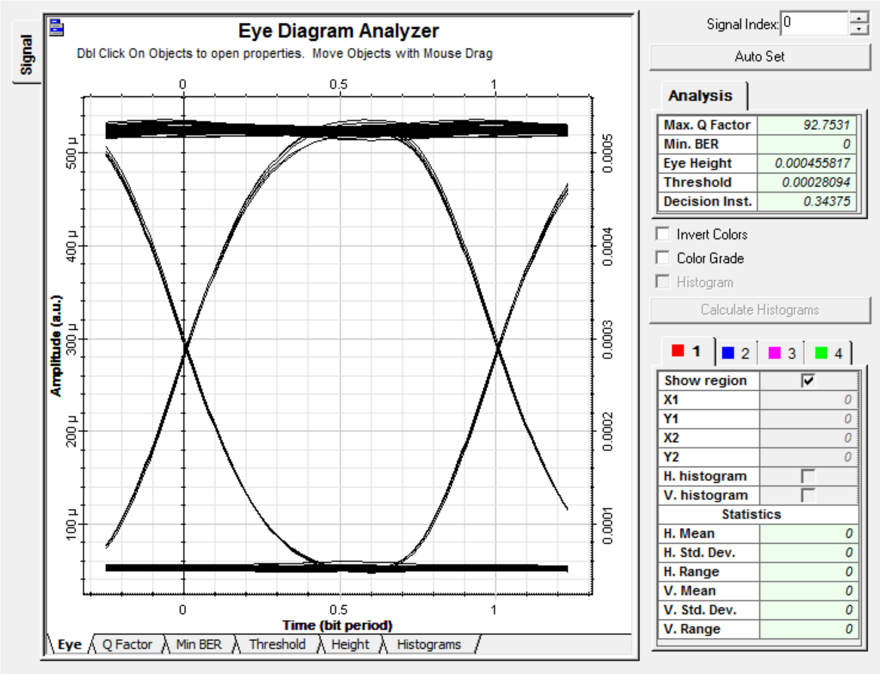

Appendix Q: Arusha Eye Diagram for April under 2km with Q factor of 93.3829 and BER of 0

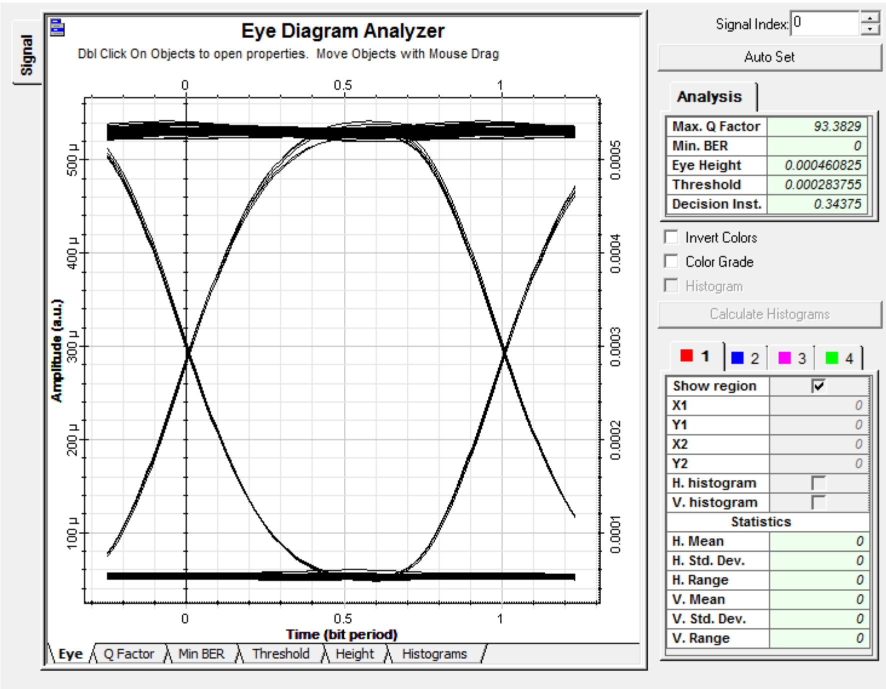

Appendix R: Arusha Eye Diagram for May under 2km with Q factor of 94.1424 and BER of 0

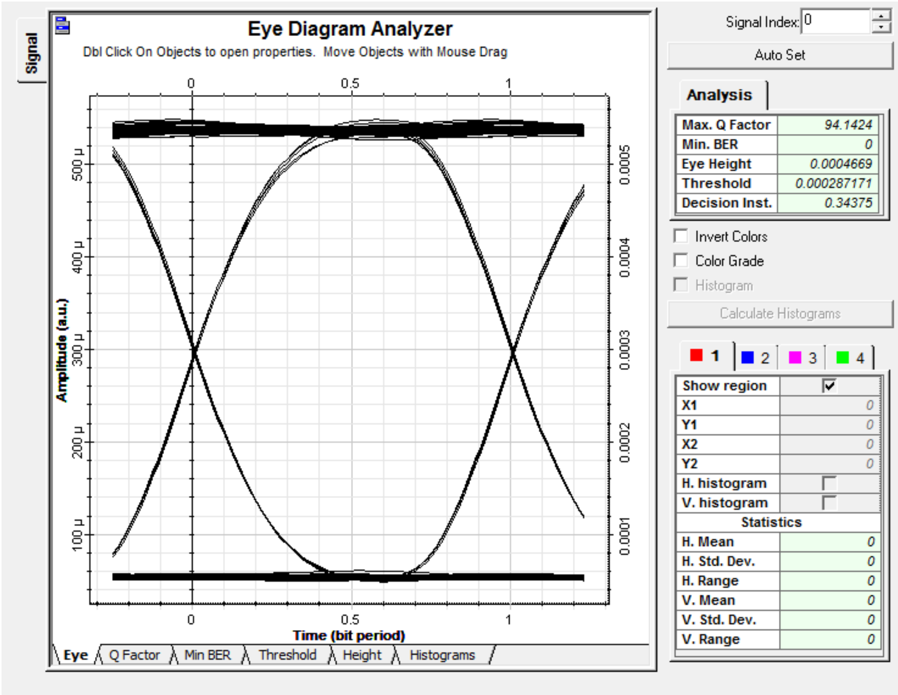

Appendix S: Arusha Eye Diagram for June under 2km with Q factor of 94.3513 and BER of 0

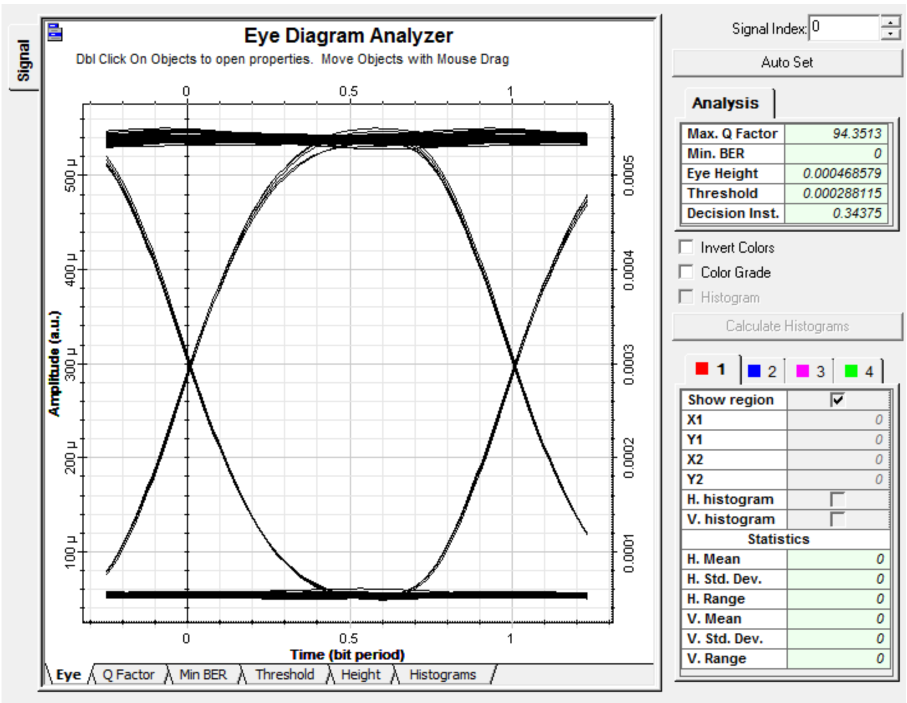

Appendix T: Arusha Eye Diagram for July under 2km with Q factor of 94.5059 and BER of 0

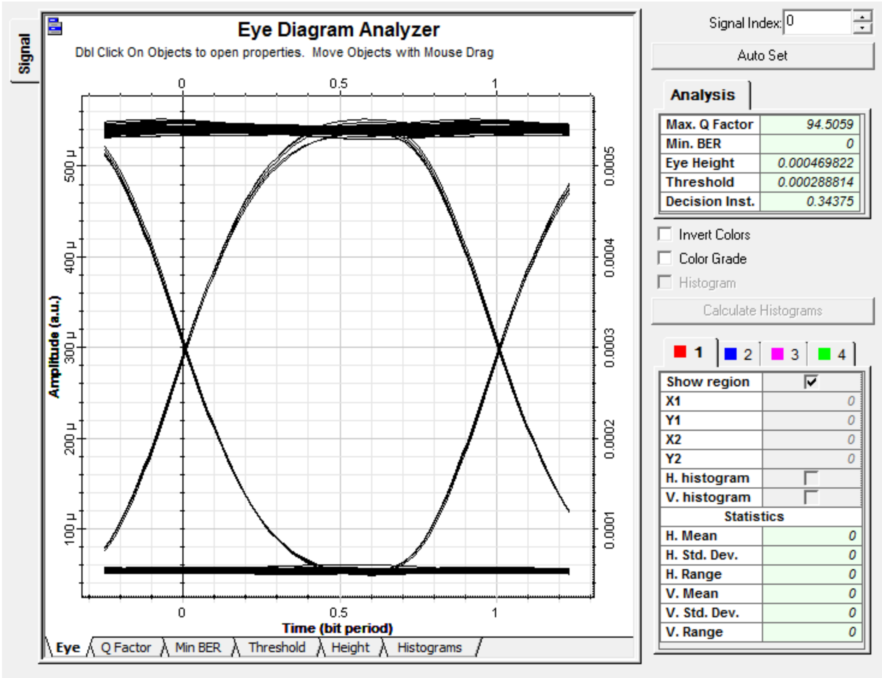

Appendix U: Arusha Eye Diagram for August under 2km with Q factor of 94.4266 and BER of 0

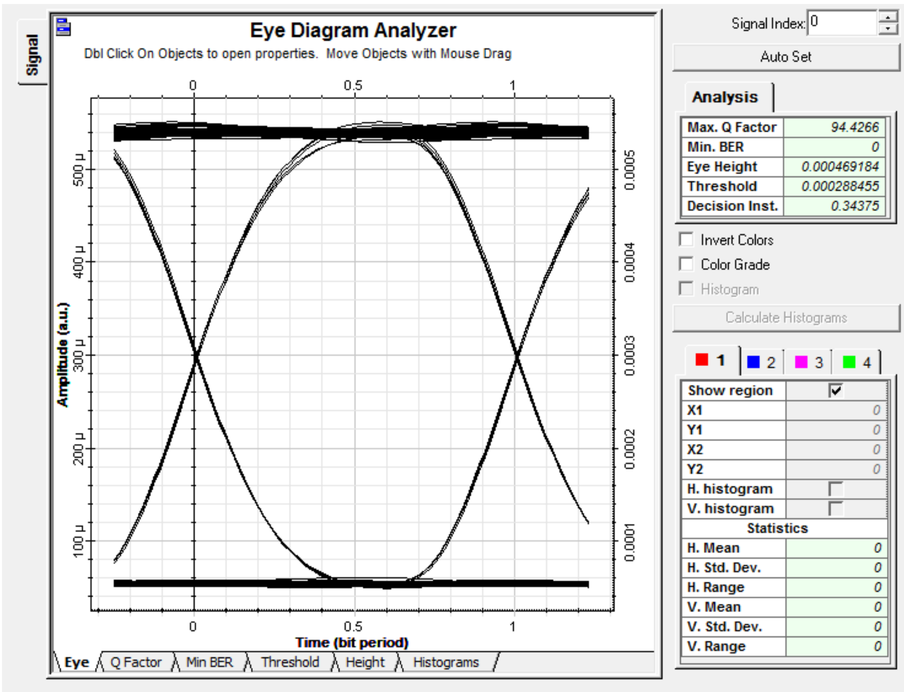

Appendix V: Arusha Eye Diagram for September under 2km with Q factor of 94.2872 and BER of 0

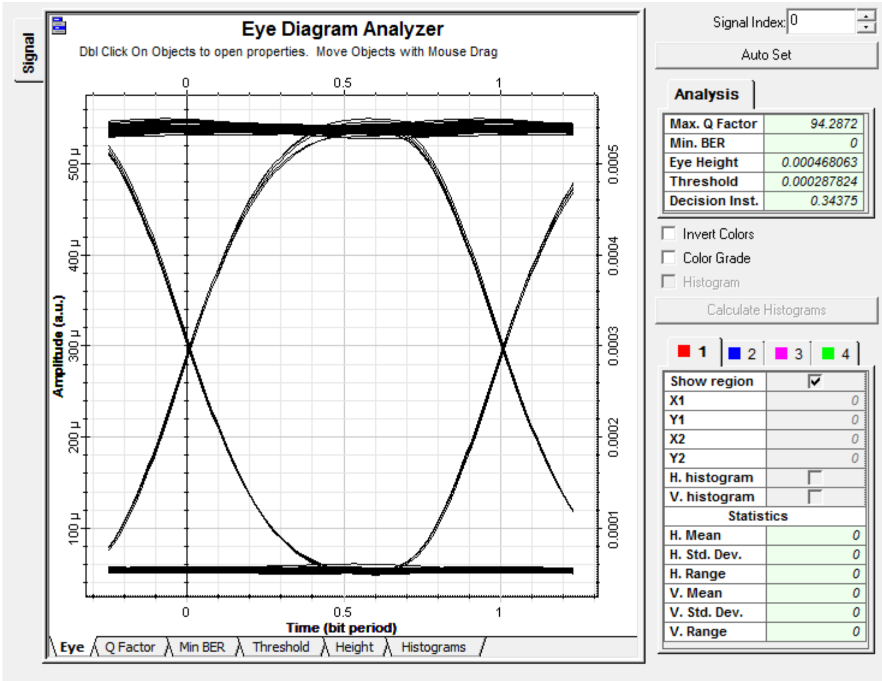

Appendix W: Arusha Eye Diagram for October under 2km with Q factor of 93.8989 and BER of 0

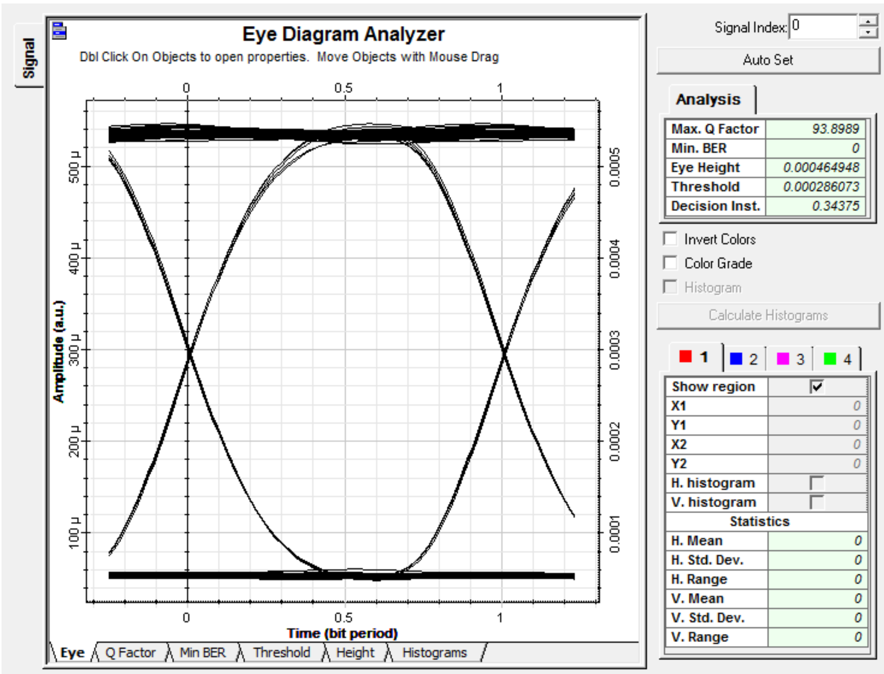

Appendix X: Arusha Eye Diagram for November under 2km with Q factor of 93.2903 and BER of 0

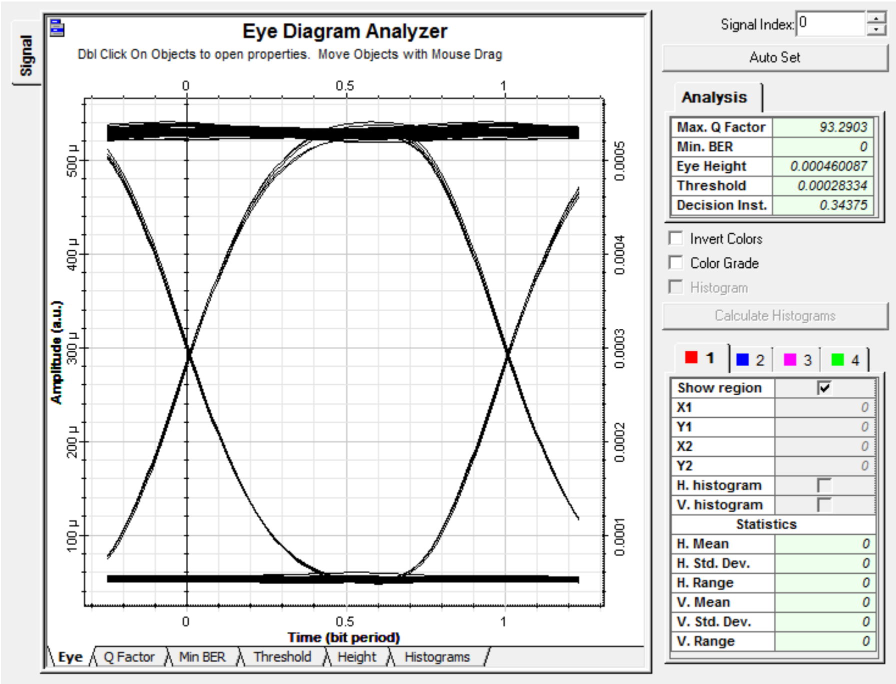

Appendix Y: Arusha Eye Diagram for December under 2km with Q factor of 992.6563 and BER of 0

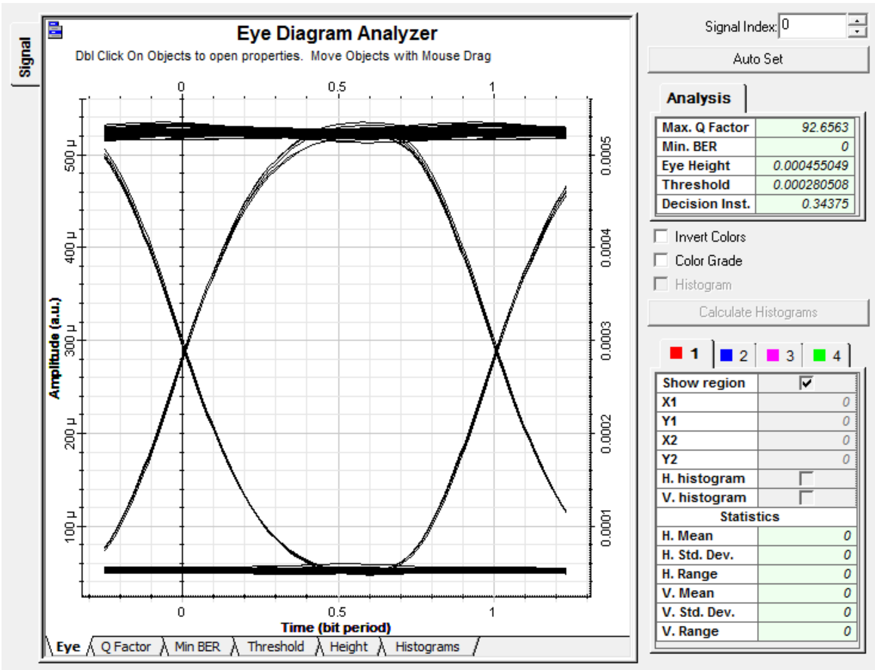

Appendix Z: Arusha Eye Diagram for January under 8km with Q factor of 5.05207 and BER of 2.19E-7

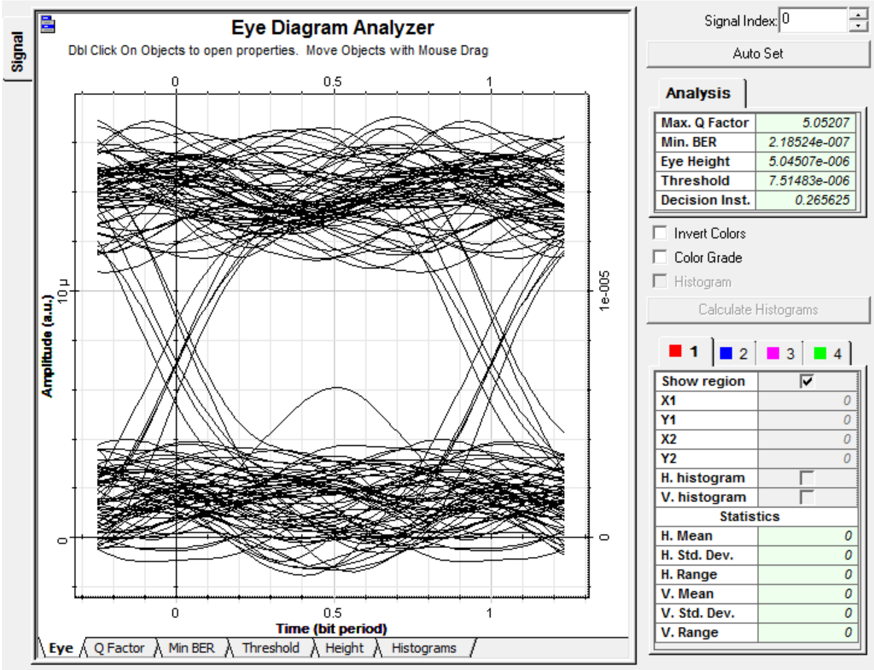

Appendix AA: Arusha Eye Diagram for February under 8km with Q factor of 5.11767 and BER of 1.55E-7

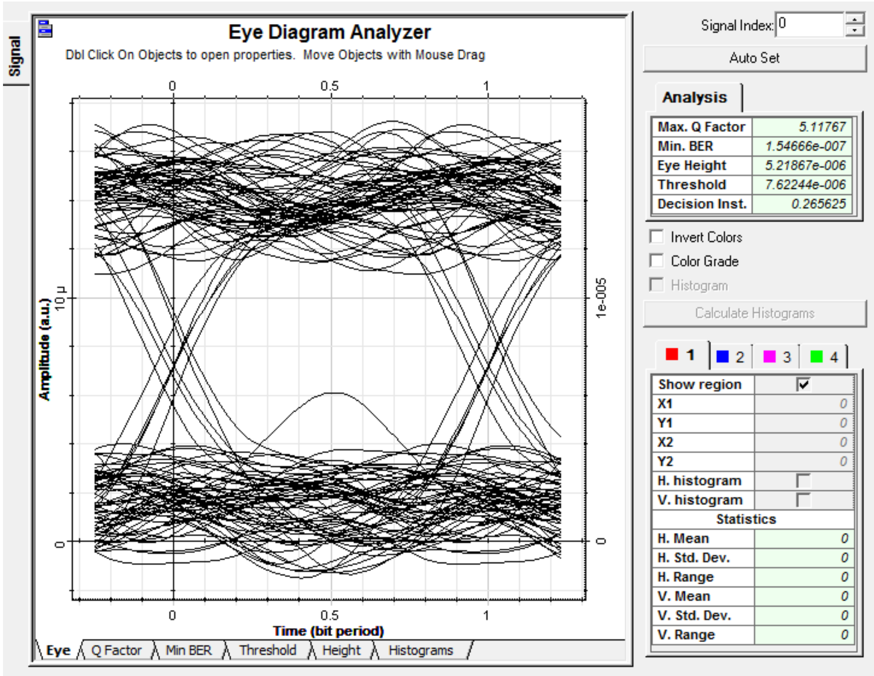

Appendix BB: Arusha Eye Diagram for March under 8km with Q factor of 5.15148 and BER of 1.29E-7

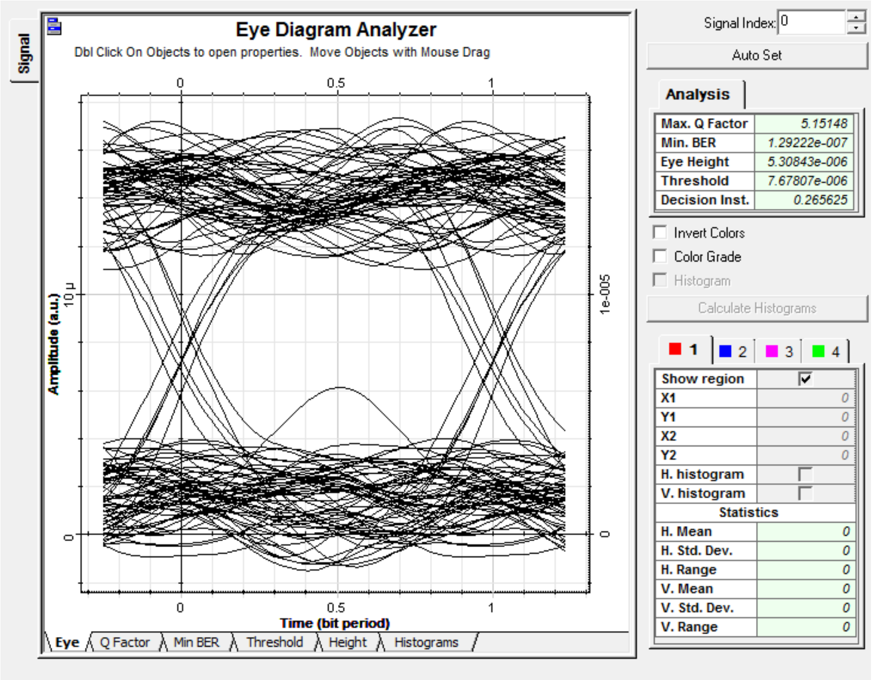

Appendix CC: Arusha Eye Diagram for April under 8km with Q factor of 5.32975 and BER of 4.92E-8

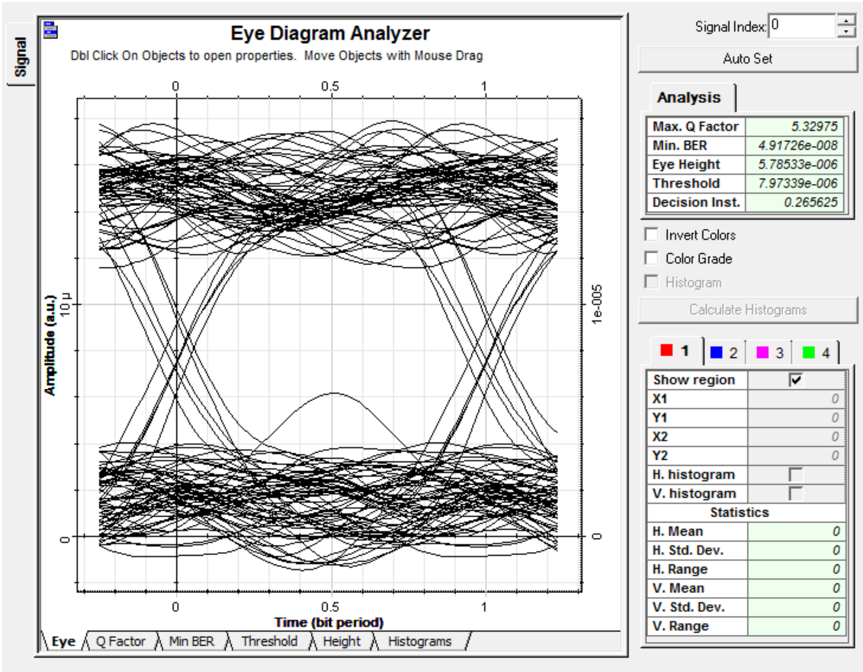

Appendix DD: Arusha Eye Diagram for May under 8km with Q factor of 5.55197 and BER of 1.41E-8

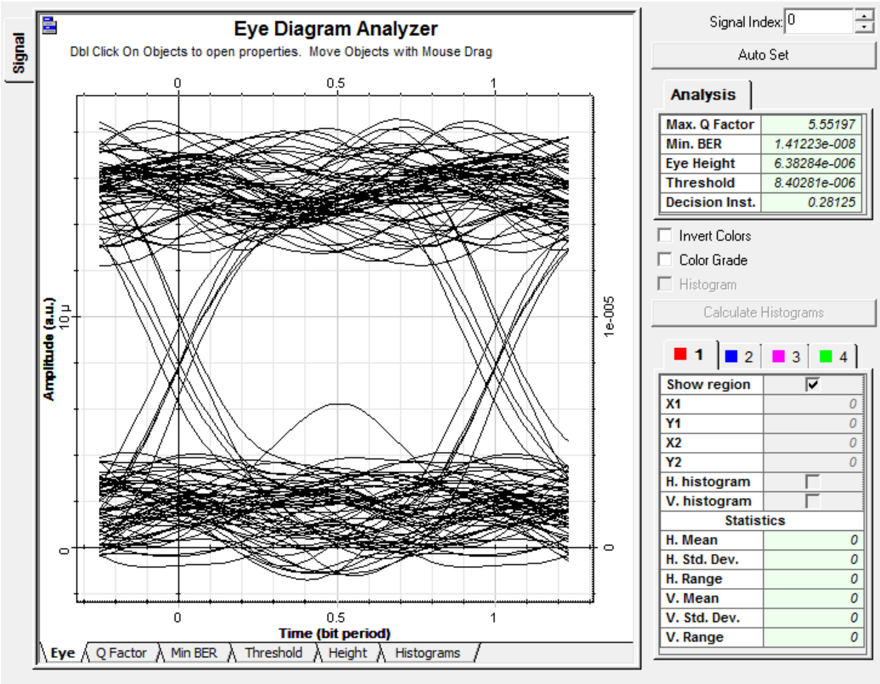

Appendix EE: Arusha Eye Diagram for June under 8km with Q factor of 5.61507 and BER of 9.82E-9

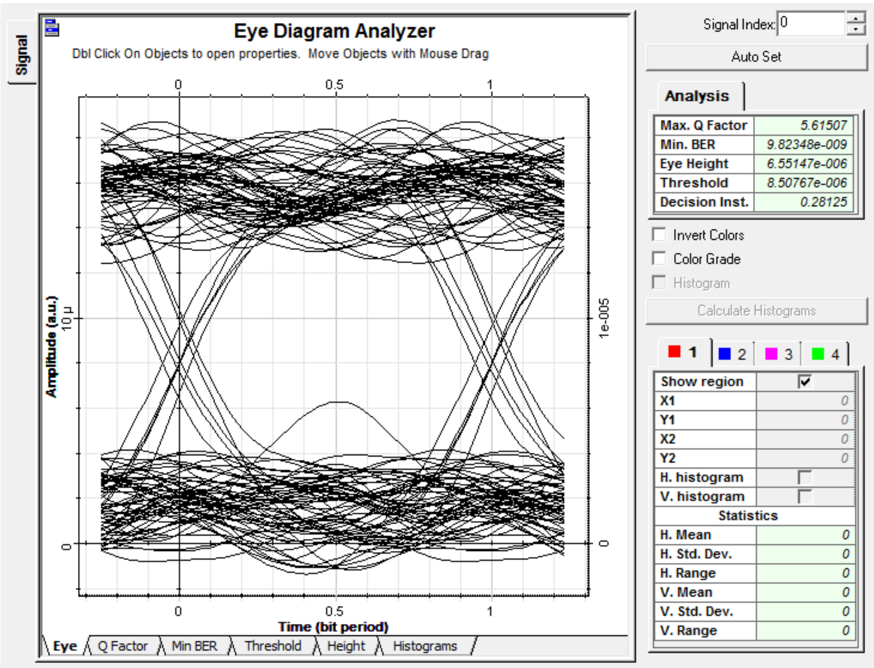

Appendix FF: Arusha Eye Diagram for July under 8km with Q factor of 5.66203 and BER of 7.48E-9

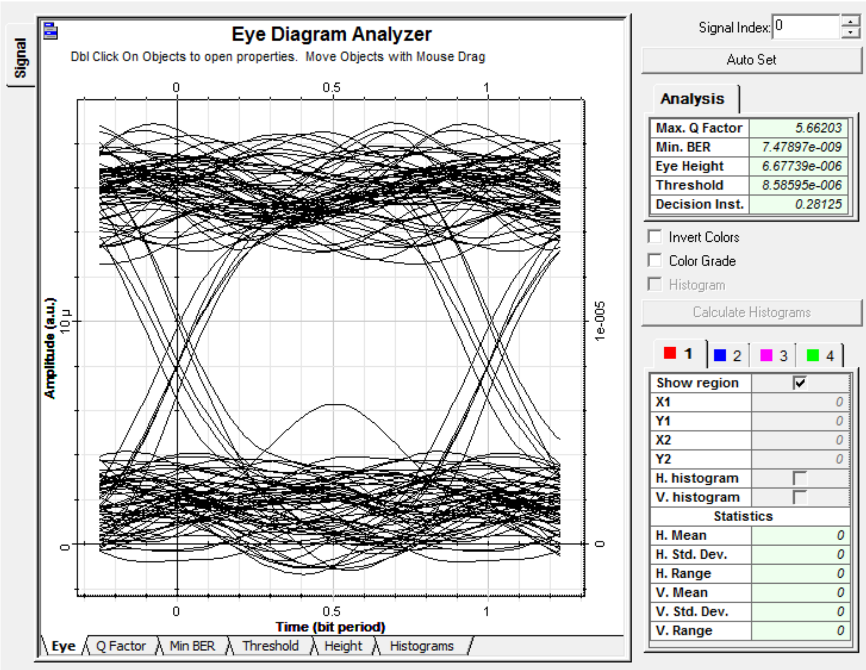

Appendix GG: Arusha Eye Diagram for August under 8km with Q factor of 5.63789 and BER of 8.61E-9

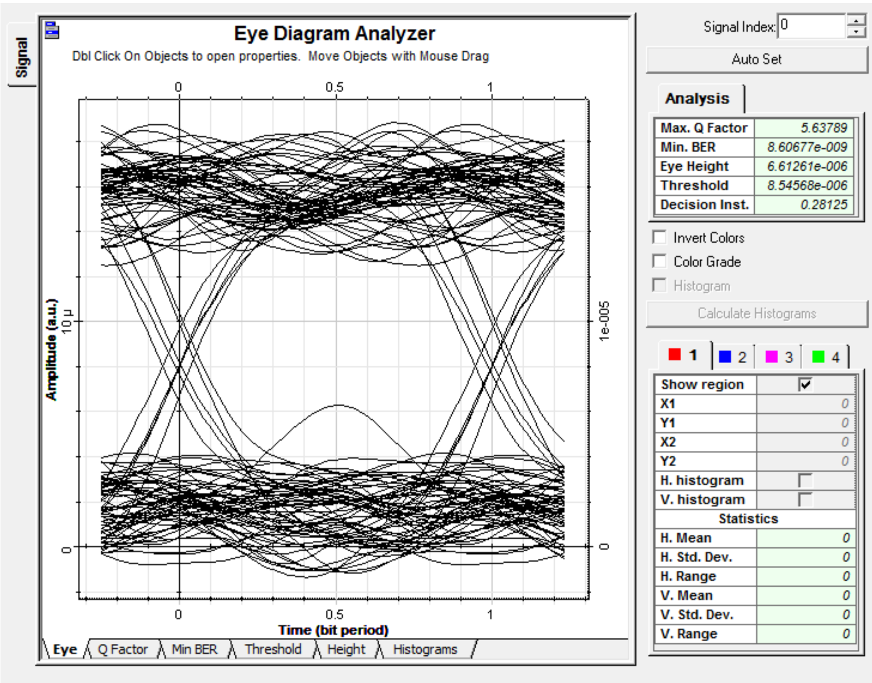

Appendix HH: Arusha Eye Diagram for September under 8km with Q factor of 5.59564 and BER of 1.10E-8

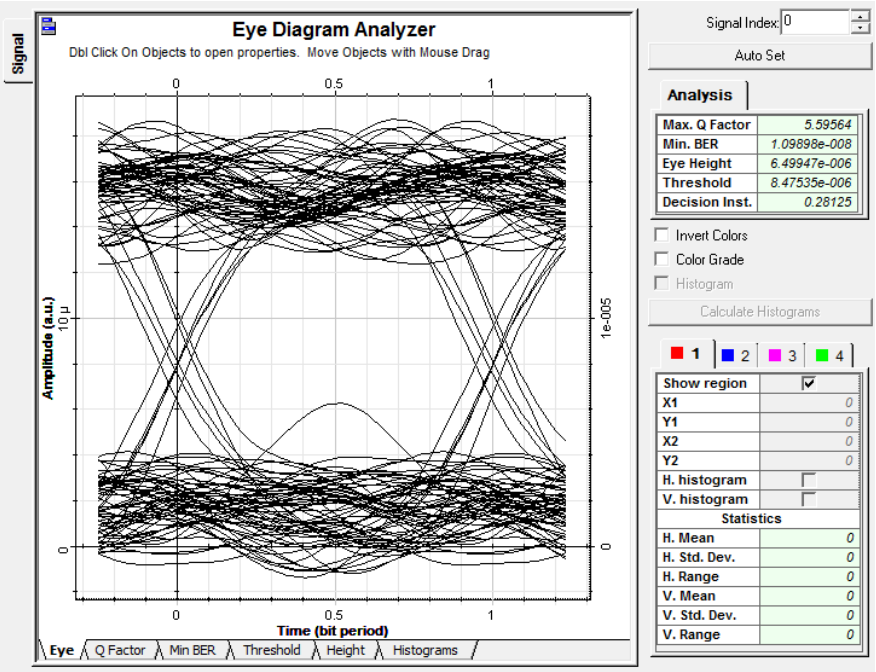

Appendix II: Arusha Eye Diagram for October under 8km with Q factor of 5.47904 and BER of 2.14E-8

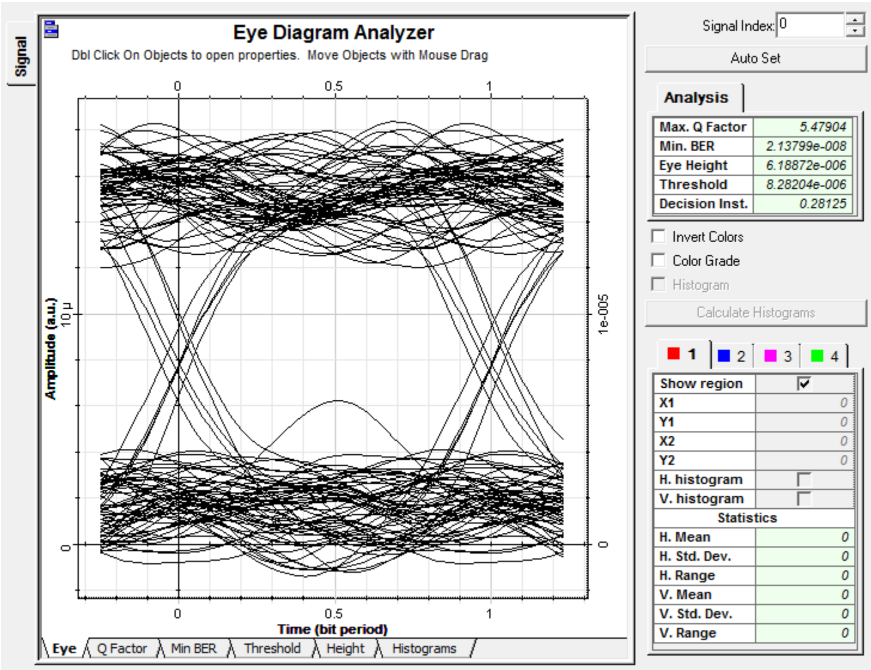

Appendix JJ: Arusha Eye Diagram for November under 8km with Q factor of 5.30332 and BER of 5.69E-8

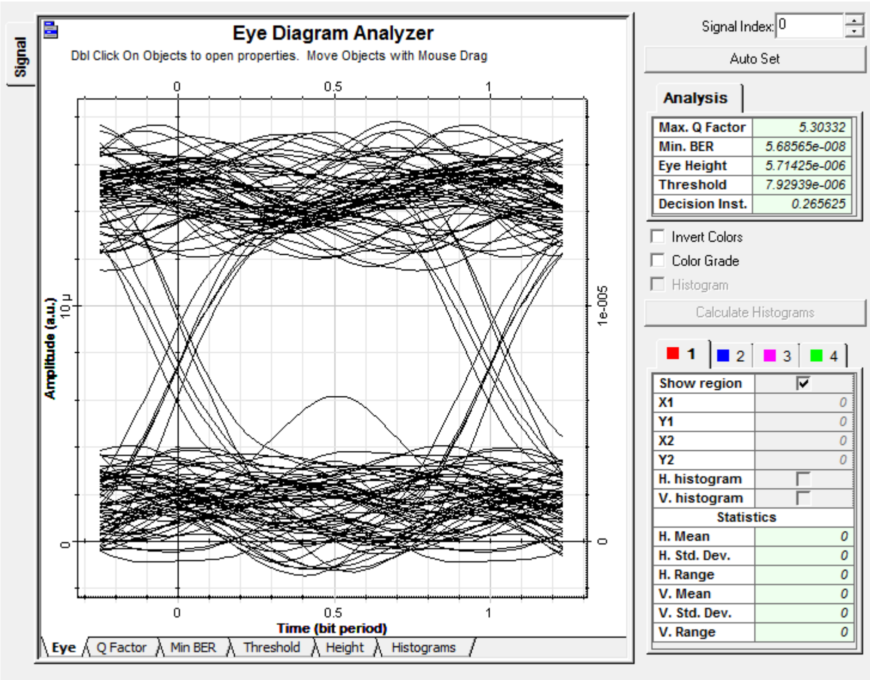

Appendix KK: Arusha Eye Diagram for December under 8km with Q factor of 5.1244 and BER of 1.49E-7

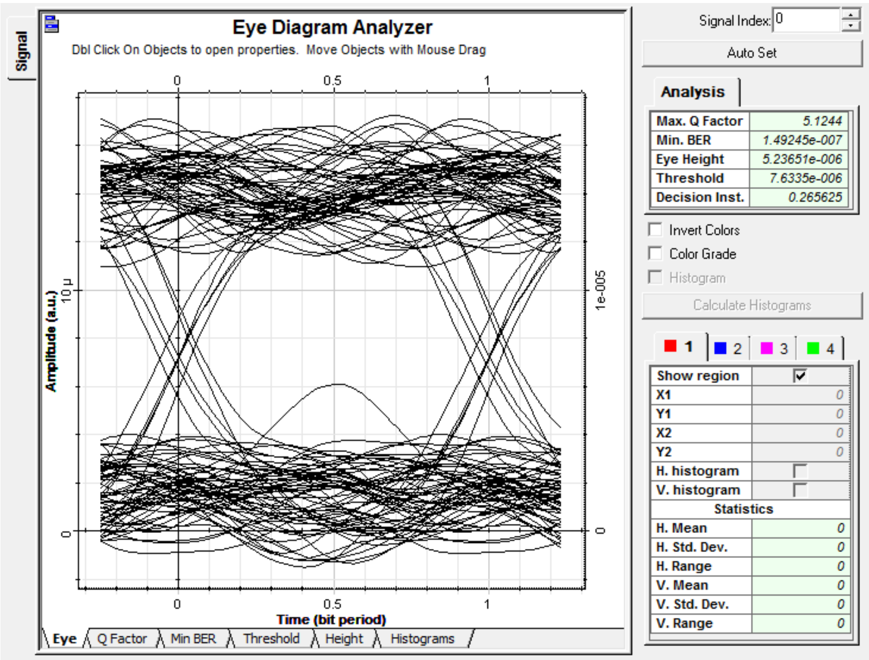

Appendix LL: Mwanza Eye Diagram for January under 4km with Q factor of 27.7607 and BER of 6.4705E-170

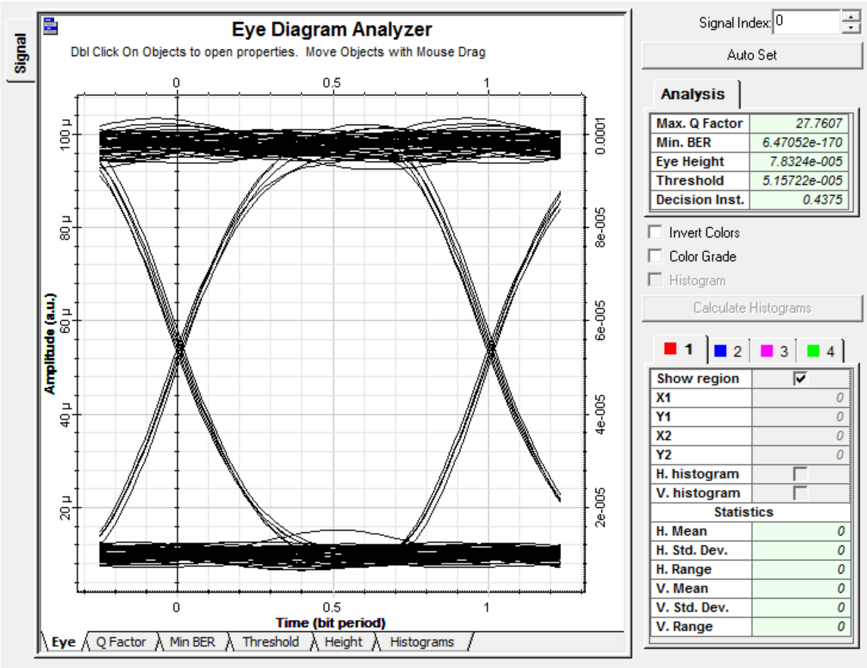

Appendix MM: Mwanza Eye Diagram for February under 4km with Q factor of 27.7803 and BER of 3.75E-170

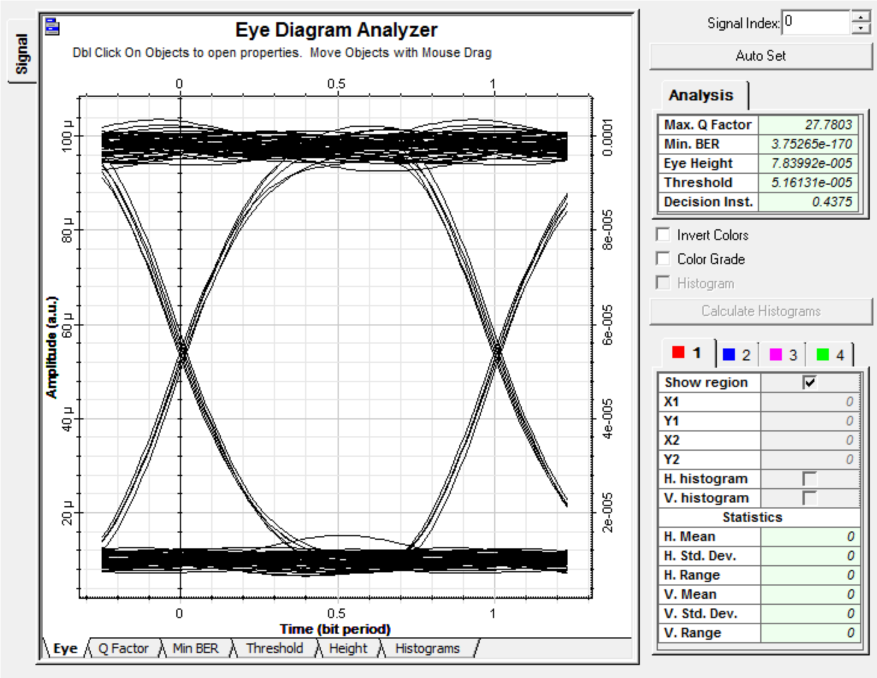

Appendix NN: Mwanza Eye Diagram for March under 4km with Q factor of 27.8283 and BER of 9.85E-171

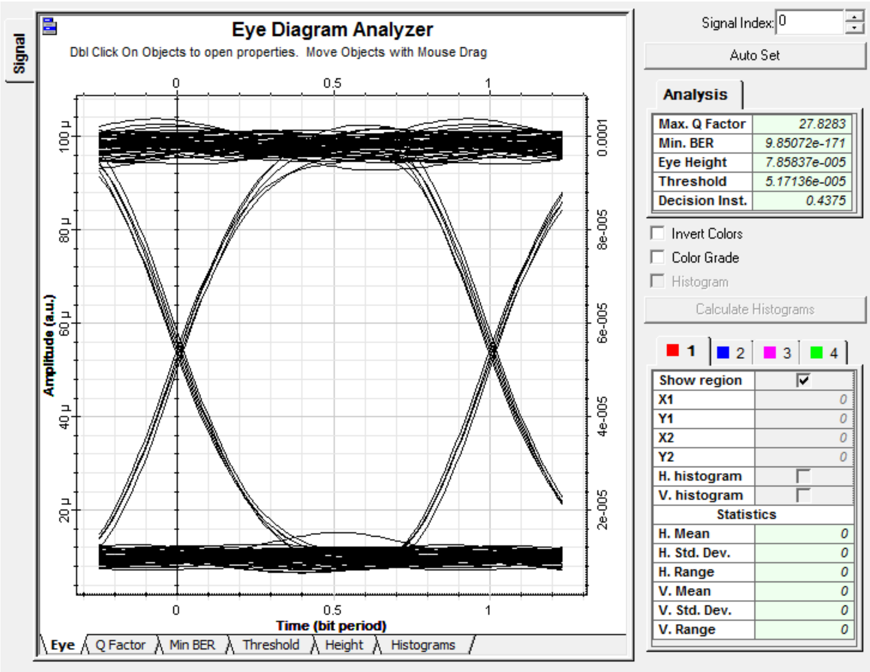

Appendix OO: Mwanza Eye Diagram for April under 4km with Q factor of 27.6475 and BER of 1.50E-168

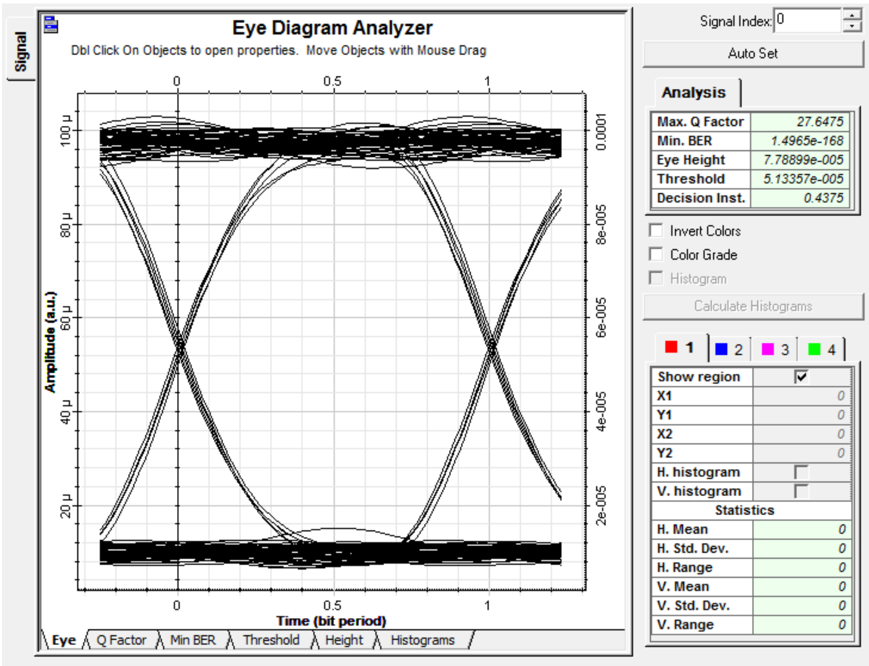

Appendix PP:Mwanza Eye Diagram for May under 4km with Q factor of 27.8289 and BER of 9.69E-171

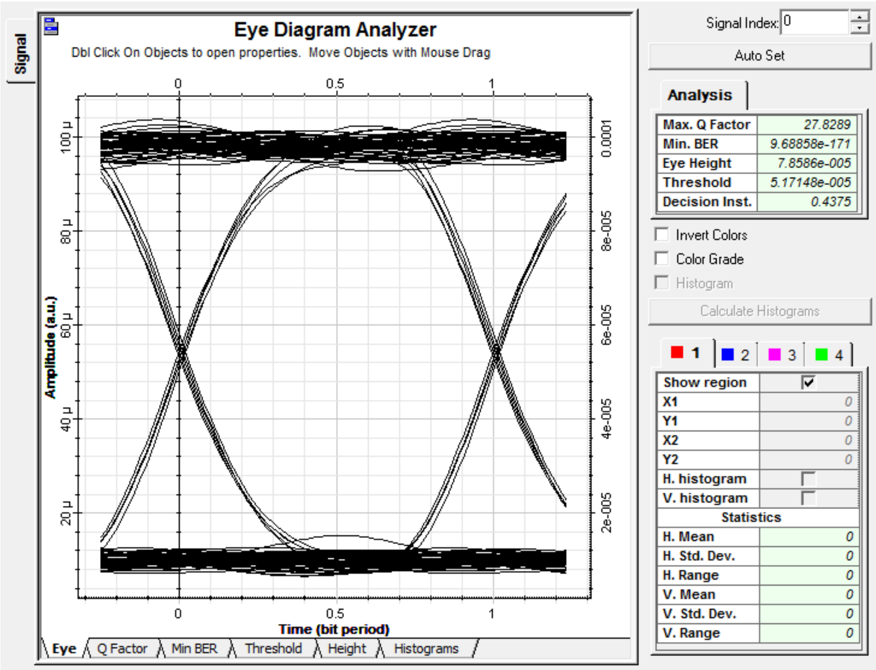

Appendix QQ: Mwanza Eye Diagram for June under 4km with Q factor of 27.887 and BER of 1.92E-171

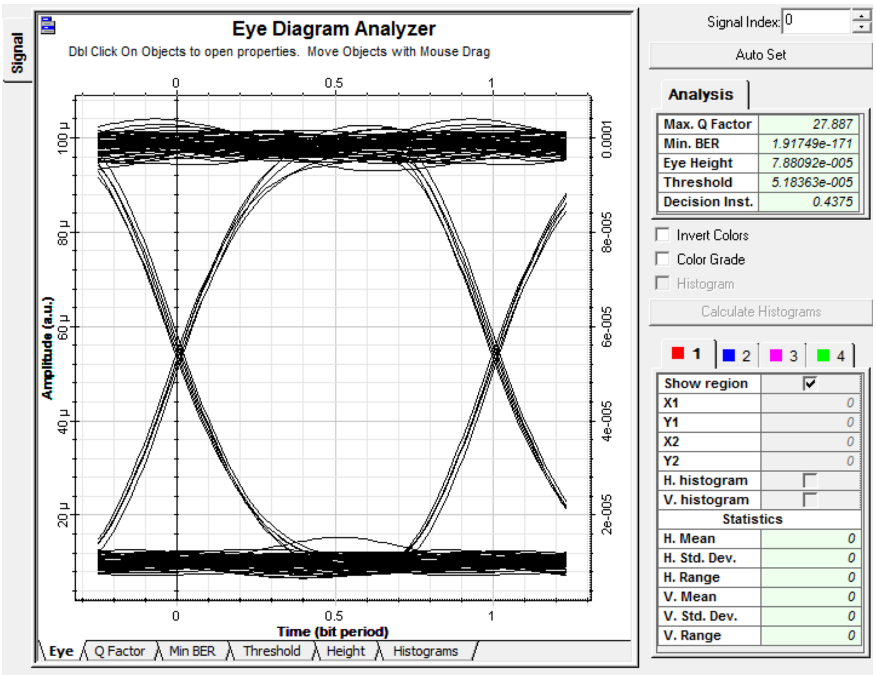

Appendix RR: Mwanza Eye Diagram for July under 4km with Q factor of 28.0867 and BER of 7.12E-174

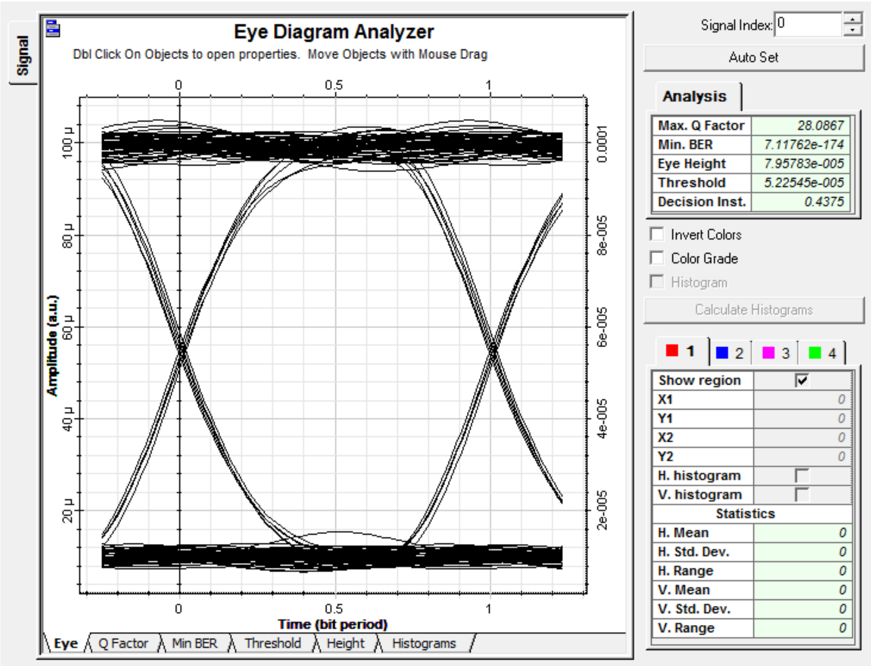

Appendix SS: Mwanza Eye Diagram for August under 4km with Q factor of 28.105 and BER of 4.2517E-174

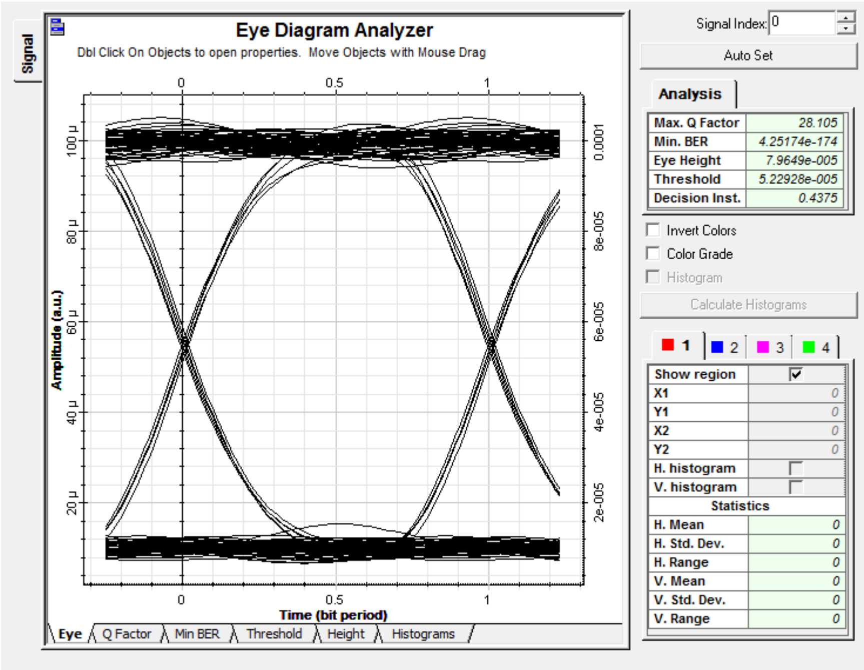

Appendix TT: Mwanza Eye Diagram for September under 4km with Q factor of 27.9588 and BER of 2.56E-172

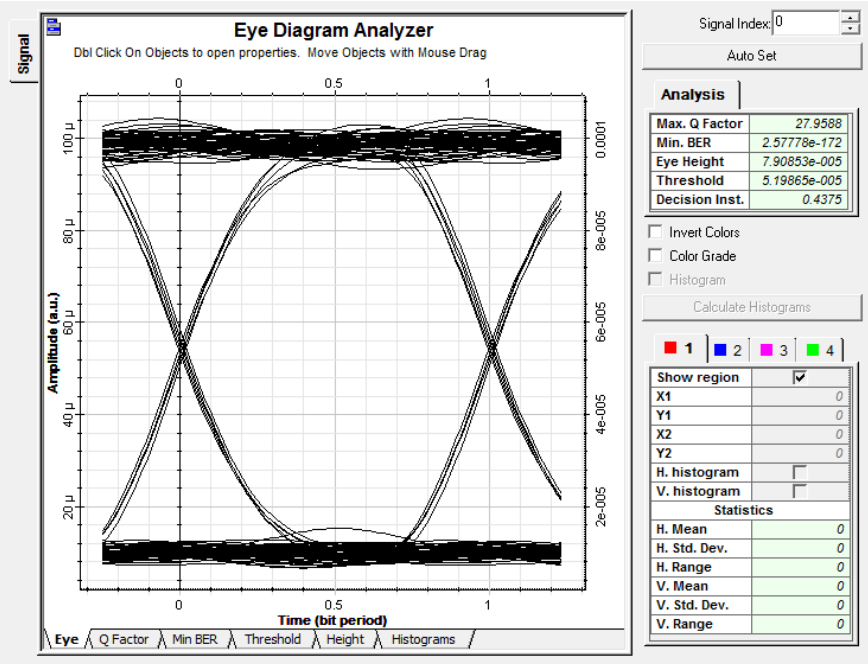

Appendix UU: Mwanza Eye Diagram for October under 4km with Q factor of 27.878 and BER of 2.46E-171

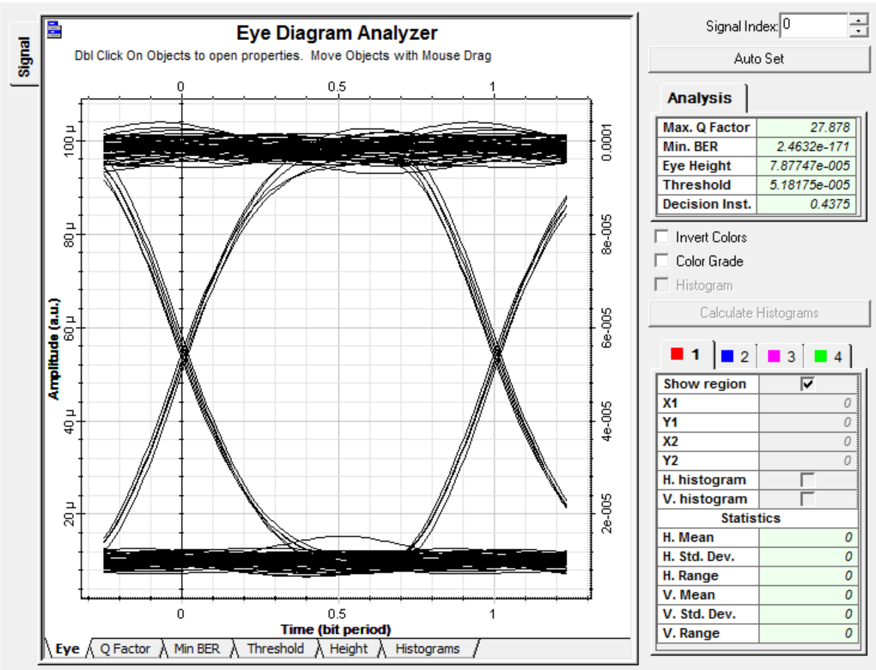

Appendix VV: Mwanza Eye Diagram for November under 4km with Q factor of 27.8318 and BER of 8.94E-171

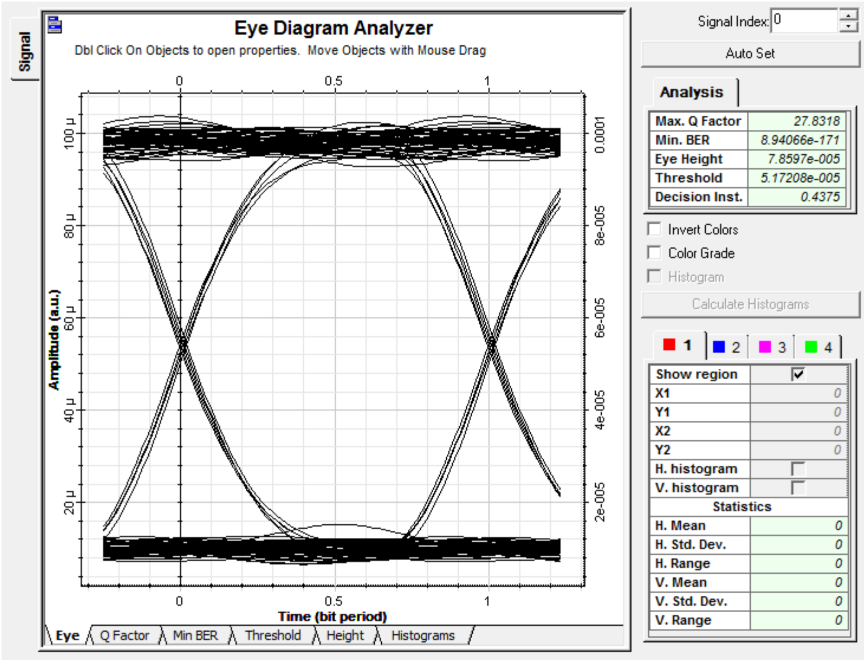

Appendix WW: Mwanza Eye Diagram for December under 4km with Q factor of 27.8559 and BER of 4.56E-171

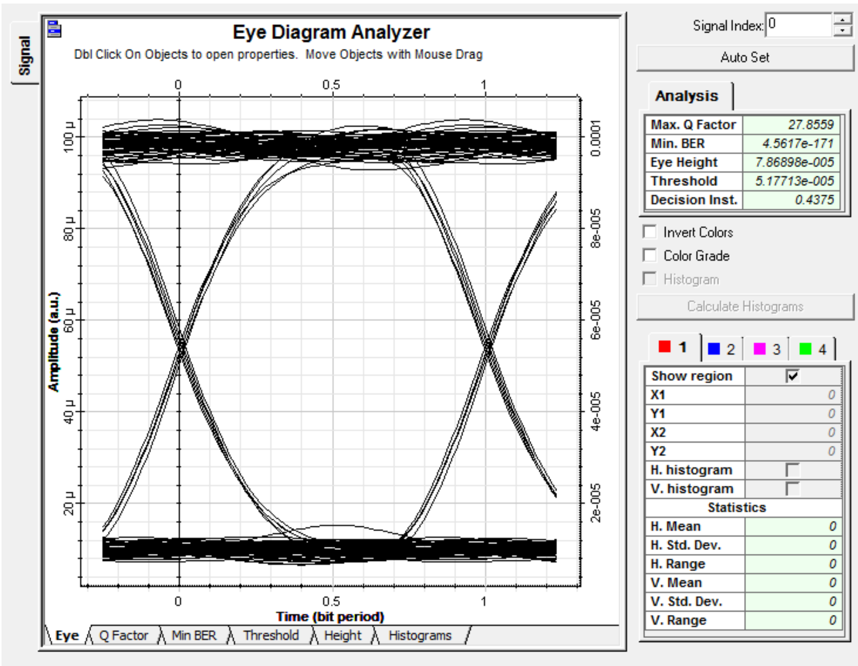

Appendix XX: Mwanza Eye Diagram for January under 6km with Q factor of 28.2377 and BER of 1.00E-175

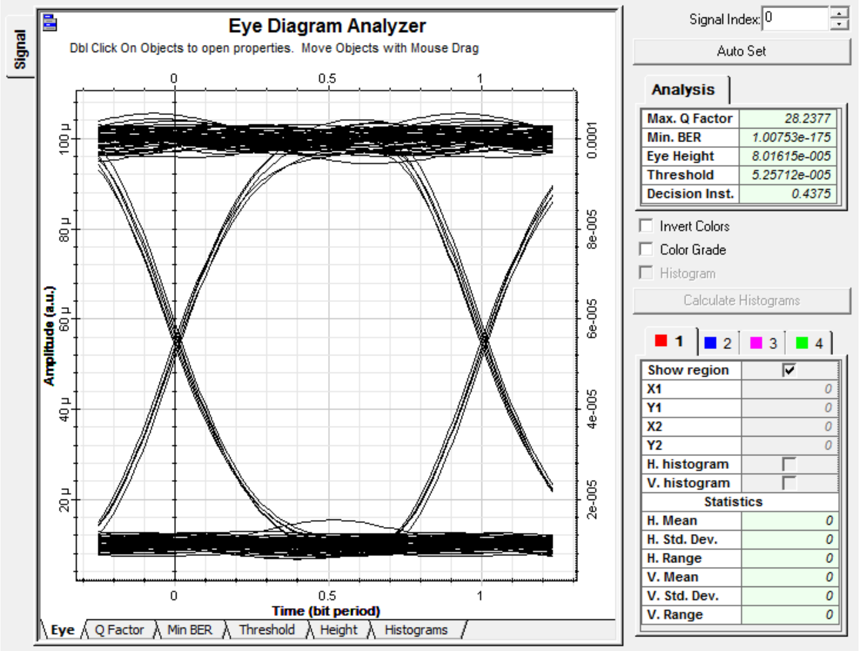

Appendix YY: Mwanza Eye Diagram for February under 6km with Q factor of 28.2569 and BER of 5.85E-176

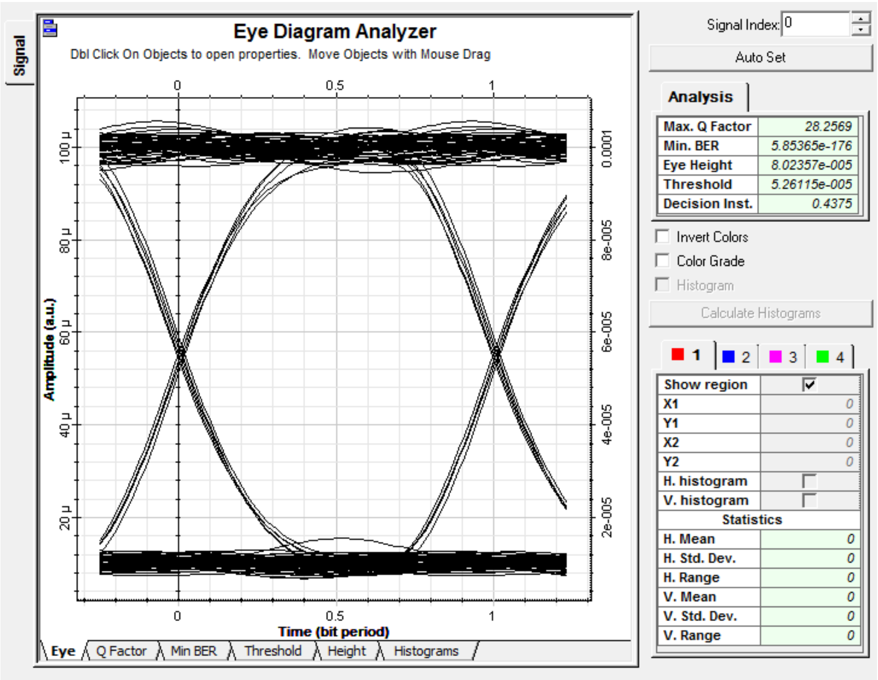

Appendix ZZ: Mwanza Eye Diagram for March under 6km with Q factor of 28.304 and BER of 1.54E-176

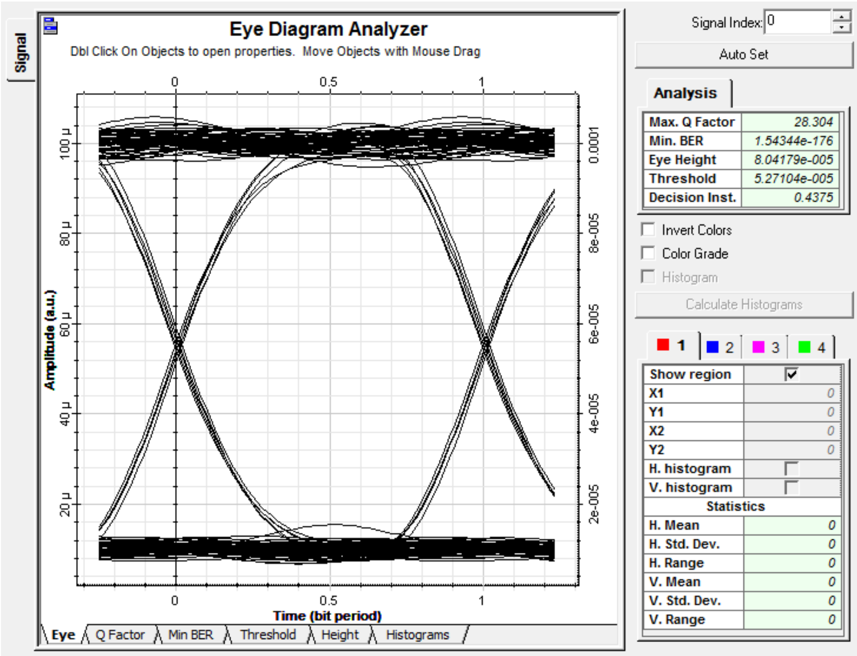

Appendix AAA: Mwanza Eye Diagram for April under 6km with Q factor of 28.1267 and BER of 2.31E-174

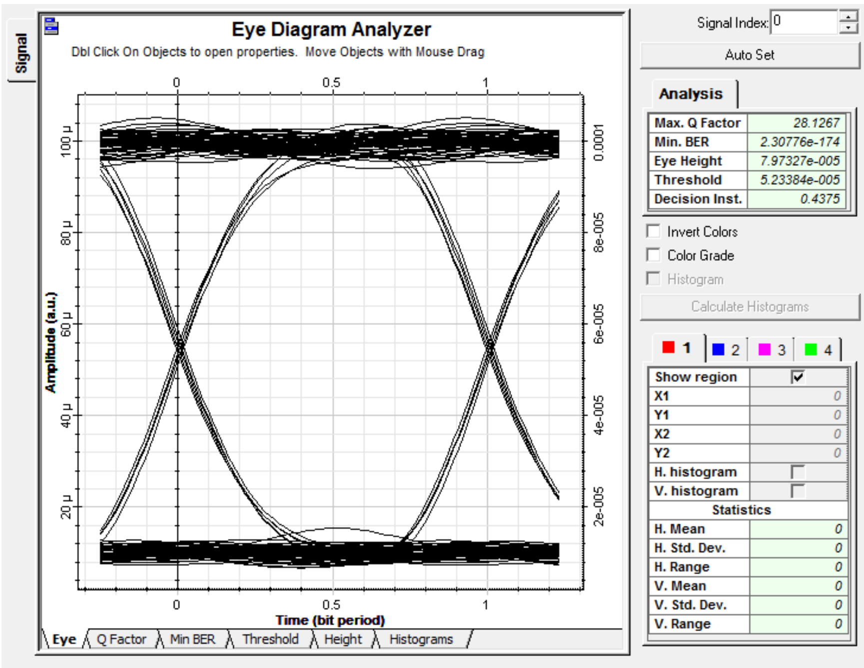

Appendix BBB: Mwanza Eye Diagram for May under 6km with Q factor of 28.3045 and BER of 1.52E-176

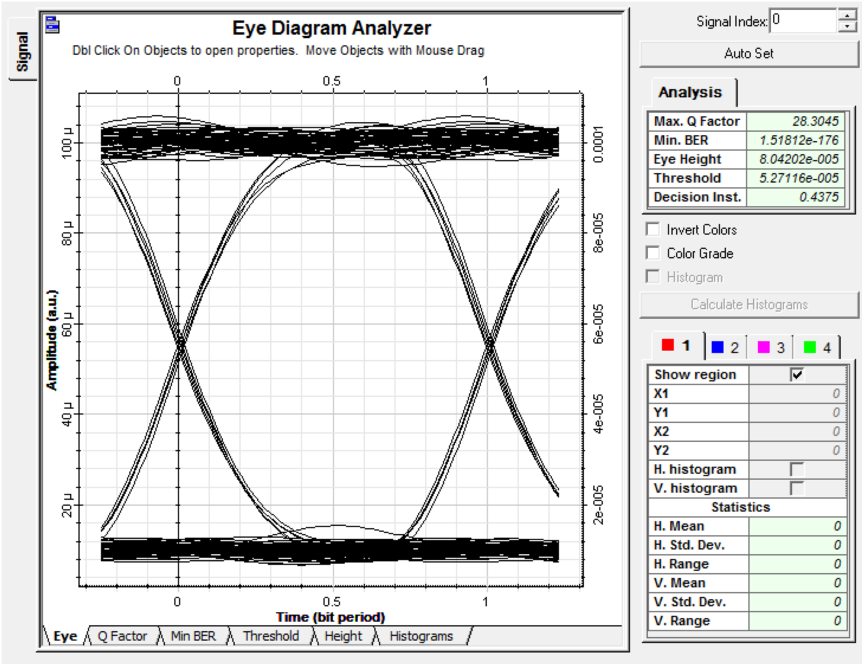

Appendix CCC: Mwanza Eye Diagram for June under 6km with Q factor of 28.3615 and BER of 3.02E-177

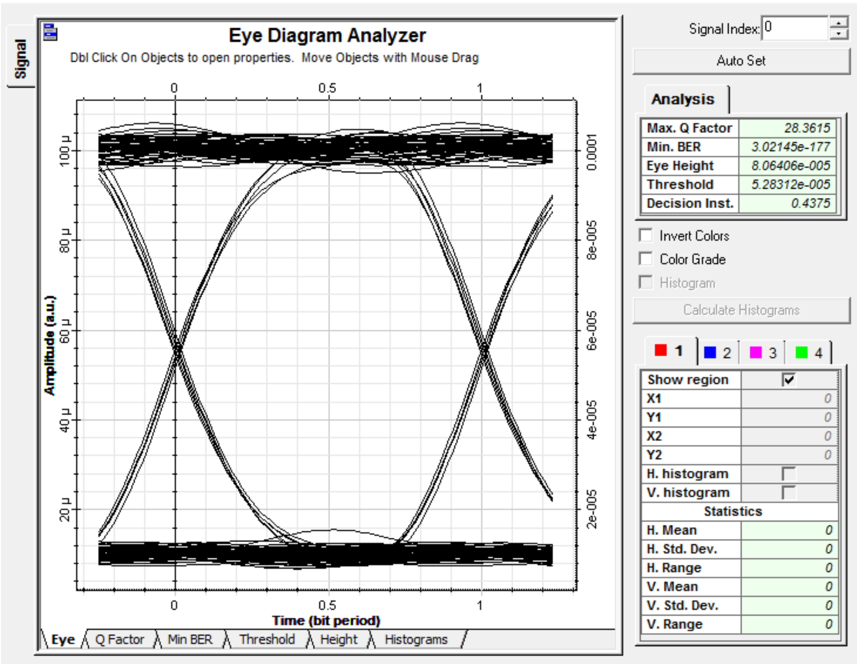

Appendix DDD: Mwanza Eye Diagram for July under 6km with Q factor of 28.5571 and BER of 1.15E-179

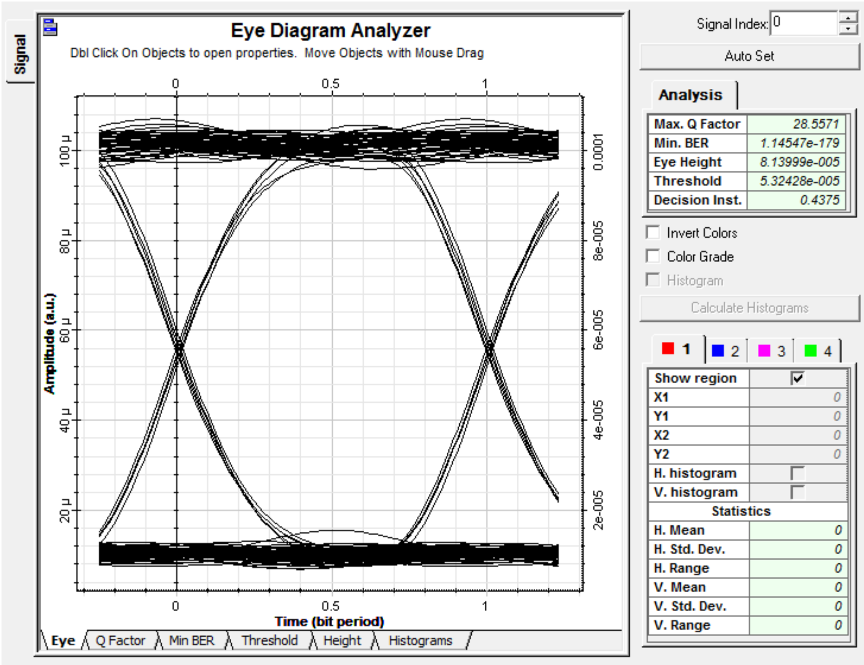

Appendix EEE: Mwanza Eye Diagram for August under 6km with Q factor of 28.5751 and BER of 6.86E-180

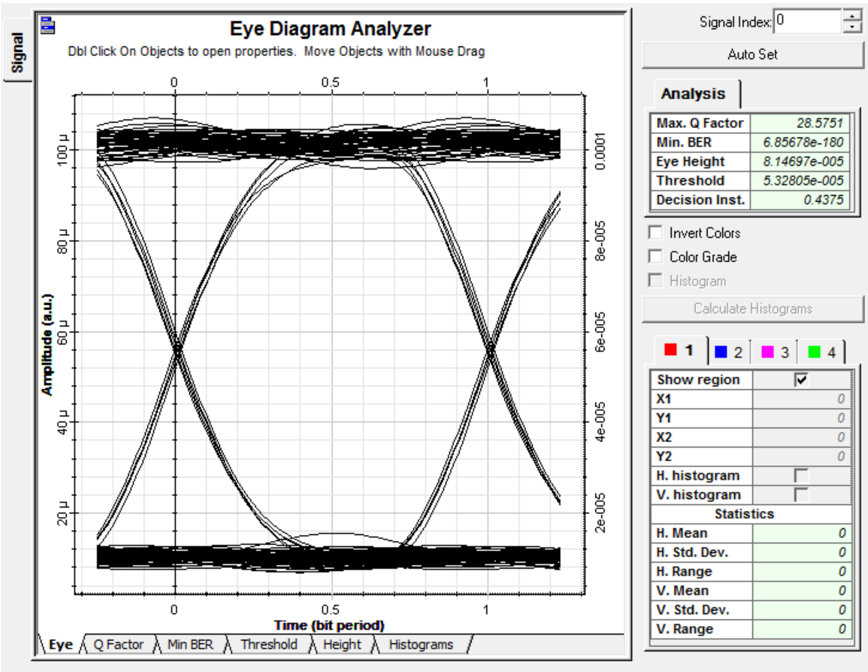

Appendix FFF: Mwanza Eye Diagram for September under 6km with Q factor of 28.4318 and BER of 4.09E-178

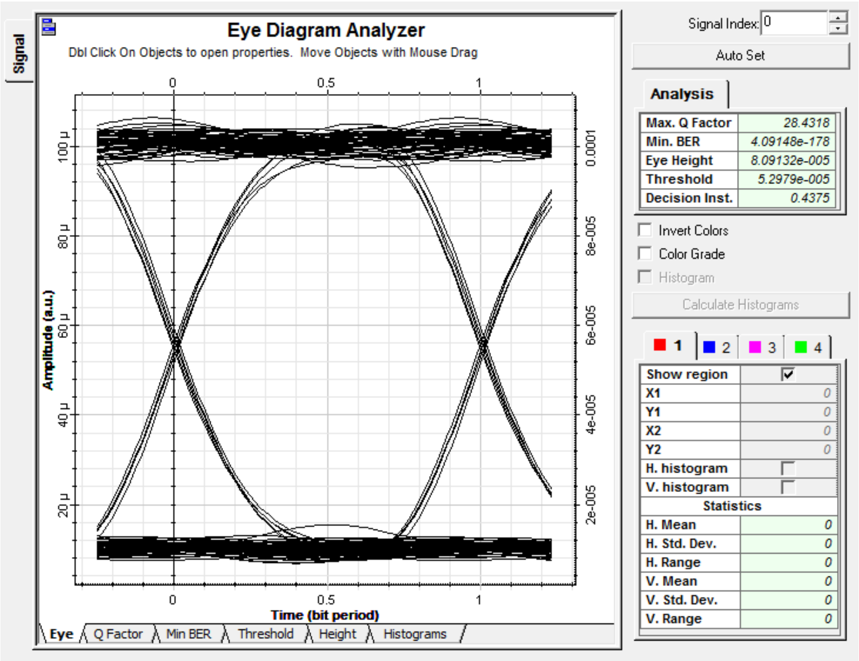

Appendix GGG: Mwanza Eye Diagram for October under 6km with Q factor of 3527 and BER of 3.88E-177

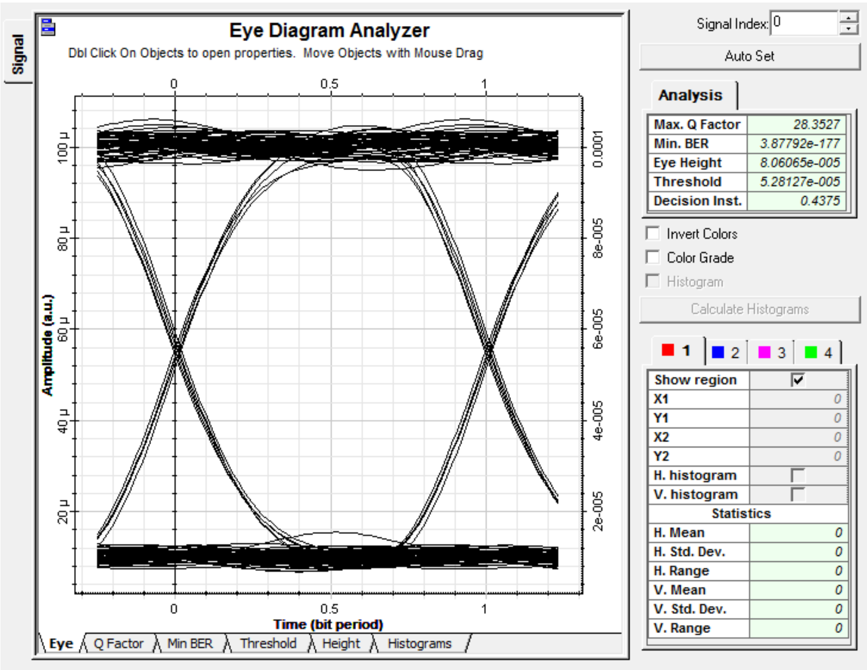

Appendix HHH: Mwanza Eye Diagram for November under 6km with Q factor of 28.3074 and BER of 1.40E-176

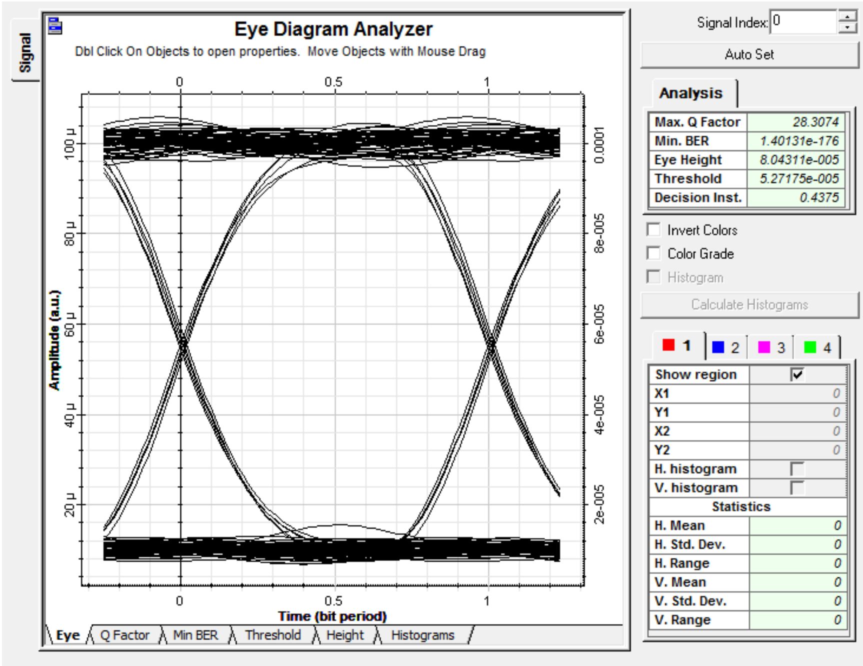

Appendix III: Mwanza Eye Diagram for December under 6km with Q factor of 28.331 and BER of 7.17E-177

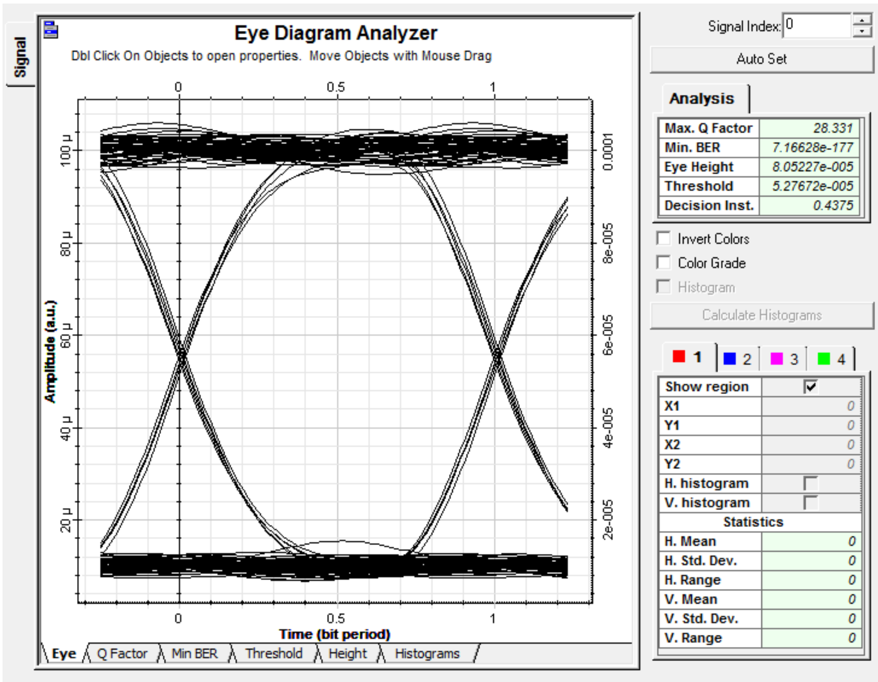

Appendix JJJ: Data from Tanzania Meteorological Agency

UNITED REPUBLIC OF TANZANIA
MINISTRY OF WORKS, TRANSPORT AND COMMUNICATION
TANZANIA METEOROLOGICAL AGENCY

Telephone: 255 22 2460735/2460706-8
Telefax: 255 22 2460735/2460700
E-mail: **met@meteo.go.tz**
Website: **www.meteo.go.tz**

3rd Floor, Ubungo Plaza
P.O. BOX 3056
DAR ES SALAAM.

In reply please quote:
Our ref.: TMA/ 1422 Vol.V
In reply please quote:

01st July, 2019

Data Delivery Report

Request No. *(yymmno)*	: 20190703
Customer Name	: EDSON JOSEPH
Customer Address	: UNIVERSITY OF DODOMA
Email Address	: edjo2011tz@yahoo.com

Description for data provided

Parameter(s) provided: Monthly Average Temperature, Relative Humidity and Wind Speed

Station(s) provided: **Mwanza** - Latitude: - 2°28' Longitude: - 32°55' Elevation: -1140m
Arusha:- Latitude: - 3°28' Longitude: - 36°38' Elevation: -1372m

Duration (Year/ Month): - November 2015 to January 2018

Data Gaps:- No gaps

Data given as: - Hard copy

For: DIRECTOR GENERAL
MINISTRY OF TRANSPORT
TANZANIA METEOROLOGICAL AGENCY
P. O. Box 3056
DAR-ES-SALAAM

Attended by:-	Joseph Ndunguru Met Supervisor	Signature	01/07/2019. Date
Verified by:-	Dr. Hashim Ng'ongolo MCC	Signature	01/07/2019 Date

Customer's signature: ....

Thank you for using meteorological data

Revision No. 00 *Effective Date: July 31, 2017*

MONTHLY AVERAGE TEMPERATURE DATA(°C)																
STATION	LAT	LONG	ALT	YEAR	Jan	Feb	Mar	Apr	May	Jun	Jul	Aug	Sep	Oct	Nov	Dec
MWANZA AIRFIELD	-2.5	32.9	1140	2015	23.0	23.5	22.5	22.4	23.9	22.9	23.0	23.8	24.2	23.6	22.8	22.6
MWANZA AIRFIELD	-2.5	32.9	1140	2016	23.4	24.2	24.9	24.3	23.6	23.3	22.2	23.3	24.0	24.3	23.9	24.0
MWANZA AIRFIELD	-2.5	32.9	1140	2017	24.6	24.1	23.8	24.6	23.6	23.9	23.1	19.3	24.4	24.4	23.5	24.0
MWANZA AIRFIELD	-2.5	32.9	1140	2018	22.8	24.8	23.2	23.4	23.0	23.1	23.0	23.4	24.8	24.1	24.2	23.2
ARUSHA AIRPORT	-3.4	36.6	1372	2015	21.9	22.3	22.8	21.8	19.9	18.5	18.6	19.4	20.7	22.8	22.4	22.0
ARUSHA AIRPORT	-3.4	36.6	1372	2016	22.5	22.3	23.9	21.6	19.8	19.0	18.1	18.9	19.7	21.5	22.4	22.1
ARUSHA AIRPORT	-3.4	36.6	1372	2017	22.5	22.5	23.1	21.8	19.8	19.0	18.3	19.7	19.9	22.3	21.7	22.2
ARUSHA AIRPORT	-3.4	36.6	1372	2018	21.7	22.7	21.8	20.9	19.4	18.4	18.2	18.4	20.5	20.9	21.5	21.3
MONTHLY AVERAGE RELATIVE HUMIDITY (%)																
					Jan	Feb	Mar	Apr	May	Jun	Jul	Aug	Sep	Oct	Nov	Dec
MWANZA AIRFIELD	-2.5	32.9	1140	2015	74	73	67	82	71	72	63	59	66	75	82	82
MWANZA AIRFIELD	-2.5	32.9	1140	2016	80	75	73	78	71	61	63	60	64	70	73	72
MWANZA AIRFIELD	-2.5	32.9	1140	2017	67	72	76	72	70	62	62	63	72	73	76	74
MWANZA AIRFIELD	-2.5	32.9	1140	2018	80	70	78	83	75	67	58	68	64	70	74	78
ARUSHA AIRPORT	-3.4	36.6	1372	2015	69	69	68	85	89	81	79	74	68	69	79	78
ARUSHA AIRPORT	-3.4	36.6	1372	2016	78	74	70	90	84	81	80	70	70	72	75	76
ARUSHA AIRPORT	-3.4	36.6	1372	2017	67	70	75	84	89	83	78	73	70	68	78	70
ARUSHA AIRPORT	-3.4	36.6	1372	2018	77	64	83	88	87	83	78	76	71	74	75	80
MONTHLY AVERAGE WIND SPEED DATA (Knots)																
					Jan	Feb	Mar	Apr	May	Jun	Jul	Aug	Sep	Oct	Nov	Dec
MWANZA AIRFIELD	-2.5	32.9	1140	2015	4	6	4	3	5	4	6	7	6	5	5	5
MWANZA AIRFIELD	-2.5	32.9	1140	2016	5	5	5	6	5	7	6	6	9	7	6	7
MWANZA AIRFIELD	-2.5	32.9	1140	2017	8	6	10	6	7	8	7	7	7	7	6	6
MWANZA AIRFIELD	-2.5	32.9	1140	2018	5	8	5	5	7	6	9	7	8	8	7	6
ARUSHA AIRPORT	-3.4	36.6	1372	2015	4	5	8	7	9	8	10	11	12	12	8	5
ARUSHA AIRPORT	-3.4	36.6	1372	2016	4	5	6	8	9	10	8	9	9	10	8	5
ARUSHA AIRPORT	-3.4	36.6	1372	2017	5	6	6	8	9	9	8	9	9	9	7	5
ARUSHA AIRPORT	-3.4	36.6	1372	2018	4	6	5	6	7	7	9	8	9	8	7	5